

EFFECTS OF FORESTRY ON MERCURY DYNAMICS IN STREAM FOOD WEBS

CUMULATIVE IMPACTS OF FOREST MANAGEMENT ON THE
ACCUMULATION AND BIOMAGNIFICATION OF MERCURY AND ITS
RELATIONSHIP TO AUTOCHTHONY IN STREAM FOOD WEBS IN NEW
BRUNSWICK, CANADA

By LAUREN NEGRAZIS, B.SC.

A Thesis Submitted to the School of Graduate Studies in Partial Fulfilment of the
Requirements for the Degree Master of Science

McMaster University MASTER OF SCIENCE (2020) Hamilton, Ontario (Biology)

TITLE: The Effects of Forest Management on the Accumulation and Biomagnification of

Mercury AUTHOR: Lauren Negrazis, B.Sc. (University of Western Ontario)

SUPERVISOR: Dr. K. Kidd NUMBER OF PAGES: xvi, 87

Lay abstract:

Forest harvesting is an essential and large part of Canada's economy, and it is important to ensure that its impacts on freshwater systems are minimal. Forest management can increase the amount of the toxic metal mercury entering streams and this can have harmful effects in top predators, like fish, since mercury concentrates through food webs. The knowledge lacking is how different harvesting practices change the amount of mercury in these food webs and whether impacts increase as streams get larger. Of the three basins I studied, the one with harvesting but little assisted regeneration (moderately impacted) had the highest mercury levels in water, leaves, and algae. From upstream to downstream the leaves and biofilm from the moderately impacted basin accumulated less mercury compared to the least harvested basin. Additionally, mercury concentrated less through the food web of this basin. The changes in the moderately impacted basin may be caused by sediments and other materials that transport mercury into the stream and increase water and food levels, but this high mercury was not being transferred to the other organisms in the food web. In conclusion, forest management had some effects on mercury at the base of food webs at a large scale, but patterns through space were inconsistent.

Abstract

Forests provide a multitude of ecological services and are one of Canada's most important natural resources that support a profitable industry, especially in New Brunswick. The activities associated with harvesting and forest management have documented ecological impacts such as the increased mobilization of mercury from the land to adjacent streams. Methylated mercury bioaccumulates and biomagnifies (concentrates) through food webs and in headwater streams forestry has been shown to change its accumulation. However, not much is known about the spatial trends of mercury accumulation and biomagnification through stream food webs and how different forest management practices affect these trends. To delineate these patterns, food webs were sampled across a spatial gradient from three basins experiencing different levels of forest management intensity. At a basin scale, methylmercury concentrations were greatest in filtered water, food sources, and one invertebrate taxa in a harvested but less intensively managed basin, likely due to increased inorganic sediments and dissolved organic carbon also observed. Biomagnification was lower in this same basin, possibly from inefficient trophic transfer of methylmercury from food sources. Longitudinally this basin also showed differences in fine particulate organic matter (FPOM) and coarse particulate organic matter (CPOM) mercury compared to the other basins, likely due to similar spatial patterns in organic matter. In conclusion, mercury dynamics in stream food webs were impacted by forestry primarily in water and basal food sources at a basin scale, but spatial patterns were inconsistent.

Acknowledgments

A thesis may seem like a one-person performance on stage (or Zoom) but really is orchestrated by countless people's support behind the curtain. I would like to thank NSERC and JD Irving for contributing funding that made the research possible. A tremendous thank you to Dr. Karen Kidd. I feel that I potentially added more grief to the process of the Masters, but you took it all in stride and with grace. I hope you're proud of the work I did and I'm very grateful to have you for a supervisor, you showed me what the world of research could be for a woman in science. My committee members Dr. Carl Mitchell and Dr. Erik Emilson, every young researcher needs guidance and I've had the privilege to have experts in their fields ensure the thesis is the best it can be. To Maitane Erdozain, you were a great role model and friend throughout the process and set the bar on what great research could look like. I appreciate the knowledge you shared with me and the guidance you gave along the way. Members of my field team: Sarah Hirtle, Zoe O'Malley, Scott Capell, and Ryan Power thanks for the memories and staying positive even when the days were long, and the weather was miserable. To the Michelle Gray lab at UNB for collecting the fish for my project, I never got to thank you in person. To everyone at the Mitchell lab at U of T Scarborough, thank you for making U of T feel like my second lab while I was running my MeHg analysis; thank you Planck Huang for being the master and all the work study students for helping me with analysis and making sure the data turned out perfect! To my lab mates in the Kidd lab: Victoria Restivo and Elise Millar (I'll be graduated with you soon!) we had lots of fun at conferences and I'll miss our networking tag team; Sally Ju, Graydon McKee, Ellie Weir, Celine Lajoie, and Jenni

Velichka, thanks for making me look forward to coming into lab and constantly reminding me why I love science! To Taylor Luu and Marcus Yurchuk, your hard work in the summer was imperative to this thesis and I loved the dynamic you had together in the lab. To my family who cheerleaded right till the finish, and especially my grandparents who always say they're proud of me for switching into a field I love and for following my passion. Huge kudos to Sergio Ráez Villanueva for motivating me to work hard everyday during the writing process and hosting thesis "bootcamps". I'm so grateful that I had someone to work with and listen to my ideas while keeping me on track, and take me out running. For anyone else that helped me along the way, and I haven't mentioned, know that I appreciate any help you contributed (scientific or otherwise, ex: Brian Hayden and Tim Jardine for answering my emails related to isotopes) I send you a huge thank you.

Table of Contents

1.0 Introduction.....	1
1.1 Forestry in Canada and impacts.....	1
1.2 Mercury background.....	4
1.3 Stable isotopes	8
1.5 Cumulative impacts	10
1.6 Objectives	12
2.0 Methods.....	13
2.1 Study site	13
2.2 Field sampling	17
2.3 Laboratory.....	21
2.4 Statistical analysis.....	26
3.0 Results.....	30
3.1 Patterns in mercury.....	30
3.1.1 Among-basin differences in mercury	30
3.1.2 Longitudinal trends in mercury within and among basins.....	33
3.2 Mercury biomagnification.....	36
3.2.1 Trophic transfer of mercury within basin	36
3.2.2 Trophic transfer of mercury among basins.....	37

3.2.3 Hg trophic transfer vs area.....	40
3.4 Autochthony and food web length	41
3.4.1 Among-basin differences in autochthony of consumers	41
3.4.2 Longitudinal trends in autochthony	42
3.4.3 Relationships between autochthony and mercury within taxa	44
3.4.4 Food web length and sculpin Hg	46
4.0 Discussion	48
4.1 Basin trends	48
4.2 Longitudinal trends in the minimal basin	51
4.3 Contrasting longitudinal trends in the intensive and extensive basins with that of the minimal basin.....	53
4.4 Biomagnification	56
4.5 Sculpin	57
4.6 Autochthony	58
4.7 Limitations/Challenges	59
4.8 Conclusions	60
References	62
5.0 Supplementary Information	73
5. 1 Isotope data	73

5.1.1 Carbon, nitrogen, and hydrogen data.....	73
5.1.2 Isotope biplots ($\delta^{15}\text{N}$ vs $\delta^{13}\text{C}$ and $\delta^{15}\text{N}$ vs $\delta^2\text{H}$).....	79
5.2 THg, MeHg and %MeHg in Sculpin.....	82
5.3 Mercury entering the food web by proxy with intercept.....	84
5.3.1 Intercept comparison of stream sites within basin.....	84
5.3.2 Intercept values vs drainage area.....	85
5.4 Autochthony	86

Table of Figures

Figure 1: Diagram of the theoretical framework used to interpret longitudinal trends of mercury concentrations and autochthony (y-axis) between streams and downstream waters (x-axis) to elucidate cumulative effects. This includes: a) the two main types of functional connectivity considered in this study, and b) the comparison of longitudinal trends between a reference (green line) and disturbed (blue line) fluvial system (Erdozain et al., 2021b). 12

Figure 2: Map of New Brunswick, Canada showing the position of the three basins and 6 stream sites within each (n=18 sites) (Erdozain et al. 2021b) 16

Figure 3: Boxplots showing the difference in MeHg concentrations in abiotic and biotic samples taken in 2018 from three basins in northern New Brunswick, Canada, with varying forest management intensity (6 sites/basin). A) Filtered water collected in September; B) Seston collected while filtering water; C-E) Basal food resources: coarse particulate organic matter (CPOM), fine particulate organic matter (FPOM) and biofilm; F-J) Macroinvertebrates: Pteronarcys, Glossosoma, Baetidae, Hydropsychidae, and Sweltsa; J) THg_{size} of female sculpin (Size Adj. F.; n=80). Letters denote significant differences among basins using Tukey's posthoc test or pairwise Wilcoxon test (p<0.05). Colours represent different basins: green is the minimal basin (NBR); light blue is the extensive basin (NBE); and dark blue is the intensive basin (NBI). 32

Figure 4: ANCOVA results for abiotic and biotic MeHg or THg (rows) versus log₁₀ of drainage area in the three basins (6 sites within each basin). The table shows p values from simple linear model (lm) ANOVAs testing the significance of drainage area and drainage area*basin for the following mixed model: linear model: log₁₀ (Hg)=log₁₀ (drainage area)*basin with interactions p<0.05 bolded. The column R² shows multiple R² values for simple linear regressions. The bar graph shows variance explained by log₁₀ (Hg)=log₁₀ (drainage area) for the simple lm; colours represent basin with green representing the minimal basin (NBR), light blue the extensive basin (NBE) and dark blue the intensive basin (NBI); length of the bar matches the R²; direction of bars represents the sign of the coefficient (+ or – relationship); asterisks denote p<0.05 and daggers represent values just over the level of significance (p=0.058-0.069). 34

Figure 5: Linear relationships between log₁₀ Hg (MeHg or THg) concentrations and log₁₀ drainage area in abiotic and biotic samples taken in 2018 from three basins in northern New Brunswick, Canada (6 sites/basin) with varying forest management intensities. A) filtered water collected in September. B) Seston from filtered water. C-E) Three different food sources: CPOM, FPOM, and biofilm. F-J) Five different taxa of macroinvertebrates: Pteronarcys, Glossosoma, Baetidae, Hydropsychidae, and Sweltsa. L) THg_{size} female sculpin (n=80). Colours represent different basins: light green is the minimal basin (NBR); light blue is the extensive basin (NBE); and dark blue is the intensive basin (NBI). p values on the graphs denote the significance of the relationship between drainage area and Hg (α=0.05). 35

Figure 6: Log₁₀ MeHg (invertebrates and food sources) or THg (fish) versus δ¹⁵N within 18 stream food webs from New Brunswick, Canada representing a gradient of harvesting intensity and increasing drainage area. A) is the minimal basin (NBR), B) is the extensive basin (NBE) and C) is the intensive basin (NBI), and streams are in order from upstream to downstream. The equation of the line and the coefficient of determination are shown in each panel (R²; p<0.001). Shading around the line represents standard error.37

Figure 7: Log₁₀ MeHg (invertebrates and food sources) or THg (fish) versus δ¹⁵N within three basins food webs from New Brunswick, Canada representing a gradient of harvesting intensity (R²; p<0.001). Data are pooled from stream sites (6/basin) to make the one regression line per basin. The equation of the line and coefficient of determination are shown in each panel. Shading around the slope represents standard error. The basins in order from minimally (NBR), extensively (NBE) and intensively managed (NBI).39

Figure 8: Trophic magnification (slope as calculated from the relationship between log₁₀Hg and δ¹⁵N) vs drainage area (km²). Data to generate the regression for each basin was generated from the slope values calculated from the five or six sites within three basins experiencing different levels of harvesting intensity in New Brunswick, Canada. The equation of the line and coefficient of determination are shown in each panel. The line and equation are colour coded by basin with the minimal (NBR) in green, extensive in light blue (NBE), and intensive in dark blue (NBI).40

Figure 9: Boxplots showing the proportion of algae in diets of benthic invertebrates and sculpin within three basins in New Brunswick that experience different levels of forest management. Taxa included are ones that had mean data from at least 3 sites in 2 different basins. Autochthony was calculated using a Bayesian 2-isotope mixing model (δ²H and δ¹³C) in MixSIAR and colours represent basin (green is the minimally managed (NBR), light blue is the extensively managed (NBE) and dark blue is the intensively managed basin (NBI)). Letters denote differences in mean proportion of autochthony with Tukey post hoc tests.42

Figure 10: Linear regressions between mean proportion of autochthony, calculated from Bayesian 2-isotope mixing model (δ²H and δ¹³C) in MixSIAR, and drainage area of 7 different benthic macroinvertebrate taxa and sculpin that had data from at least three sites for each of the three basins. Taxa are separated by FFG and given a unique shape and regression line, and basin is colour coded with the minimal basin in green (NBI), extensive basin in light blue (NBE), and intensive basin in dark blue (NBI).44

Figure 11: ANCOVA results for Hg in biota (rows) versus autochthony in the three basins (6 sites within each basin). The table shows p values from simple linear model (lm) ANCOVAs testing the significance of autochthony*basin for the following mixed model: linear model: log₁₀ (Hg)= autochthony*basin with interactions p<0.05 bolded. The column R² shows adjusted R² values for simple linear regressions. The bar graph shows variance explained by log₁₀ (Hg)= autochthony*basin for the simple lm; colours represent basin (green is the minimal basin (NBR), light blue is the extensive basin (NBE) and dark blue is the intensive basin (NBI)), length of the bar matches the R², direction of bars represents the sign of the coefficient (+ or – relationship), asterisks denote p<0.05.46

Figure 12: A) Boxplots showing FWL ($\delta^{15}\text{N}$ range (‰)) calculated from the difference between the average site $\delta^{15}\text{N}$ for sculpin and the average site $\delta^{15}\text{N}$ value for three primary producers) for three basins that experience different levels of forest management in northern New Brunswick, Canada. B) Linear regression between FWL and drainage area. Colours and shapes denote different basins, green and circles for the minimal basin (NBR), light blue and triangles for the extensive basin (NBE), and dark blue and squares for the intensive basin (NBI). The equation of the line and coefficient of determination are shown in the panel.....47

Figure 13: Linear regression comparing $\log_{10}\text{THg}$ to FWL ($\delta^{15}\text{N}$ range (‰)) calculated from the difference between average $\delta^{15}\text{N}$ for sculpin from the average $\delta^{15}\text{N}$ values from three primary consumers) for three basins that experience different levels of forest management in northern New Brunswick, Canada. Colours denote different basins (green for the minimal basin (NBR), light blue for the extensive basin (NBE), and dark blue for the intensive basin (NBI)). The equation of the line and coefficient of determination are shown in the panel.48

Figure 14: Isotope biplots for food webs of each six sites within the three basins showing either A-C) $\delta^{15}\text{N}$ vs $\delta^{13}\text{C}$ or D-F) $\delta^{15}\text{N}$ vs $\delta^2\text{H}$. Basins are ordered with the minimally managed basin first (NBR), followed by the extensively managed (NBE), then the intensively managed (NBI). Sites are ordered from most upstream from top left to right.82

Figure 15: Boxplots showing the differences in different metrics of Hg in slimy sculpin sampled in 2018 in three basins in northern New Brunswick, Canada with varying forest management intensity (5-6 sites/basin). A) shows the differences unadjusted female fish (n=80) among basins. B) shows the difference in MeHg in a subset of sculpin run for MeHg and THg (n= 19). C) shows the difference in %MeHg calculated by dividing MeHg by THg in the 19 fish. Colours represent different basins, green is the minimal basin (NBR), light blue is the extensive basin (NBE), and dark blue is the intensive basin (NBI).83

Figure 16: Longitudinal comparison of the intercepts generated from a trophic magnification regression within three basins experiencing different levels of forest management in northern New Brunswick, Canada. The data for each basin is pooled from six sites within each respective basin. Equation of the line and coefficient of determination are shown in each panel. The equation and line are coloured by basin with the minimal basin in green (NBR), extensive basin in light blue (NBE) and intensive basin in dark blue (NBI)85

Figure 17: Boxplots showing the dietary contribution of algae (in proportion) to the diets of 16 different benthic macro invertebrate taxa and sculpin separated into three FFG categories: shredders/scrapers, collector-gatherer/collector-filterer, and predator from 12 streams within 3 basins that experience different levels of forest management (northern New Brunswick, Canada). Algal contributions were calculated from a Bayesian 2-isotope mixing model ($\delta^2\text{H}$ and $\delta^{13}\text{C}$) with MixSIAR and the line in the middle of the box is the median algae diet proportion calculated from MixSIAR, the upper and lower hinges

match the upper and lower quartiles of the probability distribution around the diet proportion and the whiskers are 5th and 95th percentile of the probability distributions. Green boxes are the minimal basin (NBR), light blue the extensive basin (NBE) and dark blue the intensive basin (NBI).87

Table of Tables

Table 1: GPS coordinates (UTM 19T zone) and forest harvesting variables for all 18 stream sites from the three basins (minimally (NBR), extensively (NBE) and intensively (NBI) managed) in New Brunswick (Erdozain et al., 2021b).	17
Table 2: ANCOVA analysis to test for differences in the trophic transfer of Hg (MeHg or THg (fish only)) within three basins in northern New Brunswick, Canada in 2018. p values are included for the main effect terms, $\delta^{15}\text{N}$ and Site, as well as the interaction term $\delta^{15}\text{N}*\text{Site}$. Significant p values ($p<0.05$) are bolded. NBI6 was removed prior to analysis as no fish were collected at this site. The basins are the intensive (NBI), extensive (NBE) and minimal (NBR).	36
Table 3: P values of variables used in the ANCOVA analysis to test for differences in the trophic transfer of MeHg, or THg, within sites of similar drainage area and among the three basins in northern New Brunswick, Canada in 2018. p values are included for the main effects terms, $\delta^{15}\text{N}$ and Site, as well as the interaction term $\delta^{15}\text{N}*\text{Site}$. Significant p values ($p<0.05$) are bolded.	38
Table 4: P values from the linear regressions between autochthony in benthic macroinvertebrates/sculpin and drainage area from three basins that experience different levels of forest management. Data are from ANCOVAs testing the significance of drainage area in two different models, one within each basin with taxa as a covariate and one within each taxon and with basin as a main effect. $p<0.05$ values are bolded.	43
Table 5: Average isotopes values for biota and food sources for each stream site and number of replicates per sample	73
Table 6: Intercepts values for each site (n=18) in order of upstream to downstream separated by basin calculated from $\log_{10}\text{Hg}=\delta^{15}\text{N}+\text{Basin}$. Sites were located in northern New Brunswick, Canada in 2018.	84
Table 7: Output from the ANCOVA analysis to test for differences in intercept of MeHg, or THg, within three basins in northern New Brunswick, Canada in 2018 (6 sites/basin). p values for the terms are included for the main effect terms, $\delta^{15}\text{N}$ and Site calculated from $\log_{10}\text{Hg}=\delta^{15}\text{N}+\text{Site}$. Significant p values ($p<0.05$) are bolded.	84
Table 8: ANCOVA for Autochthony= $\log_{10}(\text{Drainage Area})*\text{Taxon}+ \log_{10}(\text{Drainage Area})+\text{Taxon}$ of data pooled from all taxa for basin. P values are included for the Drainage Area and the interaction between Drainage Area and Taxon, values bolded for $p<0.05$	86

List of all Abbreviations and Symbols

Abbreviation/Symbol	Definition
ANCOVA	Analysis of covariance
ANOVA	Analysis of variance
C	Carbon
CF-IRMS	Continuous flow-isotope ratio mass spectrometry
CPOM	Coarse particulate organic matter
ddH ₂ O	Double distilled water
DL	Detection limit
DOC	Dissolved organic carbon
DOM	Dissolved organic matter
DORM4	Fish protein certified reference material for trace metals
dw	Dry weight
FFG	Functional feeding group
FI	Fluorescence index
FPOM	Fine particulate organic matter
FWL	Food web length
GC-ICPMS	Gas chromatography-inductively couple plasma mass spectrometry
GFF	Glass-fibre filter
GIS	Geographic information system
H	Hydrogen
HCl	Hydrochloric acid
Hg	Mercury
Hg ⁰	Elemental mercury
Hg ²⁺	Oxidized, reactive form of mercury
HIX	Humification index
MeHg	Methylmercury
N	Nitrogen
NBE	Extensively managed basin
NBI	Intensively managed basin
NBR	Minimally managed basin
NSERC	Natural Sciences and Engineering Research Council
ppb	Parts per billion
PTFE	Polytetrafluoroethylene
RCC	River continuum concept
SD	Standard deviation
SFI	Sustainable Forestry Initiative
SI	Supplementary information
SUVA	Specific UV absorbance
THg	Total mercury
THg _{adj}	THg of size adjusted sculpin

THg _{size}	THg of size adjusted female sculpin
UNB	University of New Brunswick
VPDE	Vienna Pee Dee Belemenite
VSMOW	Vienna Standard Mean Ocean Water
ww	Wet weight
δ	Notation describing the ratio of heavy to light isotopes in a sample compared to a reference material
δ ¹³ C	Stable isotope of carbon
δ ¹⁵ N	Stable isotope of nitrogen
δ ² H	Stable isotope of hydrogen
‰	Per mill/ parts per thousand

1.0 Introduction

1.1 Forestry in Canada and impacts

Canada is the third most forested country in the world and contains approximately 10% of all forests (Natural Resources Canada et al., 2019; Wulder et al., 2004). This vast natural resource plays an important role in Canada's economy and contributes revenue through recreation and tourism, as well as all the jobs directly and indirectly related to forest harvesting (Natural Resources Canada et al., 2019; Wulder et al., 2004). Forestry in Canada is one of the largest sectors in the country's economy and contributed \$25.8 billion dollars in 2018 alone (Natural Resources Canada et al., 2019). In New Brunswick where this thesis work was done, forestry contributes the most to the economy even though the industry is smaller than in other provinces (Atlantic Provinces Economic Council, 2003). In 2018, forestry contributed 4.5% to New Brunswick's gross domestic product while in British Columbia it was around 2.9% (Natural Resources Canada et al., 2019). To ensure a continual supply of lumber while keeping a healthy ecosystem, informed stewardship is needed to prevent overharvesting, protect forests during climate change, and maintain biodiversity (Booth et al., 1993). To do this Canada has adopted stewardship frameworks by attaining third party certifications in sustainable forest management, which have stringent standards for certification. For instance, certification by the Sustainable Forestry Initiative (SFI) requires meeting water quality regulations, protecting riparian areas and wetlands, conducting habitat assessments, assessing the impacts from forest activities and having a mandate to invest in scientific research (Sustainable Forestry Initiative, 2015).

In addition to lumber, forests provide other essential ecological services such as producing oxygen, minimising erosion, providing habitat for countless biota and carbon sequestration, as well as water filtration among others (Krieger, 2001; Miura et al., 2015; Molnar & Kubiszewski, 2012). The brief mention of forest ecosystem services herein and the standards for certification by the SFI allude to the close connection forests have with aquatic ecosystems. To highlight the significance of this relationship, water contained in forested basins, and the filtration that occurs, supplies an estimated 60 million people in the USA with drinking water (Krieger, 2001). Forested landscapes are closely linked to aquatic ecosystems as matter and energy flows between them, especially in riparian areas because of the high surface area interface to adjacent forests (Nakano & Murakami, 2001). For instance, biota in small headwater streams that experience high levels of shade depend up to 90-99% on allochthonous carbon and nutrient inputs through litterfall that later become colonized by bacteria and become higher quality food for invertebrates, or on dissolved organic matter that comes from through-fall or drainage water (Cummins, 1979; Fisher & Likens, 1973). Fragmented litter that is not entirely used by upstream biota represents the largest organic input from headwater streams and is transported downstream providing a secondary, terrestrial source of energy (MacDonald & Coe, 2007; Richardson & Danehy, 2007).

Forestry can affect the physical conditions of aquatic systems in many ways. Reduced canopy cover allows for more light to enter a stream and for more warming of near-surface ground water, possibly raising water temperatures above those suitable for aquatic organisms (Erdozain et al., 2018). Less canopy can also change macroinvertebrate

community composition as more light entering the stream increases in-stream production and supports a higher number of grazing invertebrates, particularly shortly after harvesting in headwater streams (Nislow & Lowe, 2006). Autochthonous production is thought to be an important basal resource for consumers in larger streams (Vannote et al., 1980) but it is not known whether forestry influences the reliance of stream organisms on this food source. Alterations in water fluxes occur but depend on the topography and local climate of the basin, such as slope and mean annual precipitation (Neary, 2017). Forestry changes the permeability of soils that can lead to greater overland runoff and can result in changes in stream flow (Neary, 2017). Soil compaction from heavy machinery reduces soil porosity and limits its ability to absorb water (Moore & Wondzell, 2005). In heavy rainfalls the soil is saturated quickly and causes greater overland runoff into the neighbouring streams, increasing storm flow particularly in headwater streams (Adams & Froehlich, 1984). In areas with high snowfall, exposed areas caused by clear cut can accelerate snowmelt and result in higher water yield and daily flows during the spring (Beschta, 1978; Giles-Hansen et al., 2019; Neary, 2017). These hydrological changes can cause channel destabilization, aquatic habitat damage from streambed scouring (Giles-Hansen et al., 2019), and pose a safety hazard for people and infrastructure. Additionally, the shortened snowmelt period can cause water shortages in areas dependant on snowmelt water supply (Giles-Hansen et al., 2019).

Forest harvesting can also affect the chemical quality of headwater streams. Clear-cuts can increase the delivery of cations into adjacent streams and the implications of this exchange is nutrient leaching from the soil, potentially creating less fertile soil, as well as

altering the water chemistry (Erdozain et al., 2018; Kreutzweiser et al., 2008; Likens et al., 1969). In addition, forestry increases runoff of sediments and particulates into streams from road use/construction, poor slope integrity after the death of trees and decay of fine root networks, or other activities like preparation of planting sites using machines, particularly if they coincide during periods of high flow (Beschta, 1978; Erdozain et al., 2018; Neary, 2017). Greater inorganic sediments in streams can reduce leaf decomposition and use of this carbon source by benthic invertebrates, have physiological effects on invertebrates like damaging respiratory organs, and alter riffle microhabitats (Erdozain et al., 2018; Iwamoto et al., 1978). For fish, higher fine sediments in tributaries resulted in decreased survival for eggs and fry in chinook and coho salmon (Iwamoto et al., 1978). Decreases in population biomass have been noted for sculpin and steelhead salmon when siltation levels were elevated after forest harvesting and road construction (Iwamoto et al., 1978). In addition, terrestrial-borne particulates can be a vector for contaminants, such as pesticides (Campbell & Doeg, 1989) and mercury (Hg; Eklöf et al., 2014) into streams.

1.2 Mercury background

Hg is an environmental concern because it is a metal that has increased in the environment due to human activities and in its bioaccumulative, organic form methylmercury (MeHg) can accumulate to toxic levels. Global atmospheric Hg levels have increased from anthropogenic activities like burning of fossil fuels (coal) and mining (Pirrone et al., 2010). This gaseous Hg can travel long distances to remote ecosystems before being deposited back on the earth far from where it was originally emitted (Eckley

et al., 2018). In the atmosphere, inorganic Hg exists in a volatile form, Hg^0 . When oxidized, Hg^{2+} is more water soluble and is the dominant form that precipitates down to earth where it can complex with particulates and persist in the soil (NRC, 2000). When Hg^{2+} is deposited into aquatic, anoxic environments where sulphur and iron reducing bacteria are present, the Hg can become methylated and assimilated into food webs (NRC, 2000).

Disturbances on land from forestry affect the conversion of Hg into MeHg in terrestrial systems and the mobilization of Hg from soils into adjacent aquatic systems (Eckley et al., 2018). The changes in soil from site preparation and degradation of tree residues after harvest can increase leaching of nutrients and stimulate Hg methylation in soils and this MeHg enters streams and elevates aqueous MeHg levels several years after clearcutting (Porvari et al., 2003; Skyllberg et al., 2009). Increased production of MeHg can also occur from soil compaction caused by machines that result in soils becoming saturated with water, creating anoxic environments where bacteria convert Hg into MeHg (Bishop et al., 2009). The removal of vegetation during forest harvesting increases surface run-off and in turn the mobilization of Hg from soils into streams (Eklöf et al., 2016). In run-off, Hg is found bound to particulates and dissolved organic carbon (DOC; Eckley et al., 2018). Particulate-bound Hg is a main transporter in large watersheds, such as the Saint Lawrence River Basin, and enters rivers after high flow events that cause soil erosion (Grigal, 2002). DOC is also the predominant transporter of total mercury (THg) and MeHg because they bind to thiols and sulfides present in DOC (Lavoie et al., 2019). In many studies there is a positive relationship between DOC concentrations and aqueous

Hg in freshwater systems (Grigal 2002; Driscoll et al., 1995; Riscassi and Scanlon, 2011; Watras et al., 1998).

Bioaccumulation occurs when the excretion of MeHg in organisms is less than its assimilation into tissues. Several factors can change bioaccumulation such as the concentration of MeHg in the diet and water quality altering bioavailability of MeHg for uptake. Diet affects bioaccumulation since it is the main contributor of MeHg in aquatic biota (Hall et al., 1997). Allochthonous food sources tend to have lower MeHg levels than autochthonous sources and this is reflected in the lower MeHg in shredders (allochthonous specialists) than scrapers (autochthonous specialists; Willacker et al., 2019). Bioavailability of MeHg is affected by water quality parameters (DOC, pH, nutrient inputs) and the interaction with each other (Chaves-Ulloa et al., 2017; Tsui and Finlay, 2011). Though DOC is a transporter of MeHg to aquatic systems, higher levels of DOC can also reduce accumulation of MeHg because it has a strong binding affinity to MeHg under certain conditions. An example is in low productivity, high latitude lakes along a DOC gradient which showed a significant reduction in MeHg accumulation in biofilms and primary consumers when MeHg to DOC ratios were low (Chételat et al., 2018). Acidic conditions affect bioaccumulation by weakening the bond between MeHg and DOC, leading to increased uptake of MeHg into primary producers (Watras et al., 1998), or reducing organism growth, leading to greater MeHg in higher-trophic level organisms (Jardine et al., 2013). Additionally, greater nutrient availability can cause greater in-stream primary productivity and this can cause biodilution in the primary producers by distributing the same MeHg across more cells (Walters et al., 2015), or

faster growth of consumers leading to less MeHg per gram of tissue (Ward et al., 2010).

However, it is not known if the increased nutrient inputs from forestry have this effect.

Mercury also biomagnifies in food webs, meaning the concentration of MeHg amplifies in higher-trophic-level species compared to the lower trophic levels. Top predators that sit higher in a food web (greater food web length determined with $\delta^{15}\text{N}$ values) are at risk of concentrating greater levels of Hg compared to the same top predator supported by a shorter food web (Cabana et al., 1994). Forestry has been shown to change decrease food chain length in terrestrial systems (Woodcock et al., 2013), making it important to investigate whether aquatic food web length changes and if it affects Hg biomagnification. While the exact mechanisms influencing trophic transfer are not known, potential factors are biodilution or trophic transfer efficiency (Lavoie et al., 2013). Biodilution may affect biomagnification if the lower concentrations of MeHg in primary producers translates into lower relative uptake of MeHg by consumers. More biomass of high-quality food sources can also stimulate higher growth rates in consumers, causing biodilution of Hg at higher trophic levels (Poste et al., 2015). In some cases, higher MeHg in primary producers does not always result in increases in higher-trophic consumers, potentially because of some limitation on MeHg uptake kinetics (DeForest et al., 2007). It is important to consider biomagnification of Hg can vary across systems depending on chemical and geographic factors of the system that can interact and change how MeHg biomagnifies (Clayden et al., 2014). Few studies have examined the impact of forestry on Hg biomagnification and bioaccumulation in stream food webs despite the

considerable evidence that this resource extraction alters pH, carbon sources, nutrients, and DOC in nearby streams.

1.3 Stable isotopes

Elements can have stable variations (isotopes) that exist in much lower abundances in nature and include extra neutrons in the nucleus, making them heavier. These heavier isotopes have different reaction rates and bond strengths that result in traceable, different amounts of heavier than lighter isotopes in biota and thus can be used in aquatic ecology to delineate trophic position (nitrogen) and food sources (carbon or hydrogen) (Ben-David & Flaherty, 2012). The notation for carbon ($\delta^{13}\text{C}$), hydrogen ($\delta^2\text{H}$), and nitrogen ($\delta^{15}\text{N}$) is used to describe the ratio of heavy (extra neutron variation) to light (most common) isotopes in samples to that of a reference material. Trophic enrichment is the difference in stable isotope ratios between an organism and its diet (Caut et al., 2009; Fry, 2006). Organisms become more “enriched” if they incorporate more heavy isotopes and “depleted” if they fractionate against the heavier isotopes and incorporate the lighter ones instead. The differences in trophic enrichments of $\delta^{13}\text{C}$, $\delta^2\text{H}$ and $\delta^{15}\text{N}$ isotopes are used to assess reliance on autochthonous and allochthonous food sources and trophic position, respectively, in a food web.

Because the trophic enrichment of $\delta^{13}\text{C}$ is usually low in freshwater systems, it can be used to trace primary producers in a food web since consumers typically reflect the same signature (France & Peters, 1997; Post, 2002). Delineating food sources can be done because $\delta^{13}\text{C}$ values in terrestrial sources have values consistently around -28‰ while

aquatic sources, like algae, are typically more depleted (more negative; Finlay, 2004).

However, the stream biofilms collected and used to represent autochthonous sources often do not give a reliable source separation for algae. The $\delta^{13}\text{C}$ of algae varies considerably within a stream because biofilms are a matrix of algae, bacteria and fungi, and because CO_2 available for photosynthesis is more variable in streams than air (Finlay, 2004; Jardine et al., 2014a). In this case $\delta^2\text{H}$ isotopes may give better separation between allochthonous and autochthonous sources supporting the food web. This is because aquatic plants fractionate against the heavier isotope, becoming very depleted in $\delta^2\text{H}$ while terrestrial plants become more enriched due to the loss of lighter H isotopes during the evaporation of water from leaves (Doucett et al., 2007). The trophic enrichment for $\delta^2\text{H}$ is considered negligible (Doucett et al., 2007; Solomon et al., 2009), or indiscernible for $\delta^{13}\text{C}$ if lipid correction (adjusting isotope values in fatty tissues because lipids have depleted $\delta^{13}\text{C}$ values compared to bulk tissue) is needed (Jardine et al., 2009). $\delta^{15}\text{N}$ is used to delineate trophic position because there is typically a clear enrichment in $\delta^{15}\text{N}$ from basal food sources to primary consumers up to top predators; the most commonly reported trophic enrichment factor is 3.4‰ (Fry, 2006; Post, 2002). However, the trophic enrichment of $\delta^{15}\text{N}$ can differ in food webs depending on the diet of the consumer, among other factors, and can range between 1.4-3.4‰ if invertebrates, plant matter, or vertebrates are consumed (McCutchan et al., 2003).

Stable isotope analysis can be used to detect effects of forestry on stream food webs through changes in macroinvertebrate and fish reliance on autochthonous or allochthonous primary producers or their relative trophic levels. For example, forestry-

induced changes in forest cover alter crayfish $\delta^{13}\text{C}$ signatures away from terrestrial matter due to less CPOM entering streams (England & Rosemond, 2004). Additionally, models estimating food source using $\delta^{13}\text{C}$ found that invertebrates had a higher reliance on terrestrial material in intensively managed systems because roads were contributing to higher water-borne terrestrial inputs (Erdozain et al., 2019).

1.5 Cumulative impacts

Streams and rivers are a large, connected system with the downstream continually receiving inputs from upstream sources and this makes them inherently cumulative (Fritz et al., 2018). The basic model that outlines the relationship between upstream and downstream is the river continuum concept (RCC) and it describes spatial hierarchy of streams by the change in energy dynamics (respiratory vs. productive), invertebrate communities, and nutrient availability (Vannote et al., 1980). These longitudinal patterns in reference forested basins can be either sink (materials/energy decrease downstream) or source (increase downstream) functions. For example, nutrient concentrations in headwaters typically decrease downstream because of biological uptake (sink) while sediments increase (source) from multiple stream inputs (Leibowitz et al., 2018). Because stream networks are so closely linked, disturbances from forestry can also be propagated spatially and the effects can be dissipative or cumulative compared to the source or sink function in a reference basin. Drainage area is used as a proxy for stream size in analysis of longitudinal trends because there is a positive relationship between drainage and stream size (Downing, 2012). The interactions between drainage area and basin are used to infer effects of forestry (Figure 1). In a study done at the same time as this thesis,

longitudinal impacts from forestry included cumulative effects on inorganic sediments and dissipative effects on organic sediments, water temperature, phosphorous, and nitrogen (Erdozain et al., 2021b). Research from my study will link these downstream impacts to the spatial dynamics of Hg in biota and address the knowledge gaps about the impacts of forestry on Hg bioaccumulation, biomagnification and food web structure at larger spatial scales. One similar, but smaller-scale study using paired catchments, found aqueous and caddisfly (Hydropsychidae) MeHg was greater at up and midstream sites in harvested catchments but did not accumulate at downstream sites; however, a cumulative effect was seen in MeHg biomagnification factors in Hydropsychids (Charbonneau, 2018).

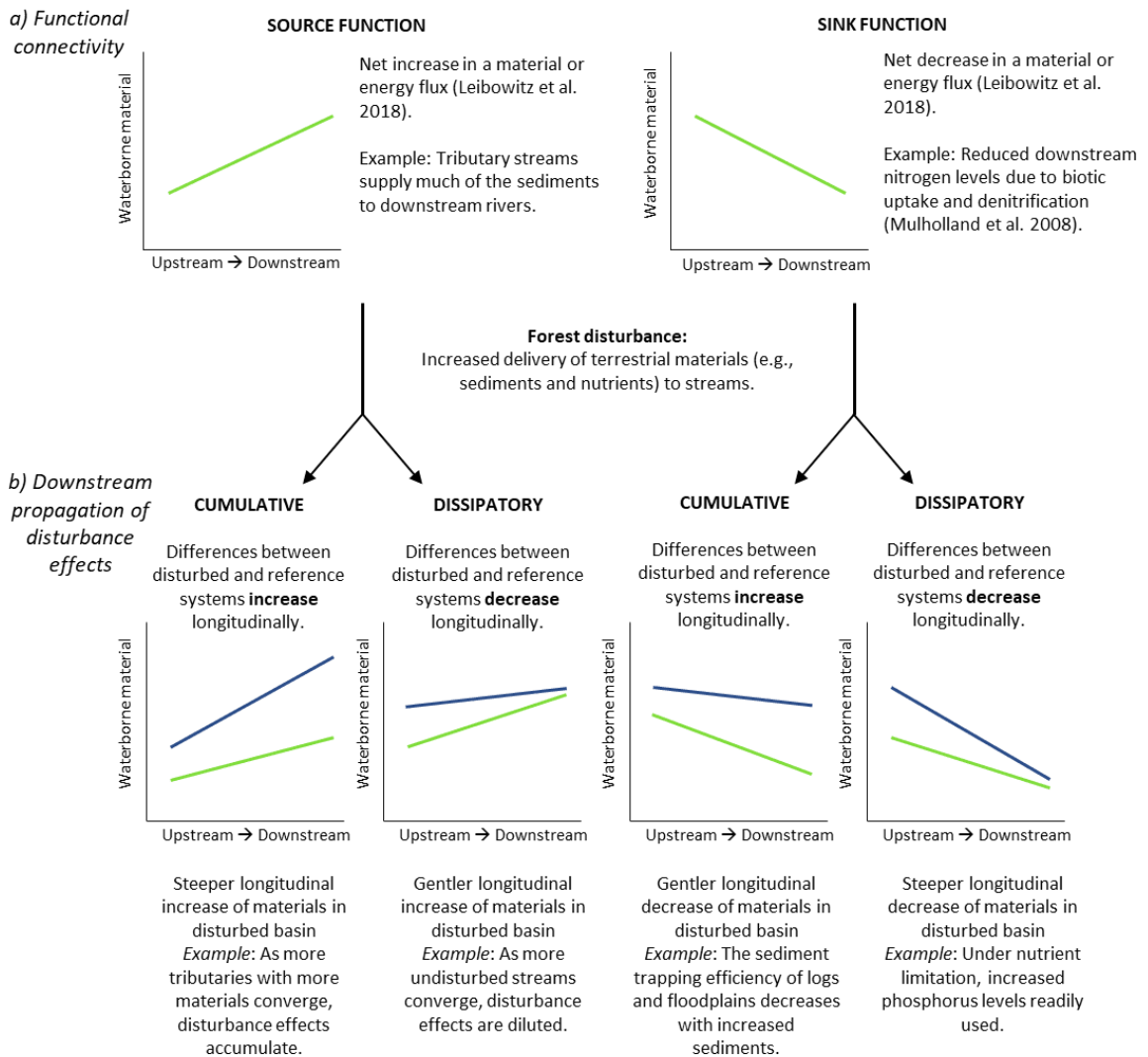


Figure 1: Diagram of the theoretical framework used to interpret longitudinal trends of mercury concentrations and autochthony (y-axis) between streams and downstream waters (x-axis) to elucidate cumulative effects. This includes: a) the two main types of functional connectivity considered in this study, and b) the comparison of longitudinal trends between a reference (green line) and disturbed (blue line) fluvial system (Erdozain et al., 2021b).

1.6 Objectives

This thesis addresses knowledge gaps about how forestry affects the bioaccumulation and biomagnification of MeHg in stream food webs and their structure,

and whether there are cumulative or dissipative impacts at larger downstream sites. Here I use three river basins in New Brunswick with different forest management (see below) and by sampling sites within each basin along a longitudinal gradient to address if : 1) MeHg in abiotic and biotic samples, MeHg biomagnification, autochthony in macroinvertebrates and fish, and food web length changes among three basins in New Brunswick with different forest management intensities; and 2) longitudinal trends in MeHg in abiotic and biotic samples, MeHg biomagnification, autochthony in macroinvertebrates and fish, and food web length are affected by forest harvesting.

2.0 Methods

2.1 Study site

Samples were collected from three basins with different forest management in northern New Brunswick, Canada, management determined by total disturbance in the basin, which is the sum % of all harvesting methods (partial and clear cut) + regeneration between 2009-2018 (Figure 2). The region that was most intensively managed (NBI) is within the Restigouche River watershed and called the Black Brook forestry district; this district is owned, managed and harvested by J.D. Irving, Ltd. Management includes, thinning, assisted forest regeneration, and implementing various stand improvement techniques following guidelines set by the SFI. It is a part of the Central Uplands ecoregion within the Madawaska ecodistrict in northwestern New Brunswick. This region's geology is characterized by non-calcareous Ordovician-Devonian metasedimentary rocks and the dominant vegetation is mixed hardwood and softwood forest, with a high proportion of cultivated spruce within the intensive basin since it is a

preferred tree species in the forestry industry. Approximately 475 to 525 mm of precipitation falls between late spring and early fall and between 1400-1600 degree days are above 5°C annually. The extensively managed basin (NBE) is within the Quisibis River watershed close to the Restigouche River. Extensively managed means that there is less intervention after cutting as tree stands are left to naturally regenerate, while in the intensive basin there is assisted regeneration. The extensively managed basin is within the same ecoregion as the intensively managed basin and has similar geology, vegetation and local climate. The minimally managed basin (NBR) is within the Charlo River watershed and has less harvesting compared to the extensive and intensive basins as it is drinking water source for the local communities. Harvesting trees in the minimal basin must have a 30 m buffer from streambanks if harvesting is less than 1 km from a surface water supply intake and at least a 15 m buffer if more than a kilometre away. Trees can only be felled from November 1st to March 31st with no more than 30% of tree stems being removed every five years. Clearcut of up to 25 hectares is allowed beyond 75 m from streams and clearcut blocks must be separated by an unharvested, 100 m buffer unless near a property parcel, and left to regenerate for 10 years (Government of New Brunswick, n.d.). The minimally managed basin is located in the northeastern part of New Brunswick and is part of the Northern Uplands ecoregion and touches three ecodistricts (Upsalquitch, Tetagouche and Tijigog). The geology of this region is primarily Silurian-Devonian calcareous rocks with volcanic igneous rock intrusions, and the dominant vegetation is also mixed hardwood and softwood forest. The local climate is similar to the extensive and intensive basin, but the region has marginally less precipitation and cooler

temperatures. It was not possible to locate a large enough reference region closer to the other two basins.

Within each basin 6 sites along the stream were selected that capture a spatial gradient from upstream to downstream. Due to limited access, not all stream sites flow into each other (Figure 2). Within the minimal basin one of the flow paths is sites 6, 5, 4, and 1, another flow path is sites 2, 4 and 1, and lastly site 3 flows into site 1. In the extensive basin, sites 3 and 2 are along the same flow path and sites 6, 5 and 4 are on a separate flow path. In the intensive basin sites 3 and 2 are along the same flow path and sites 6, 5, and 4 are along a separate flow path. All sites numbered with 1 (e.g., NBI1, NBE1, and NBR1) were the largest of the six stream sites and received water from all 5 of the upstream sites in their respective basin. The area of the catchment of each stream site was determined using the 20-m provincial digital elevation model. Forest harvesting variables for each site were determined from GIS layers provided by the province (extensive and minimal basin) or J.D. Irving (intensive basin). Harvest metrics were summarized into cumulative area harvested within the last 5 or 10 years for three different methods of harvesting which included clearcut (>80% tree removal), partial harvest (35-50% tree removal), and total disturbance (% of site catchment harvested by all methods plus regeneration). The metrics shown in Table 1 includes % clearcut within the last 10 years, and total disturbance since % clearcut within 10 years was significantly correlated with % clearcut within 5 years and total disturbance was correlated with partial harvest within 5 and 10 years and total disturbance within 5 years (Erdozain et al., 2021b). Road

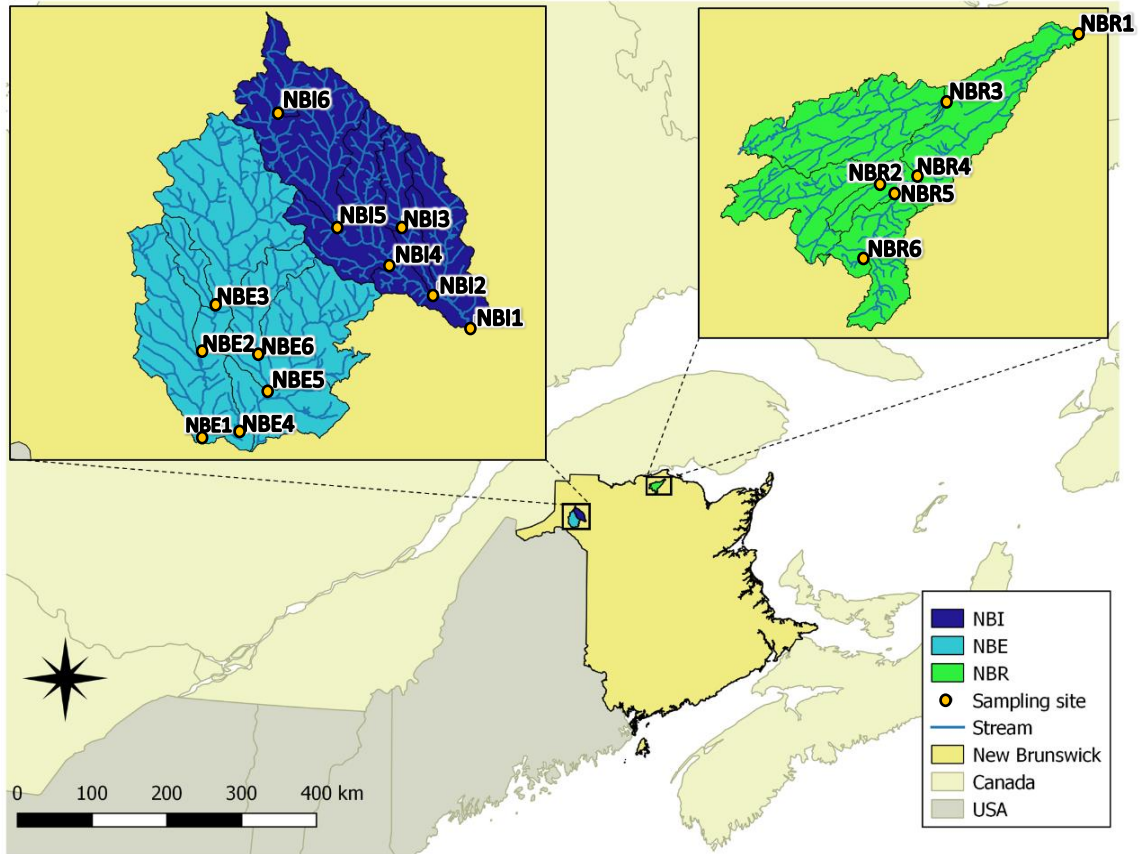


Figure 2: Map of New Brunswick, Canada showing the position of the three basins and 6 stream sites within each (n=18 sites) (Erdozain et al. 2021b)

and crossing densities were calculated by dividing the length of the roads by the area of the study catchment and by dividing the number of road crossings by stream length, respectively, with data that came from road shapefiles provided by GeoNB. Comparing harvesting variables across the basins, the intensive basin had the greatest amount of total disturbance, road crossing density and the smallest forest height and % clearcut compared to the other basins, while the extensive basin had the greatest road density. Measures of total disturbance, road crossing density, forest height, and clearcut did not differ between

the extensive and minimal basins but the mean value for clearcut and total disturbance was higher in the extensive basin (Erdozain et al., 2021b).

Table 1: GPS coordinates (UTM 19T zone) and forest harvesting variables for all 18 stream sites from the three basins (minimally (NBR), extensively (NBE) and intensively (NBI) managed) in New Brunswick (Erdozain et al., 2021b).

Stream -site	X	Y	Catchment Area (km ²)	Total disturbance (% , 10 y)	Clearcut (% , 10 y)	Crossing density (#/km)	Road density (m/ha)
NBR1	47.94969	-66.40167	167.47	7.35	4.07	0.35	19.91
NBR2	47.86021	-66.57194	33.19	5.54	4.08	0.36	19.47
NBR3	47.91020	-66.51417	51.05	11.46	3.63	0.37	21.35
NBR4	47.86387	-66.54222	73.24	6.82	5.79	0.36	19.99
NBR5	47.85406	-66.55833	28.52	7.76	6.82	0.38	20.37
NBR6	47.81680	-66.58472	12.53	7.25	7.24	0.17	17.02
NBE1	47.36078	-68.07194	233.52	14.14	5.42	0.45	24.10
NBE2	47.41159	-68.07556	85.34	17.76	4.36	0.56	26.88
NBE3	47.43935	-68.06444	9.19	0.00	0.00	0.08	35.82
NBE4	47.36435	-68.04194	93.16	13.77	7.67	0.34	21.65
NBE5	47.39061	-68.01389	67.98	16.58	8.59	0.31	23.06
NBE6	47.41004	-68.02500	18.10	20.75	10.13	0.48	27.29
NBI1	47.43016	-67.83639	163.03	24.28	2.56	0.78	24.27
NBI2	47.45257	-67.87028	20.61	22.33	2.03	0.47	21.33
NBI3	47.48940	-67.90139	11.80	21.66	2.61	0.61	19.08
NBI4	47.46766	-67.90750	102.54	22.48	1.33	0.92	24.85
NBI5	47.49055	-67.95722	62.01	21.41	1.07	0.83	23.34
NBI6	47.55868	-68.00972	0.66	6.39	0.00	0.00	13.02

2.2 Field sampling

2.2.1 Water sampling and preservation

Water samples were collected from all sites in both September and October (n=1-3/site). A Geotech peristaltic pump and acid-washed polytetrafluoroethylene (PTFE) tubing were used to collect subsurface water from the middle of the stream in 2018. Before collecting the sample, the tubing was flushed with stream water. Next a 47 mm

single stage Sallivex filter unit that had been acid washed overnight (10-20% HCl) and then rinsed with distilled water was loaded with a pre-ashed and preweighed 1.2 μm VWR® glass-fibre filter (GFF) and attached to the pump. To fill the sterile graduated 125 mL square-bottom Nalgene bottles, a "Clean Hands/Dirty Hands" procedure was used with powder-free nitrile gloves. "Dirty Hands" handled the tubing and filtration unit and opened the outer bag that contained the sample bottle. "Clean Hands" opened the inner bag with the sample bottle and held the bottle while and it was filled and examined the sample for particles. If the water sample contained particles because the filter ripped, the sample was discarded and the whole procedure was repeated. If the sample was clear it was sealed in the inner bag by "Clean Hands", then sealed in the second, outer bag by "Dirty Hands" and placed in the dark until it could be preserved at the end of the day. Three replicates of filtrate were taken at one randomly chosen site for each basin. A field blank consisting of a bottle prefilled with distilled water was opened at the first site on each day samples were taken and then processed similarly. Water samples were preserved using a similar "Clean Hands/Dirty Hands" procedure described above and approximately 0.5% of sample volume of 37% OmniTrace HCl was added to each sample. Preserved water samples were kept cool and dark until analysis.

2.2.2 Filters for seston

After filtered water was collected, water was run through the same filter unit until water flow slowed considerably as the filter clogged with seston or until 15 L had been filtered. The volume of water filtered was recorded. The filter was then folded using precleaned tweezers and the "Clean Hands/Dirty Hands" procedure, put into a petri dish

and kept with the water sample until it was frozen at the end of the day (n=1-3/site).

Seston mass was calculated by subtracting the freeze dw mass of unused filters from mass of the filters with seston after they had been freeze dried.

2.2.3 Food sources

Three samples of each food source were taken at each site with one replicate from each of the upper, middle, and lower part of the reach. To collect biofilm, 3-4 rocks were randomly selected and the tops scraped with a toothbrush. The slurry was rinsed off the toothbrush with stream water into Whirl-paks®. A turkey baster was used to collect fine particulate organic matter (FPOM) from depositional areas of the stream and stored in Whirl-paks®. Decaying leaves — typically sugar maple or alder— that were snagged on objects (i.e. branches, logs, boulders) within the stream were collected as coarse particulate organic matter (CPOM) and stored in Whirl-paks®. All the samples were stored in a cooler until they could be frozen in a -20°C freezer at the end of the day (n=3/site).

2.2.4 Benthic macroinvertebrates

In September 2018, aquatic invertebrates were collected by electroshocking riffles along the study reach and collecting the stunned inverts downstream with drift nets, as well as by hand for taxa that lived in structures adhered to rocks or found in submerged leaf litter. Each taxon was sorted to the lowest taxonomic level possible (usually family) and placed into Whirl-paks® with stream water. The Whirl-paks® were kept in a cooler

until they could be frozen at -20°C at the end of the day. Additional sampling was done in October 2018 to collect extra biomass for some taxa.

The ten different taxa targeted represented one of five functional groups: scrapers (*Glossosoma* and *Heptageniidae*), shredders (*Pteronarcys* and *Tipula*), collector gatherers (*Baetidae*, *Ephemerella/Paraleptophlebia*), collector filterers (*Hydropsychidae* and *Philopodidae*), and predators (*Sweltsa* and *Perlodidae/Perlidae*). Five of the genera – *Heptageniidae*, *Tipulidae*, *Ephemerella* and *Paraleptophlebia*, *Philopodidae* – were only used for stable isotope analyses to determine food web structure, and the other five were used for both MeHg and stable isotope analyses (n=6-10/taxon/site).

2.2.5 Sculpin collection and preparation

Sculpin were collected by electroshocking in October 2018 and then lethally sampled using procedures approved by the UNB Animal Care Committee (Animal Use Protocol 18029). Approximately 20 male and 20 female fish were collected from each site (except none were found in NBI6). Fish were processed at UNB and then shipped to McMaster. They were received frozen with heads and internal organs already removed and of those fish 144 were selected for analysis. In the lab, partially thawed sculpin were filleted. Skinless fillets for stable isotope analyses were put into acid washed 7 mL vials that had been pre-weighed and wet weight of the fillet recorded (g). The remaining whole bodies were placed in acid washed 20 mL vials for Hg analyses. On average, 10 fish per site were used for analysis, aiming for equal numbers of males and females within a similar size range at all sites.

2.3 Laboratory

2.3.1 Invertebrate sorting

All invertebrates were sorted to genus except *Baetidae*, which was sorted to family to have enough mass for isotope and MeHg analyses. For sorting, small numbers of invertebrates were thawed in the fridge, and then identified and separated on precleaned petri dishes in ddH₂O using precleaned tweezers. After the genus/family was determined, they were pooled in scintillation vials and then frozen (n=1-317/taxon) until analyzed. Samples were sorted to genus or family using morphological features (Merritt et al., 2008).

2.3.2 CPOM processing

Leaves collected from each site were rinsed with ddH₂O water and any invertebrates were removed. Three replicates of approximately 4-8 leaves were taken at each site at the upper, lower and middle section of the reach and frozen before being processed. Before freeze drying, each replicate was stored in acid washed scintillation vials and after drying, ground with an acid washed glass rod. Nitrile gloves were used to handle the samples to prevent contamination.

2.3.3 FPOM and biofilm processing

FPOM samples were thawed and then filtered through a precleaned 1 mm sieve into an acid washed, glass petridish to remove larger particles. The samples were then examined under a dissecting microscope for invertebrates that were removed using precleaned tweezers before the sample was processed further. The sample was then

transferred into a sterile falcon tube using an acid washed, borosilicate pipette. When the falcon tube was full, it was centrifuged at 7000 gs for 8 minutes to separate out the FPOM, and the water was removed and discarded. Biofilm samples were processed similarly to FPOM with the exception that they were not filtered through a 1 mm sieve. FPOM and biofilm samples were frozen until further processed.

2.3.4 Freeze drying and homogenizing

All samples were freeze dried before being homogenized and subsampled for stable isotope, MeHg, or THg analysis. CPOM, biofilm, FPOM, seston filters, fish fillets, and invertebrate samples were freeze dried for 48 hours, while fish carcasses were freeze dried for 96 hours. All samples, except fish carcasses, were pulverized with an acid cleaned glass rod in the scintillation vials until they were a fine powder. Fish carcasses were homogenized using a precleaned Retsch Mixer Mill MM400 ball mill for 2 minutes at a frequency of 30 hertz.

2.3.5 MeHg analysis

MeHg analyses were completed at the University of Toronto Scarborough using isotope dilution-gas chromatography-inductively couple plasma mass spectrometry (GC-ICPMS) (Hintelmann & Evans, 1997). For water, ~39 mL was used in a distillation vessel but because of the low amount of MeHg in that volume, a second distillation of the same sample was done and both extracts were combined to improve MeHg detection. Increasing the total volume of water analyzed per sample to ~80 mL. For seston, whole filters from the field were used in the distillation after they were freeze dried and

reweighed (~1.5-20 mg dw of seston). For CPOM and FPOM samples, approximately 200 mg of dry mass was used. Approximately 30-50 mg of dry biofilm was used, however some replicates did not have enough mass and had to be combined with other replicates from the same stream to reach a target mass for reliable results. For invertebrate samples, the target sample mass was between 10-50 mg dw, however not all samples reached these targets. Low mass samples were still run, but if Me¹⁹⁹Hg recovery was low the values were not included since the calculated Me²⁰²Hg values would not be reliable. Approximately 10-15 mg dw of whole-body fish sample was used for MeHg analysis that also had been measured for THg (n=19). The subset of fish was ~50/50 males and females and from a range of sizes. Before analysis, water, seston and food sources underwent steam distillation and fish and invertebrate samples underwent KOH extraction in methanol to separate MeHg from the sample matrices (Horvat, Bloom, et al., 1993; Horvat, Liang, et al., 1993). A known amount of enriched Me¹⁹⁹Hg was added to each distillation extraction vessel to account for analytical variability via the isotope dilution approach. The distillates or extracts were then buffered and ethylated with sodium tetraethylborate in bubblers, where the volatile ethylated MeHg was trapped in Tenax-filled glass traps. The traps were then thermally desorbed along a stream of argon gas and species of Hg were separated by gas chromatography and Hg isotopes detected by ICPMS. For quality control, certified reference materials, duplicates and blanks were run with every set of samples. Recovery (%) of MeHg spikes or standard reference material (mean ± standard deviation) was 97 ± 6% (n = 5) for water, 106 ± 6% (n = 6) for seston, 109 ± 15% (n = 12) for CPOM/FPOM, 98 ± 3% (n = 4) for biofilm, and 83 ± 4% (n = 10)

invertebrates/fish. The differences in duplicates was 7.64% (n = 1 pair) for water, $4 \pm 3\%$ (n = 8 pairs) for CPOM/FPOM, $18 \pm 29\%$ (n = 5 pairs) for biofilm, and $5 \pm 3\%$ (n = 15 pairs) for invertebrates/fish. The reference materials used were marine sediment (IAEA158) for food sources, and dogfish muscle (DORM3) for invertebrates and fish. Samples that did not have a reference material (water and seston) used a blank spike, or in the case reference material ran out (one run of biofilm and one of FPOM) a matrix spike was added which received 30-200 μ L 1ppb MeHg stock. There was only one water replicate since water samples were double distilled leaving not enough sample for a double distilled duplicate. Seston also had no duplicates since the whole filters were used at a time. The method detection limits calculated as 3*standard deviation of blanks were 0.006 ng/L for water, 0.021 ng/g for seston, 0.022 ng/g for CPOM/FPOM, 0.11 ng/g for biofilm, and 4.1 ng/g for invertebrates/fish.

2.3.6 THg analysis

THg (ng/g dw) in whole-body slimy sculpin was analyzed using a Milestone Tri-Cell Direct Mercury Analyzer-80® (DMA-80) following the method outlined in the US Environmental Protection Agency (US EPA) method 7473 and with DORM-4 Fish Protein as the reference material (US EPA, 2007; NRCC, 2012). In this analysis mercury is quantified using thermal decomposition, gold amalgamation and atomic absorption spectrophotometry. For QA/QC, method blanks, two liquid standards with known Hg concentrations (3 ng, 0.3 ng), certified reference material, and a duplicate sample were run with each 10-15 samples ($\pm 20\%$ variability was deemed acceptable for standards or reference materials). A liquid standard stability check (10 ng MeHg) was also run at the

start and end of each day. All Hg data for solid samples are expressed on a dry weight (dw) basis unless otherwise noted. Recovery (%) of reference material (mean \pm standard deviation) was $108 \pm 8\%$ (n=21) and differences in duplicates was $1.2 \pm 1.2\%$ (n=14 pairs).

2.3.7 Isotope analysis

Isotopes are expressed in delta (δ) notation, which is the ratio between the heavy and light isotopes of an atom relative to a standard in parts per thousand (‰). The equation for this calculation is:

$$\delta X = \left(\frac{R_{\text{sample}}}{R_{\text{standard}}} - 1 \right) * 1000 ,$$

Where X is ^2H , ^{13}C , or ^{15}N and R is the respective $^2\text{H}/^1\text{H}$, $^{13}\text{C}/^{12}\text{C}$, $^{15}\text{N}/^{14}\text{N}$ ratio.

After samples have been processed, freeze-dried, and homogenized, they were weighed (1.00-1.20 mg of animal tissue and 3.00-3.20 mg of plant tissue) into tin capsules for C/N analysis and weighed (0.20-0.25 mg) into silver capsules for H analysis. They were then sent to the Stable Isotope in Nature Laboratory (SINLab, New Brunswick, Canada) where stable isotope ratios were measured using continuous flow-isotope ratio mass spectrometry (CF-IRMS). Samples are analyzed for both $\delta^{13}\text{C}$ and $\delta^{15}\text{N}$ with a Costech 4010 elemental analyzer coupled to Delta^{Plus} XP IRMS with Conflo III continuous flow. The analysis for $\delta^2\text{H}$ is done with a Thermo-Finnigan High-Temperature Conversion Elemental Analyzer and Delta V Plus IRMS with Conflo IV.

The stable isotope measurements were normalized to international standards, which is Vienna Pee Dee Belemnite (VPDE) for carbon and atmospheric air for nitrogen. Measurements of internal standards indicate a precision of $\pm 0.06\text{‰}$ (SD) in the C isotope ratios and $\pm 0.21\text{‰}$ (SD) in the N isotope ratios, on average.

The H results are normalized to the international standard Vienna Standard Mean Ocean Water (VSMOW). Non-exchangeable $\delta^2\text{H}$ in samples is determined with the comparative equilibrium approach, which has the samples and two keratin standards exposed to the local atmosphere for 72 hours before analysis to exchange H atoms between ambient water and tissue (Wassenaar and Hobson, 2003). Measurements of internal standards indicated that the precision of the H isotope ratios was $\pm 3.4\text{‰}$ (SD), on average.

2.4 Statistical analysis

Food web length (FWL) was calculated as the difference between average of the three primary consumers that had the lowest $\delta^{15}\text{N}$ and individual sculpin $\delta^{15}\text{N}$ from that site.

Mixing models were used to calculate the proportion of algae (autochthony) in the diet in sculpin and invertebrates from a Bayesian 2-isotope ($\delta^2\text{H}$ and $\delta^{13}\text{C}$) 2-source (biofilm and FPOM) mixing model with MixSIAR (Stock and Semmens, 2016). Before running the mixing models, isotope biplots of the food source and invertebrate data were made and used to determine which food sources to use. For terrestrial inputs FPOM was chosen over CPOM as it fell better within the mixing polygon for consumers in $\delta^{15}\text{N}$ vs

$\delta^2\text{H}$ biplots. Biofilm was originally sampled to represent the autochthonous food source but its values fell outside of the mixing polygon for the food sources supporting invertebrates, likely because it is a matrix of algae, bacteria and fungi and because invertebrates can selectively graze specific components of the biofilm (e.g. algae; McNeely et al., 2006). Because of these issues, the isotopic values ($\delta^2\text{H}$ and $\delta^{13}\text{C}$) of algae were calculated instead. For $\delta^2\text{H}$, 170‰ was subtracted from stream water $\delta^2\text{H}$ values because primary producers fractionate against ^2H by 160-170‰ during photosynthesis (Solomon et al., 2009). No $\delta^2\text{H}$ data exists for site NBE6 so $\delta^2\text{H}$ values were estimated using an average of the site above and below it. $\delta^{13}\text{C}$ values of algae were calculated from primary consumers if they had $\delta^{13}\text{C}$ values more depleted than biofilm, which was dominantly the scrapers *Eperous* and *Glossosoma*, and calculated by subtracting a $\delta^{13}\text{C}$ fractionation factor of $0.4 \pm 1.20\text{‰}$ selected from published data and backed by a previous caging experiment in Black Brook (Erdozain et al., 2019; McCutchan et al., 2003) from the $\delta^{13}\text{C}$ values for those scrapers. Separate mixing models were run for primary consumers using taxa as a fixed factor, predatory invertebrates with taxa as a fixed factor, and sculpin from each site. Before accepting the results of the mixing models, results from Geman-Rubin and Geweke diagnostic tests were checked to ensure the posterior distributions of each model had converged. Fractionation factors used in the models were $0.4 \pm 1.20\text{‰}$ for $\delta^{13}\text{C}$ and an assumed 0‰ for $\delta^2\text{H}$. It is common to correct consumer $\delta^2\text{H}$ for the fraction that comes from water in addition to assimilated (DeNiro & Epstein, 1981; Vander Zanden et al., 2016) but in this case consumers were not corrected for the contribution of $\delta^2\text{H}$ from water because consumers adjusted for body

water fell outside of isotope mixing polygon. $\delta^{15}\text{N}$ was not used in the mixing models of there is such a high variability in trophic fractionation factors. All data analysis was done in R 4.0.0 (R Core Team 2020).

Response variables (mean Hg and autochthony within taxa collected at each site) were compared among basins using ANOVA and Tukey post hoc tests for samples that met the assumption of normality and equal variance. If variance was not equal, sample means were compared with a Welch one-way test. Kruskal Wallance rank on sums tests were used if assumptions for normality did not pass followed by pairwise wilcoxon post-hoc tests (*car* package).

All water MeHg data were used in the overall basin analysis because there were no differences between September or October within any of the basins after running two factor ANOVAs ($\text{Hg} \sim \text{Basin} * \text{Month}$; p month and interaction terms=0.11, 0.91). However, only water data from September ($\text{Water}_{\text{Sept}}$) were used in the longitudinal analyses because of significant model interactions between Month, Area and Basin.

Female sculpin were size standardized for THg (hereafter THg_{size} ; n=80) because sizes of female fish differed among sites (Kruskal-Wallis; p= 0.011) and THg versus length was significantly related (linear regression; p<0.001). To size-standardize the data, a simple regression between log THg and fish length was made for each site, then the amount of mercury for a 66 mm fish was estimated from that model by adding the intercept to the slope value multiplied by 66. Variability was propagated back into the THg estimate for each fish by adding the residuals from the original regression. Percent

MeHg (%MeHg) was calculated by dividing MeHg by THg measured on the same individuals.

ANCOVA regressions were run using simple linear models and categorical covariates because sample sizes were too limited to run mixed models with random effects. ANCOVAs were used to assess the longitudinal trends in the dependant variables Hg, biomagnification, autochthony, and FWL, as well as relationships between Hg vs autochthony. For longitudinal trends the equation was “dependant variable = $\log_{10}(\text{Drainage Area}) * \text{Basin} + \log_{10}(\text{Drainage Area}) + \text{Basin}$ ”, where drainage area is used in the models to examine the longitudinal trends and the interaction between basin and drainage area is used to infer cumulative or dissipative effects. ANCOVAs were run to compare slopes (log Hg vs $\delta^{15}\text{N}$) of all sites within each basin and slopes of sites with the same relative size among basins, and then data were pooled across all sites within a basin to assess among-basin differences. Equations for these ANCOVAs were “slope = $\delta^{15}\text{N} * \text{Basin}(\text{or Site}) + \delta^{15}\text{N} + \text{Basin}(\text{or Site})$ where $\delta^{15}\text{N}$ shows whether Hg is related to relative trophic position and an interaction indicates that slopes vary between basins or streams. If the interaction term was significant, the slopes of lines were compared using a Tukey pairwise comparison (*lsmeans* package). If the interaction term was not significant, the model was rerun without it for comparisons of intercepts. This was done because the intercept may represent the baseline MeHg input to the food web (Borgå et al., 2012). Significant differences in intercepts were compared using a Tukey’s test (*multcomp* package) to understand whether inputs to the base of the food web differed among locations: (results shown in SI file). An ANCOVA using

$\log_{10}\text{Hg}=\text{autochthony}*\text{Taxa}/\text{Basin}+\text{Taxa}+\text{Basin}$ was run to determine whether Hg was related to the amount of algae in the diet and a significant interaction indicated different relationships between basins or taxa.

3.0 Results

3.1 Patterns in mercury

3.1.1 Among-basin differences in mercury

Mercury concentrations in water and food sources varied among sites and showed some among-basin differences when values from each stream site were combined. MeHg in water ranged from < DL to 0.15 ng/L and was highest in the extensive basin compared to the other basins ($p<0.005$) (Figure 3A). MeHg in biofilm ranged from 1.28 to 13.0 ng/g dw and the overall basin average was greater in the extensive than minimal basin ($p=0.001$; Figure 3E). CPOM MeHg ranged from 0.09 to 5.74 ng/g dw across all sites, and the extensive basin had significantly higher levels of MeHg compared to the intensive and minimal basins ($p<0.05$; Figure 3C). FPOM MeHg ranged from 0.074 to 7.74 ng/g dw and did not differ among basins ($p= 0.66$; Figure 3D). Similarly, the range in seston MeHg concentrations was 0.196 to 11.0 ng/g dw and did not differ among basins ($p=0.26$; Figure 3B).

Although levels of MeHg or THg in the macroinvertebrates and fish showed some trends among basins, with results tending to be higher for most taxa from the extensive basin, most comparisons were not statistically significant (exception Hydropsychidae). In Hydropsychidae, MeHg concentrations ranged from 6.00 to 302 ng/g dw and were greater

in the extensive basin compared to the intensive basin (pairwise wilcoxon test $p=0.026$; Figure 3I). For the scraper, *Glossosoma*, MeHg concentrations ranged between 4.55 to 133 ng/g dw and the concentrations were highest in the extensive basin compared to the intensive and minimal basins ($p=0.17$; Figure 3G). The collector-gatherers Baetidae (MeHg values between 4.70 to 217 ng/g dw) also showed a similar trend as *Glossosoma* where MeHg values in the extensive basin samples tended to be greater than in the other basins but not significantly different ($p=0.16$; Figure 3H). Within the shredder *Pteronarcys*, MeHg ranged between 13.5 to 86.3 ng/g dw but did not show any clear trend among basins ($p=0.62$; Figure 3F). In the predatory invertebrate, *Sweltsa*, MeHg ranged between 2.5 to 373 ng/g dw and the extensive basin shows slightly higher MeHg than the other basins ($p=0.27$; Figure 3J). THg_{size} ($n=22-30$ /basin) in sculpin ranged from 228 to 772 ng/g dw did not show any significant differences among basins ($p=0.85$; Figure 3L).

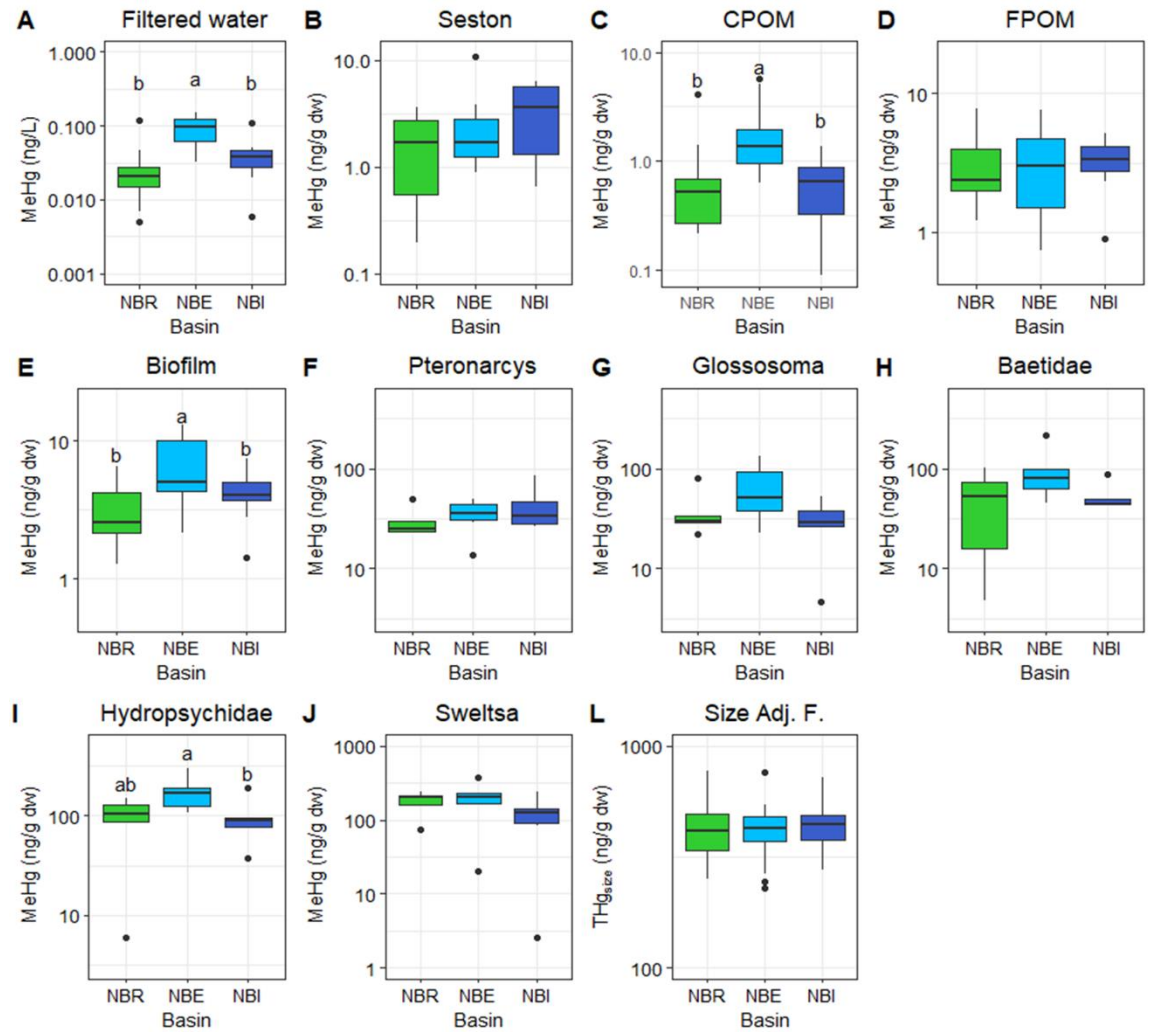


Figure 3: Boxplots showing the difference in MeHg concentrations in abiotic and biotic samples taken in 2018 from three basins in northern New Brunswick, Canada, with varying forest management intensity (6 sites/basin). A) Filtered water collected in September; B) Seston collected while filtering water; C-E) Basal food resources: coarse particulate organic matter (CPOM), fine particulate organic matter (FPOM) and biofilm; F-J) Macroinvertebrates: *Pteronarcys*, *Glossosoma*, Baetidae, Hydropsychidae, and *Sweltsa*; J) THg_{size} of female sculpin (Size Adj. F.; n=80). Letters denote significant differences among basins using Tukey's posthoc test or pairwise Wilcoxon test (p<0.05). Colours represent different basins: green is the minimal basin (NBR); light blue is the extensive basin (NBE); and dark blue is the intensive basin (NBI).

3.1.2 Longitudinal trends in mercury within and among basins

There were some longitudinal trends in MeHg and THg concentrations within basins. In the minimal basin, MeHg and THg tended to increase from upstream to downstream for water_{Sept}, CPOM, *Pteronarcys* and fish (indicated by * in Figure 5; Figures 4 and 5). This increase was also observed in the intensive basin for five of the ten groups (biofilm, CPOM, FPOM, Hydropsychidae and *Sweltsa*) analyzed for MeHg, and a similar but non-significant trend was also observed for water_{Sept}. In contrast, in the extensive basin the data showed either no trends or insignificant decreases from upstream to downstream in MeHg in Hydropsychidae, *Sweltsa*, *Pteronarcys*, with FPOM having a near significant longitudinal decrease in MeHg ($p=0.059$).

The spatial patterns in MeHg and THg varied significantly among basins for CPOM, FPOM, and Baetidae (drainage area*basin term; Figure 5). More specifically, MeHg in CPOM significantly increased downstream similarly in the minimal and intensive basins, but only the minimal basin differed compared to the extensive basin, which showed no strong longitudinal trend (1strends; $p=0.034$). MeHg in FPOM increased downstream similarly in the minimal and intensive basins but decreased in the extensive basin (1strends; $p=0.014$ and 0.037). For Baetidae, the slope in the minimal basin was positive and differed from that of the intensive basin (1strends $p=0.040$), which showed an insignificant longitudinal decrease in MeHg.

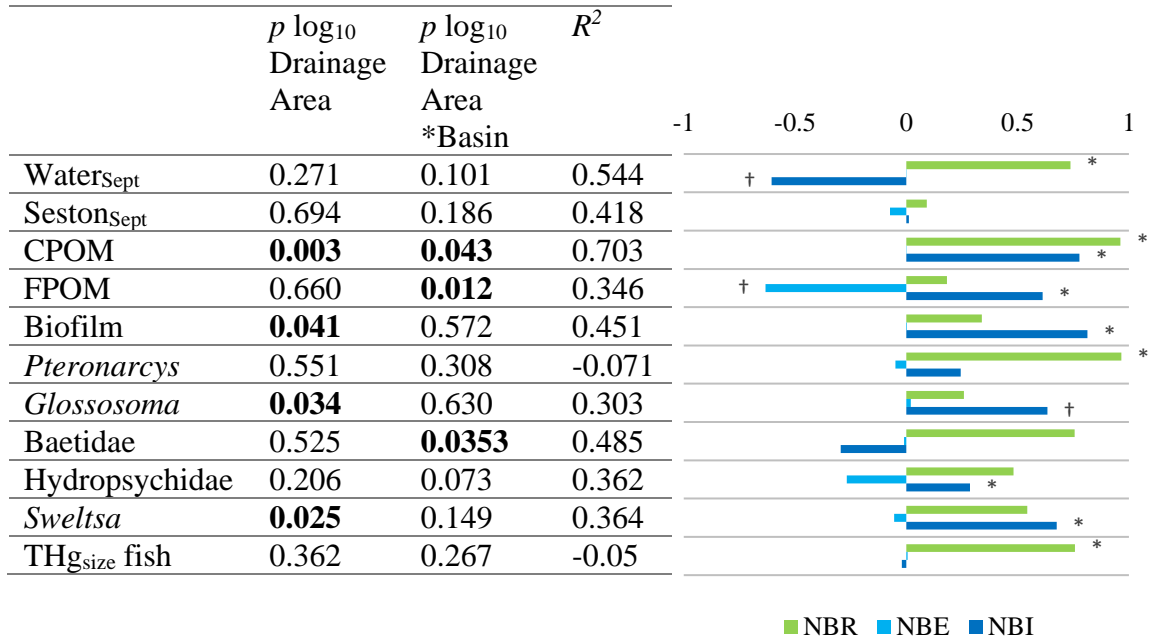


Figure 4: ANCOVA results for abiotic and biotic MeHg or THg (rows) versus \log_{10} of drainage area in the three basins (6 sites within each basin). The table shows p values from simple linear model (lm) ANOVAs testing the significance of drainage area and drainage area*basin for the following mixed model: linear model: $\log_{10}(\text{Hg}) = \log_{10}(\text{drainage area}) * \text{basin}$ with interactions $p < 0.05$ bolded. The column R^2 shows multiple R^2 values for simple linear regressions. The bar graph shows variance explained by $\log_{10}(\text{Hg}) = \log_{10}(\text{drainage area})$ for the simple lm; colours represent basin with green representing the minimal basin (NBR), light blue the extensive basin (NBE) and dark blue the intensive basin (NBI); length of the bar matches the R^2 ; direction of bars represents the sign of the coefficient (+ or – relationship); asterisks denote $p < 0.05$ and daggers represent values just over the level of significance ($p = 0.058-0.069$).

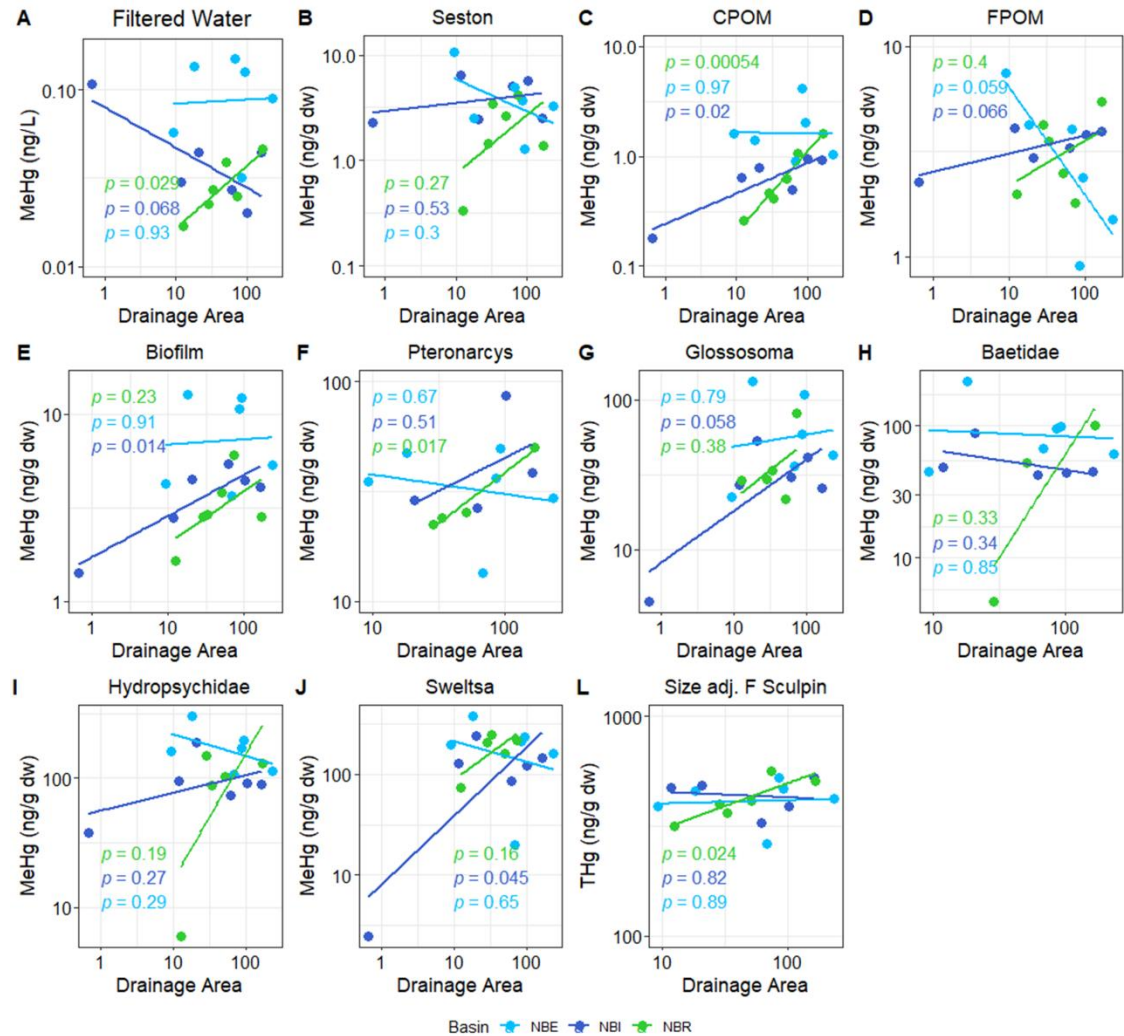


Figure 5: Linear relationships between \log_{10} Hg (MeHg or THg) concentrations and \log_{10} drainage area in abiotic and biotic samples taken in 2018 from three basins in northern New Brunswick, Canada (6 sites/basin) with varying forest management intensities. A) filtered water collected in September. B) Seston from filtered water. C-E) Three different food sources: CPOM, FPOM, and biofilm. F-J) Five different taxa of macroinvertebrates: *Pteronarcys*, *Glossosoma*, Baetidae, Hydropsychidae, and *Sweltsa*. L) THg_{size} female sculpin (n=80). Colours represent different basins: light green is the minimal basin (NBR); light blue is the extensive basin (NBE); and dark blue is the intensive basin (NBI). p values on the graphs denote the significance of the relationship between drainage area and Hg ($\alpha=0.05$).

3.2 Mercury biomagnification

3.2.1 Trophic transfer of mercury within basin

Log-transformed mercury concentrations in food sources and biota (THg in fish, MeHg in all other samples) were significantly related to their $\delta^{15}\text{N}$ within all the stream sites from each basin (Figure 7). Among sites the regression slopes ranged between 0.32-0.39 in the minimal basin, 0.25-0.30 in the extensive basin, and 0.29-0.38 in the intensive basin (Figure 7). The amount of variance described by the regression models for streams within each basin was 86-94% in the minimal, 73-92% in the extensive and 84-97% in the intensive (NBI6 had no sculpin and was therefore not included in any of the following analyses) basins. There were no significant interactions between $\delta^{15}\text{N}$ and stream site, indicating that slopes did not differ between the stream sites within any of the three basins (Table 2).

Table 2: ANCOVA analysis to test for differences in the trophic transfer of Hg (MeHg or THg (fish only)) within three basins in northern New Brunswick, Canada in 2018. *p* values are included for the main effect terms, $\delta^{15}\text{N}$ and Site, as well as the interaction term $\delta^{15}\text{N}*\text{Site}$. Significant *p* values ($p < 0.05$) are bolded. NBI6 was removed prior to analysis as no fish were collected at this site. The basins are the intensive (NBI), extensive (NBE) and minimal (NBR).

Basin	Terms		
	<i>p</i> $\delta^{15}\text{N}$	<i>p</i> Site	<i>p</i> $\delta^{15}\text{N}:\text{Site}$
NBR	<0.001	0.407	0.772
NBE	<0.001	0.237	0.809
NBI	<0.001	0.371	0.285

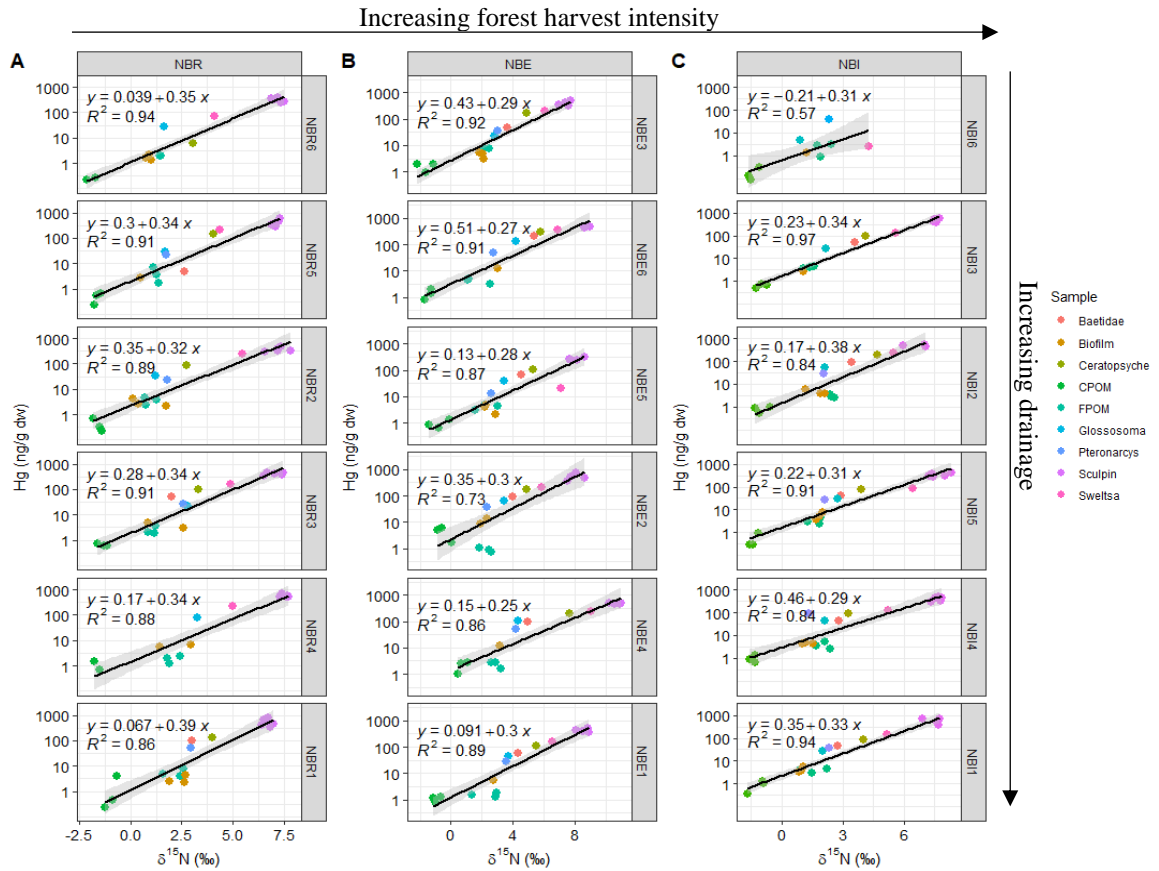


Figure 6: Log₁₀ MeHg (invertebrates and food sources) or THg (fish) versus $\delta^{15}\text{N}$ within 18 stream food webs from New Brunswick, Canada representing a gradient of harvesting intensity and increasing drainage area. A) is the minimal basin (NBR), B) is the extensive basin (NBE) and C) is the intensive basin (NBI), and streams are in order from upstream to downstream. The equation of the line and the coefficient of determination are shown in each panel (R^2 ; $p < 0.001$). Shading around the line represents standard error.

3.2.2 Trophic transfer of mercury among basins

The biomagnification of Hg was compared among basins for stream sites with similar, relative sizes and only one comparison showed differences (Figure 7). The interaction between basin and $\delta^{15}\text{N}$ was significant at the second smallest site ($p=0.047$); the slopes of the minimal and intensive basins were greater than in the extensive basin, but not significantly different after a Tukey pairwise test ($p=0.074-0.10$; Table 3). Although not

statistically significant, it is interesting to note that, within sites of similar sizes, the slopes for the minimal basin were highest at the three largest sites (Figure 6). Due to the presence of the interaction in the second smallest site it was excluded from analyses of intercepts described in the Supplementary Information Section 5.3.

Data were pooled among sites to assess whether overall Hg biomagnification differed among basins. The overall slopes were 0.34 in the minimal basin, 0.27 in the extensive basin, and 0.32 in the intensive basin (Figure 8). The interaction between $\delta^{15}\text{N}$ and basin was significant ($p < 0.001$) and the slopes in the minimal and intensive basins were significantly greater than the slope of the extensive basin (Istrends $p = 0.0001$ and $p = 0.001$, respectively) and not significantly different from each other ($p = 0.468$).

Table 3: *P* values of variables used in the ANCOVA analysis to test for differences in the trophic transfer of MeHg, or THg, within sites of similar drainage area and among the three basins in northern New Brunswick, Canada in 2018. *p* values are included for the main effects terms, $\delta^{15}\text{N}$ and Site, as well as the interaction term $\delta^{15}\text{N} \times \text{Site}$. Significant *p* values ($p < 0.05$) are bolded.

Site Size	Terms		
	<i>p</i> $\delta^{15}\text{N}$	<i>p</i> Basin	<i>p</i> $\delta^{15}\text{N}:\text{Basin}$
smallest*	<0.001	0.034	0.065
2 nd smallest	<0.001	0.199	0.047
3 rd smallest	<0.001	0.009	0.125
4 th smallest	<0.001	0.532	0.614
5 th smallest	<0.001	0.283	0.159
largest	<0.001	0.227	0.097

*Comparison to the smallest sites in the minimal and extensively managed basins only

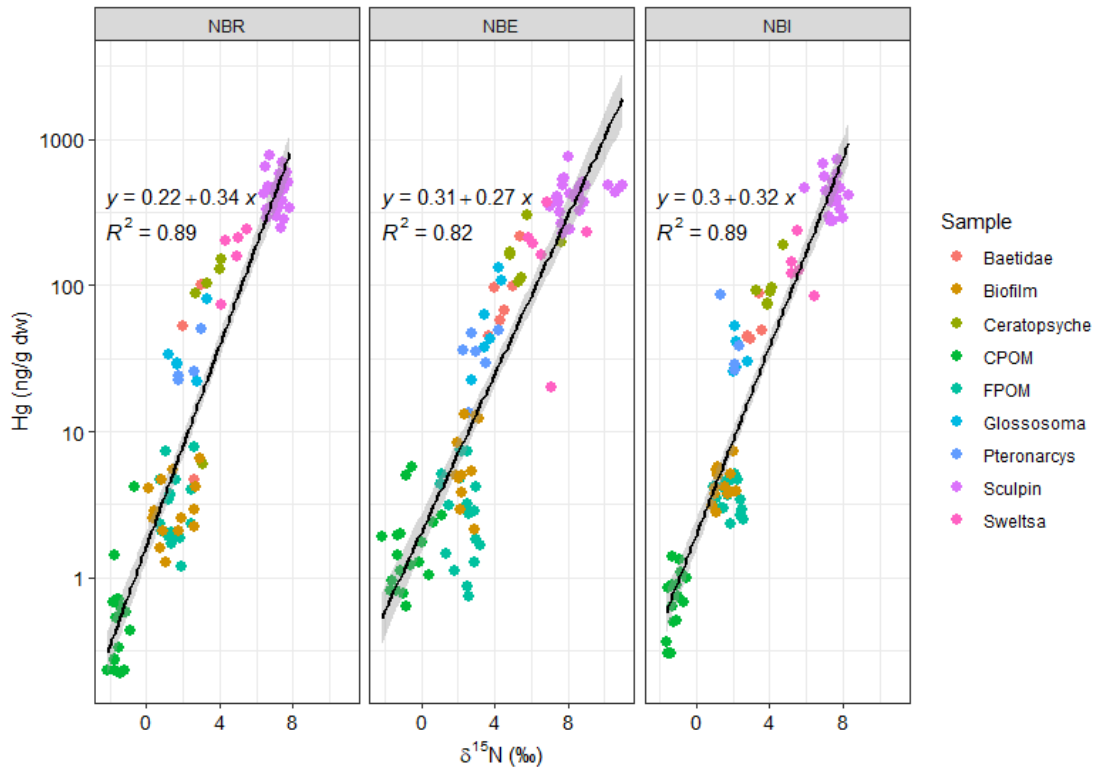


Figure 7: Log₁₀ MeHg (invertebrates and food sources) or THg (fish) versus δ¹⁵N within three basins food webs from New Brunswick, Canada representing a gradient of harvesting intensity (R^2 ; $p < 0.001$). Data are pooled from stream sites (6/basin) to make the one regression line per basin. The equation of the line and coefficient of determination are shown in each panel. Shading around the slope represents standard error. The basins in order from minimally (NBR), extensively (NBE) and intensively managed (NBI).

3.2.3 Hg trophic transfer vs area

There were no effects of drainage area on the slopes of log Hg vs. $\delta^{15}\text{N}$ (ANCOVA, basin*log₁₀(drainage area), p=0.122), indicating that biomagnification slopes did not differ from upstream to downstream (Figure 8). As a note, the slope values in the extensive basin showed little among-site variation in values and were consistently lower than those of the other two basins. When the interaction term was removed from the model, basin was significant because the slopes of the extensive basin were consistently lower compared to the intensive and minimal basins (basin p=0.003). The trends and

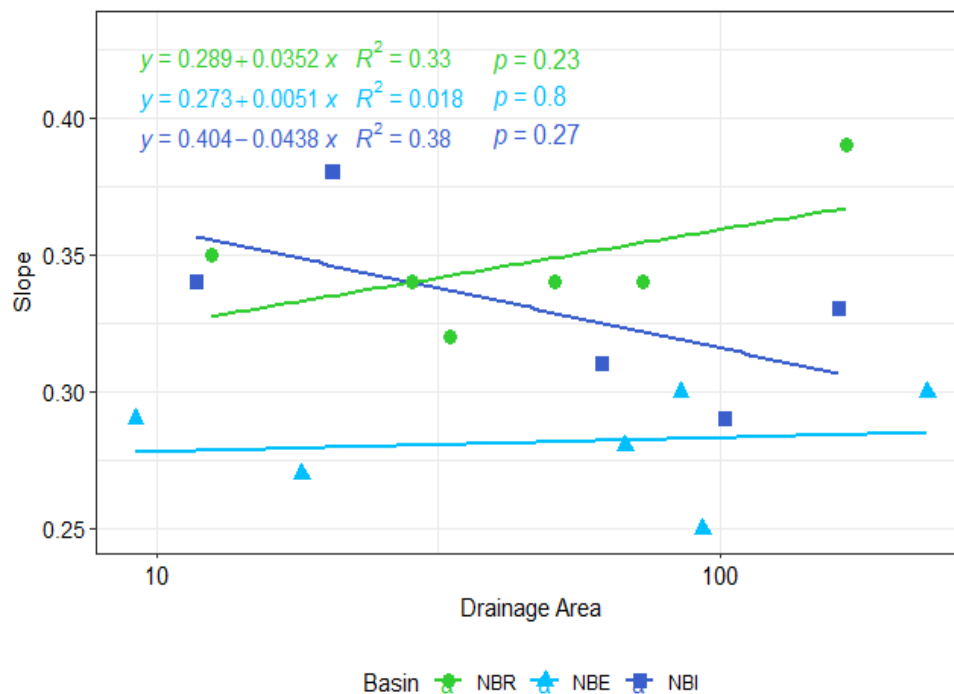


Figure 8: Trophic magnification (slope as calculated from the relationship between log₁₀Hg and $\delta^{15}\text{N}$) vs drainage area (km²). Data to generate the regression for each basin was generated from the slope values calculated from the five or six sites within three basins experiencing different levels of harvesting intensity in New Brunswick, Canada. The equation of the line and coefficient of determination are shown in each panel. The line and equation are colour coded by basin with the minimal (NBR) in green, extensive in light blue (NBE), and intensive in dark blue (NBI)

analyses should be interpreted with caution as the variance in the model was not well captured with a linear line and five or six points.

3.4 Autochthony and food web length

3.4.1 Among-basin differences in autochthony of consumers

After pooling mean data for all taxa, analyses (Autochthony=Basin*Taxon+Basin+Taxon; basin $p=0.14$, taxon $p<0.001$) showed that there were no differences in autochthony among basins (basin*taxon; $p=0.80$). For taxa with data from at least 3 sites in 2 basins, among-basin comparisons of site means indicated that only two predators (*Diura* and sculpin) had significant differences in mean autochthony. The *Diura* from the minimal basin were supported more by algae than those in the intensive basin (mean autochthony = 0.52 and 0.36 for the minimal and intensive basins, respectively), while sculpin in the extensive basin had a greater proportion of algae in their diets compared to those in the minimal basin (mean autochthony = 0.61 and 0.48 for the extensive and minimal basins, respectively; Figure 9).

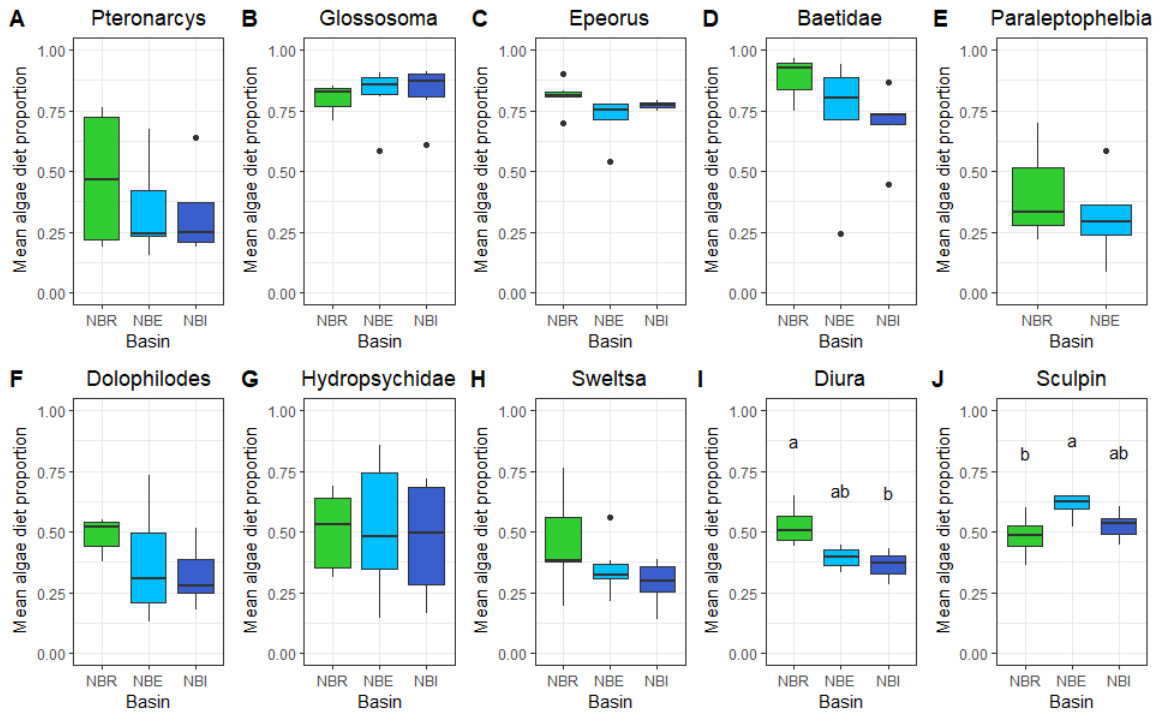


Figure 9: Boxplots showing the proportion of algae in diets of benthic invertebrates and sculpin within three basins in New Brunswick that experience different levels of forest management. Taxa included are ones that had mean data from at least 3 sites in 2 different basins. Autochthony was calculated using a Bayesian 2-isotope mixing model ($\delta^2\text{H}$ and $\delta^{13}\text{C}$) in MixSIAR and colours represent basin (green is the minimally managed (NBR), light blue is the extensively managed (NBE) and dark blue is the intensively managed basin (NBI)). Letters denote differences in mean proportion of autochthony with Tukey post hoc tests.

3.4.2 Longitudinal trends in autochthony

Within each basin, the longitudinal trends in autochthony were drainage area and taxon dependant in the minimal and intensive basins but only taxon dependant in the extensive basin (Table 4). Because the interaction term was not significant, it indicated that the slopes among taxa did not differ significantly. When taxa were examined separately the interaction between drainage area and basin was significant for *Diura* and sculpin, with autochthony for *Diura* increasing downstream in the minimal and intensive

basins and decreasing downstream in the extensive basin. For sculpin, the minimal basin had the greatest increase in autochthony downstream compared to the intensive and extensive basins, which both had slopes that were not as steep (Figure 10).

Table 4: P values from the linear regressions between autochthony in benthic macroinvertebrates/sculpin and drainage area from three basins that experience different levels of forest management. Data are from ANCOVAs testing the significance of drainage area in two different models, one within each basin with taxa as a covariate and one within each taxon and with basin as a main effect. $p < 0.05$ values are bolded.

Within Basin¹			
	Log ₁₀ Drainage Area	Taxon	Log ₁₀ Drainage Area*Taxon
Minimal	0.014	<0.001	0.529
Extensive	0.169	<0.001	0.681
Intensive	0.002	<0.001	0.633
Within Taxa²			
	Log ₁₀ Drainage Area	Basin	Log ₁₀ Drainage Area*Basin
<i>Pteronarcys</i>	0.099	0.172	0.133
<i>Glossosoma</i>	0.698	0.268	0.176
<i>Epeorus</i>	0.646	0.838	0.869
Baetidae	0.556	0.944	0.859
Hydropsychidae	0.486	0.854	0.877
<i>Dolophilodes</i>	0.912	0.427	0.476
<i>Sweltsa</i>	0.697	0.960	0.995
<i>Diura</i>	0.001	0.008	0.002
Sculpin	<0.001	0.006	0.021

¹model: Algae in diet = $\log_{10}(\text{Drainage Area}) * \text{Taxon} + \log_{10}(\text{Drainage Area}) + \text{Taxon}$

²model: Algae in diet = $\log_{10}(\text{Drainage Area}) * \text{Basin} + \log_{10}(\text{Drainage Area}) + \text{Basin}$

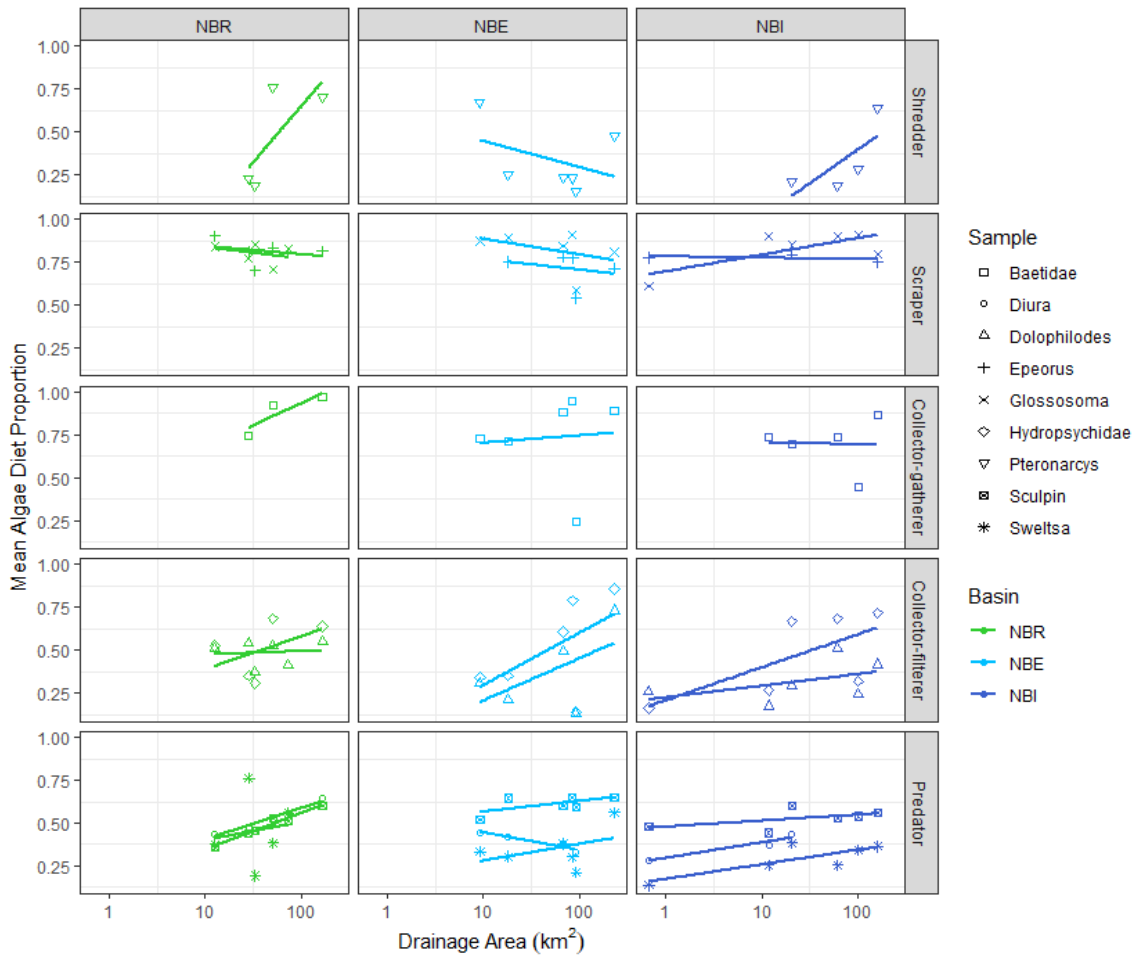


Figure 10: Linear regressions between mean proportion of autochthony, calculated from Bayesian 2-isotope mixing model ($\delta^2\text{H}$ and $\delta^{13}\text{C}$) in MixSIAR, and drainage area of 7 different benthic macroinvertebrate taxa and sculpin that had data from at least three sites for each of the three basins. Taxa are separated by FFG and given a unique shape and regression line, and basin is colour coded with the minimal basin in green (NBR), extensive basin in light blue (NBE), and intensive basin in dark blue (NBI).

3.4.3 Relationships between autochthony and mercury within taxa

Pooling autochthony data from each taxon by basin showed that the minimal and extensive basins had a significant interaction between taxa and autochthony ($p < 0.01$).

Within taxa, there was a significant increase in Hg concentrations as autochthony

increased within four (Baetidae, THg_{size}, *Glossosoma* and *Sweltsa*) of the six groups but only in one of the three basins (indicated by * on Figure 11 bars). Baetidae and THg_{size} had higher Hg concentrations with greater autochthony in the minimal basin, whereas *Glossosoma* and *Sweltsa* showed the same relationship, but in the intensive basin. The relationships in other basins and taxa were either insignificant decreases in Hg concentrations with autochthony (ex: Hydropsychidae) or no relationship at all.

There were also spatial differences in Baetidae, *Glossosoma*, and *Sweltsa* as indicated by the interaction term (Figure 11). For Baetidae, there was a greater increase in MeHg with autochthony in the minimal basin compared to both the extensive and intensive basins ($p=0.003-0.007$), which showed an insignificant decrease in MeHg with autochthony or no relationship. For *Glossosoma* the slope in the intensive basin was greater compared to the extensive basin ($p=0.04$), which had an insignificant decrease in MeHg with autochthony. For *Sweltsa* the increase in MeHg with autochthony was greater in the intensive basin than both the extensive and minimal basin ($p=0.018-0.02$).

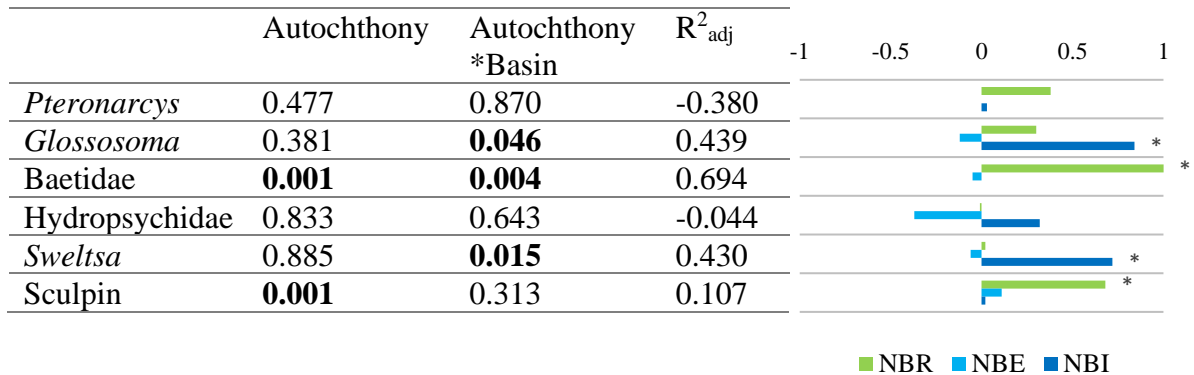


Figure 11: ANCOVA results for Hg in biota (rows) versus autochthony in the three basins (6 sites within each basin). The table shows p values from simple linear model (lm) ANCOVAs testing the significance of autochthony*basin for the following mixed model: linear model: $\log_{10}(\text{Hg}) = \text{autochthony} * \text{basin}$ with interactions $p < 0.05$ bolded. The column R^2 shows adjusted R^2 values for simple linear regressions. The bar graph shows variance explained by $\log_{10}(\text{Hg}) = \text{autochthony} * \text{basin}$ for the simple lm; colours represent basin (green is the minimal basin (NBR), light blue is the extensive basin (NBE) and dark blue is the intensive basin (NBI)), length of the bar matches the R^2 , direction of bars represents the sign of the coefficient (+ or – relationship), asterisks denote $p < 0.05$.

3.4.4 Food web length and sculpin Hg

Average FWL was similar within basins and was not different among basins ($p=0.52$; $\text{NBI}=5.06 \pm 0.20$, $\text{NBE}=4.99 \pm 0.27$, $\text{NBR}=4.67 \pm 0.28$; Figure 13A). Results from an ANCOVA showed FWL had no longitudinal relationships ($\log_{10}(\text{drainage area})$, $p=0.84$) or relationship to basin (basin $p=0.49$). The interaction term between FWL and drainage area ($p=0.17$) was also not significant, indicating that longitudinal relationships in FWL did not differ among basins, which was not surprising considering the insignificant relationship of the line and the variability in the 5-6 data points within the basins (Figure 15B). Similarly, THg_{size} also showed no relationship to FWL ($p=0.48$), basin ($p=0.63$), or interaction between FWL and basin ($p=0.34$; Figure 14).

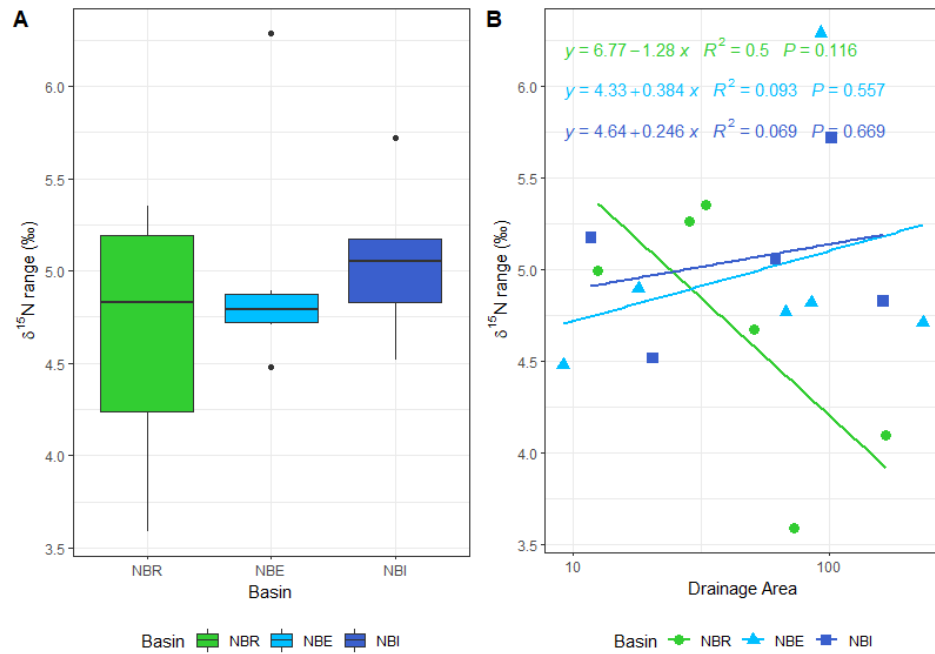


Figure 12: A) Boxplots showing FWL ($\delta^{15}\text{N}$ range (‰)) calculated from the difference between the average site $\delta^{15}\text{N}$ for sculpin and the average site $\delta^{15}\text{N}$ value for three primary producers) for three basins that experience different levels of forest management in northern New Brunswick, Canada. B) Linear regression between FWL and drainage area. Colours and shapes denote different basins, green and circles for the minimal basin (NBR), light blue and triangles for the extensive basin (NBE), and dark blue and squares for the intensive basin (NBI). The equation of the line and coefficient of determination are shown in the panel.

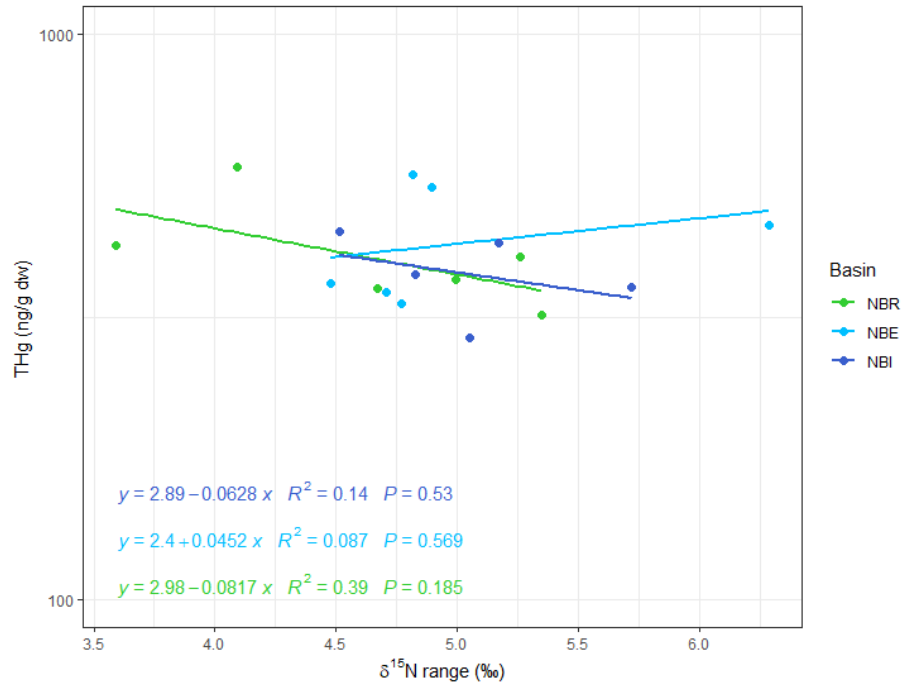


Figure 13: Linear regression comparing \log_{10} THg to FWL ($\delta^{15}\text{N}$ range (‰)) calculated from the difference between average $\delta^{15}\text{N}$ for sculpin from the average $\delta^{15}\text{N}$ values from three primary consumers) for three basins that experience different levels of forest management in northern New Brunswick, Canada. Colours denote different basins (green for the minimal basin (NBR), light blue for the extensive basin (NBE), and dark blue for the intensive basin (NBI)). The equation of the line and coefficient of determination are shown in the panel.

4.0 Discussion

4.1 Basin trends

The extensive basin had the greatest MeHg concentrations in water, CPOM, biofilm, and Hydropsychidae compared to the minimal and intensive basins, and these trends may be related to differences in water quality among basins. The extensive basin had lower conductivity compared to the other two basins, lower nitrates compared to the minimal basin, and greater phosphorus, inorganic/organic sediments, DOC, and humic, terrestrial, less aromatic DOM (humification by HIX, origin determined by FI, aromaticity by SUVA) compared to the other basins (Erdozain et al., 2021b). Lower

conductivity means fewer cations in the water, causing biofilm membranes to be more permeable and increase passive uptake of Hg into cells (Daguené et al., 2012; Dranguet et al., 2017). Even though the extensive basin had the highest phosphorus levels of the three basins, it had the lowest nitrates/nitrites, which could mean nitrogen was a limiting nutrient for biofilm growth resulting in less growth dilution (Pickhardt et al., 2002; Tank & Dodds, 2003). DOC may also explain the higher MeHg levels in the extensive basin water and biofilm because terrestrial inputs of DOC are linked to increased transport of MeHg and Hg into aquatic systems (Eckley et al., 2018; Pinheiro, 2000; Zhang et al., 2016). Higher water MeHg concentrations can lead to higher biofilm MeHg levels, as aqueous MeHg can cross tissue membranes through facilitated transport or passive diffusion (Dranguet et al., 2017). While DOM and DOC in terrestrial runoff increases water MeHg concentrations, it could also play a role attenuating uptake in biota. DOM that has higher aromaticity is thought to protect against metal toxicity by having a strong metal binding potential (Al-Reasi et al., 2013; Ravichandran, 2004); even though the extensive basin DOM had the lowest SUVA (measurement of aromaticity) it still may have had a protective effect. Additionally, DOC concentrations were greatest in the extensive basin and MeHg levels did not differ in the majority of invertebrates and fish. Limited incorporation of MeHg at high levels of DOC has been seen in caddisflies (Tsui & Finlay, 2011), chironomids and riparian spiders (Bundschuh & McKie, 2016), and yellow perch from the Adirondacks (Driscoll et al., 1995). Because Hg in leaves comes dominantly from foliar uptake, the elevated CPOM MeHg could be due to differences in foliar uptake across species or atmospheric Hg deposition, but it may also be due to differences in soil

MeHg (Ericksen et al., 2003; Miller et al., 2005; Yang et al., 2018). These parameters were not measured and could be done in future studies.

Some of the among-basin patterns in invertebrate MeHg may be due to their feeding habits. Because MeHg is mainly obtained from the diet, it was surprising that the elevated MeHg in the extensive basin autochthonous and allochthonous food sources did not translate into higher MeHg in most invertebrates, particularly the specialists. Despite being classified as an obligate consumer of terrestrial matter, mixing model results found that the shredder *Pteronarcys* relied ~25% on autochthonous sources. Mixing models were not run with CPOM but *Pteronarcys* may not be consuming enough terrestrial CPOM to reflect the higher MeHg in this food source and relying also on FPOM as a terrestrial food source (Plague et al., 1998). Additionally, *Pteronarcys* could eat the bacteria/fungi community colonizing the leaves that may not have the same MeHg levels as the leaves (Bueler, 1984). Similarly, the scrapers *Glossosoma* are obligate consumers of algae but did not reflect among-basin differences in biofilm MeHg likely because they were selectively eating autotrophic components of biofilm (McNeely et al., 2006) and not consuming more algae in the extensive basin compared to the other basins. The lack of among-basin differences may also be due to low sample sizes since *Glossosoma* MeHg in the extensive basin did seem to be higher than in the other basins. MeHg in the filterers, Hydropsychidae, in the extensive basin may have been impacted by the overall higher inorganic sediments getting caught in their nets, making it more difficult to obtain food and hindering growth, therefore concentrating MeHg in their tissues.

The invertebrate MeHg concentrations had a wide range, particularly for *Glossosoma*, Hydropsychidae, and *Sweltsa*, and tended to have higher fold differences (29, 49 and 148, respectively) among sites than has been observed elsewhere. In another study conducted in New Brunswick, the fold difference for stream primary consumer invertebrates spanning different genera and functional feeding groups was 32 while in predatory inverts it was approximately 5 (Jardine et al., 2013). Scrapers from California streams (including *Glossosoma*) had a 12-fold difference in MeHg concentrations, a 4-fold difference in MeHg concentrations in Hydropsychidae genera, and a 4-fold difference in MeHg concentrations for predatory invertebrates (Tsui et al., 2009). Most of the very low MeHg values in this study came from the smallest site in the intensive basin, which had the smallest drainage area of any site from any of the three basins. This site also had the highest phosphorous levels and fairly high nitrogen that could have caused more food source growth and growth dilution in consumers. It has been removed from some biomagnification analysis herein for its lack of fish and in other analyses because its smaller drainage area had disproportionately large influence on the results (Erdozain et al., 2021b).

4.2 Longitudinal trends in the minimal basin

In the minimal basin there was an upstream to downstream increase in MeHg or THg in water, CPOM, biofilm, *Pteronarcys*, and sculpin, an increase in autochthony across all consumers (SI Table 9) and taxon specific increases in autochthony for sculpin and *Diura*. The longitudinal trends in biofilm may be explained by the downstream dissipation in DOM humification and in nitrates/nitrites. DOM that is less humic has a

lower affinity to bind MeHg, making it more bioavailable for uptake, and the lower nitrogen, a limiting nutrient, could result in decreased growth of biofilms and subsequent higher MeHg concentrations downstream, especially if these sites are receiving more light, stimulating biofilm growth and increasing demand for nutrients (Ylla et al., 2007). The downstream increase in sculpin THg could be related to its longitudinal increase in autochthony as there was a positive relationship between THg and autochthony in this species, indicating that sculpin at downstream sites were more exposed to THg from autochthonous sources. Top predators supported by a longer food web (herein FWL) may have higher Hg than the same species from a shorter underlying food web because the former are consuming prey higher in Hg and likely growing larger and living longer, both of which result in greater accumulation of Hg (Ouédraogo et al., 2015). Herein, FWL did not explain the spatial patterns in THg of sculpin because it did not change with drainage area; the same trend in FWL with drainage area was also seen in 2017 (Erdozain et al., 2021b). The spatial patterns for *Pteronarcys* MeHg were likely related to the increasing CPOM MeHg, as this is their main food source. The spatial patterns seen in biota from the minimal basin differ from other basins where Hg in shredders and forage fish decreased with hydrologic transport distance (Riva-Murray et al., 2011). Finally, the overall increase in downstream autochthony when all taxa were pooled is consistent with results from another study done in 2017 in the same system and continues to reflect the change in food source origin predicted by the RCC (Erdozain et al., 2021b).

4.3 Contrasting longitudinal trends in the intensive and extensive basins with that of the minimal basin

Longitudinal trends in the harvested basins differed from patterns observed in the minimal basin for some measures of Hg and suggests that forest management changed the dissipative/cumulative patterns. There were significant downstream increases in biofilm, Hydropsychidae, and *Sweltsa* MeHg (and near significant increase in *Glossosoma*) in the intensive basin that were not seen in the minimal basin. The biofilms may have had more access to nutrients since there was a dissipative trend in aqueous nitrogen and phosphorous (suggesting greater uptake) in the intensive basin compared to the minimal basin (Erdozain et al., 2021b) as well as no change in biofilm quality (Erdozain et al., 2021a). Growth dilution was likely not seen because scraper abundance also increased in the intensive basin, causing competition for food sources (Erdozain et al., 2021a). MeHg in *Glossosoma* and *Sweltsa* were significantly related with their increased autochthony so diet can explain the spatial trends for these taxa and the filter feeding of Hydropsychidae may have been impacted by the increased inorganic sediments at downstream sites which would have slowed their growth rates. For the intensive basin, the inorganic sediments and increased terrestrial DOM inputs were likely driving the differences from what was seen in the minimal basin.

The extensive basin showed significantly different spatial patterns in CPOM and FPOM MeHg when compared to the minimal basin. There were no longitudinal changes in CPOM MeHg in the extensive basin, but all data points were higher compared to the minimal basin, which could be explained by soil Hg levels, or foliar uptake, but no

supporting data are available. The decrease in FPOM MeHg to downstream in the extensive basin could be a result of the high loading of organic sediment in the upstream sites, which could be terrestrial matter bound with MeHg, and then quickly degraded/assimilated by biota through space. The dissipative results for Baetidae are difficult to interpret because there were fewer data points since not all sites had enough biomass for analysis. However, Charbonneau (2018) found that MeHg in Hydropsychids was greater in upper and middle reach sites compared to downstream in harvested catchments and this may be occurring for biota in my study as well. It is possible some effects of forestry on FPOM MeHg longitudinal trends possibly were not observed because stream sites were not all along the same flow path to carry the organic matter to downstream locations (Erdozain et al., 2021b).

Some among-basin differences in the longitudinal trends in autochthony of biota were observed and suggest that forest harvesting affects food web structure. Unlike in the minimal basin, there was no longitudinal trend in overall autochthony of taxa in the extensive basin. This is supported by the lack of trends from upstream to downstream in nitrogen or phosphorous as nutrients dissipated in the other basins, and no spatial change in biofilm mass (Erdozain et al., 2021a, 2021b); however autotrophic index also declined longitudinally in the extensive basin potentially from the higher sediment loads (Erdozain et al. 2021). The longitudinal patterns in autochthony also differed in individual taxa; there were dissipative trends in *Diura* in the extensive basin compared to the minimal basin, and dissipative trends in sculpin in both the extensive and intensive basins compared to the minimal basin. The differences in overall and longitudinal patterns in

autochthony between the extensive and the intensive basin is likely due to the differences in sediments. The higher sediment loads in the extensive basin at the downstream sites may have reduced the autochthony of the organisms (Erdozain et al., 2021b).

The lack of congruence between basin and spatial comparisons of isotopes and mercury in water to biotic samples may be because food sources were collected in September at the same time as the consumers. Consumers are longer-lived and their tissues reflect longer time periods whereas biofilms and water show greater temporal variation, especially for stable isotopes. For instance, sculpin have been seen to be isotopically out of sync with prey items and biofilms because both can have quick tissue turnover rates in $\delta^{13}\text{C}$ and $\delta^{15}\text{N}$ (Jardine et al., 2014). For this reason, the estimation of autochthony made herein may not be as accurate as it could be since the September isotope values of food sources may be different from what was assimilated by the biota. MeHg concentrations in water also show seasonal variation and consumer tissue sampled in September could be reflecting the aqueous MeHg weeks prior to sampling (Bradley et al., 2011). Fish were sampled in October so they may have had enough time to assimilate Hg and isotope values from samples collected in September.

As in this study, drainage area has not been a consistent predictor of autochthony (Jonsson et al., 2018) and Hg in fish that are in the same ecoregion (Riva-Murray et al., 2020). Forest harvesting variables (such as canopy openness, forest cover, road density/crossing, and % clearcut) may be better at explaining trends in biotic Hg than space at these relatively smaller scales as they are linked to the delivery of terrestrial

material into streams and the type of basal resources used by invertebrates (Erdozain et al., 2019, 2021; Jonsson et al., 2018).

4.4 Biomagnification

As in other studies, $\delta^{15}\text{N}$ significantly predicted Hg levels and confirmed its biomagnification within all stream food webs examined herein. An average slope for stream food webs was 0.24 (Lavoie et al., 2013) compared to 0.32 (all 18 slopes averaged) from this study and 0.30 from another study in New Brunswick assessing biomagnification in 21 streams (Jardine et al., 2013). The range in site slope values in this study (0.25- 0.39) was also comparable to those (0.22-0.39) in Jardine et al. (2013), which also calculated slopes from MeHg in biofilm and invertebrates and THg in fish. These values are also within the range reported for other streams across Canada (0.06-0.39) (Lavoie et al., 2013). Overall, this suggests that the trophic transfer of MeHg within sites in my study were comparable to those of other systems.

Interestingly, there were no within-basin differences in the biomagnification slopes from upstream to downstream in this study, suggesting that the size of the lotic system does not affect the trophic transfer of this metal. This differs to lentic systems that show Hg biomagnification increases with area and is also related to aqueous phosphorous (Kidd et al., 2012).

The overall slope values for each basin after pooling sites was significantly lower in the extensive basin compared to the minimal and intensive basins, and this appears to be driven by the higher MeHg concentrations in the lower trophic levels (CPOM, biofilm)

of the extensive basin food webs that were not propagated up to sculpin. Inefficient trophic transfer of MeHg can start at food sources to primary consumers due to differences in dietary assimilation efficiencies (Jardine et al., 2013; Reinfelder et al., 1998). Dampened Hg biomagnification has also been seen in several species of fish when dietary Hg concentrations were high (DeForest et al., 2007). Overall, forest harvesting intensity did affect biomagnification among basins and this seemed to be related to greater uptake of MeHg in primary producers and the inefficient transfer of Hg from lower to higher trophic levels.

4.5 Sculpin

THg in all sculpin ranged between 133-822 ng/g dw and was converted to wet weight (ww) to give a range of 33.1-249 µg/kg ww. For female sculpin only it ranged between 218-822 ng/g dw and was 58.4-249 µg/kg ww. These values compare to sculpin collected across Ontario that had THg concentrations between 130-740 ng/g dw (Lescord et al., 2018) and other small-bodied fish collected in New Brunswick with average THg_{adj} concentrations between ~404-707 ng/g dw across two years of sampling (Reinhart et al., 2018) compared to the average THg_{adj} in this study of 434 ng/g dw. The Tissue Residue Guidelines to Protect Wildlife from Mercury Toxicity recommends animals should not consume fish with mercury concentrations exceeding 33 µg/kg ww and all fish are above this guideline. This indicates that animals that are sensitive to Hg, like Belted Kingfisher (Lazorchak et al., 2003) that breed in northern New Brunswick, could be at risk for mercury poisoning by consuming these fish and feeding their young high mercury fish.

4.6 Autochthony

Some among-basin differences in autochthony were observed in this study, suggesting that forest management can change carbon flow in riverine food webs. *Diura* had overall higher autochthony in the minimal basin compared to the intensive basin, which could be explained by the fact that *Diura* can also be facultative scrapers (Merritt et al., 2008), however their $\delta^{15}\text{N}$ values were not similar to scraper values. *Diura* may also be consuming taxa, such as Baetidae, *Epeorus*, or *Dolophilodes*, that have higher proportions of algae in their diets in the minimal basin compared to the other basins. Sculpin had overall higher autochthony in the extensive basin compared to the minimal basin, but because higher autochthony was not seen in their invertebrate prey the reason for the overall spatial trends for this fish is unclear.

Mixing model results did not concur completely with similar data from these sites collected in 2017 (Erdozain et al., 2021b). In 2017, overall basin autochthony was greater in the minimal and the extensive basins compared to the intensive basin whereas in my data there were no differences in overall basin autochthony. Also, in 2017, overall autochthony increased from upstream to downstream in the minimal basin only but in my study both the minimal and intensive basins increased longitudinally. Longitudinal trends in autochthony for each taxon within the minimal basin also showed some differences among years as autochthony increased in *Baetis*, *Ephemerella*, and Hydropsychidae in 2017, while only *Diura* and sculpin increased in 2018. The intensive and extensive basins showed differences in spatial patterns when compared to the minimal basin in Heptageniidae and *Ephemerella* in 2017 but this was not seen in 2018. Sculpin was the

only taxa that showed the same pattern across years and basins, with autochthony increasing longitudinally in the minimal basin compared to the intensive and extensive basins, both of which did not show significant spatial trends. In future studies it may be better to compare autochthony to harvesting variables rather than space. Autochthony increases with decreasing forest cover related to logging and differences in autochthony in filter-feeders and other taxa were better explained by forest management variables than spatial differences (Erdozain et al., 2021b; Jonsson et al., 2018).

4.7 Limitations/Challenges

My thesis work was part of a larger study assessing the cumulative effects of forestry on rivers that was designed to assess many abiotic and biotic endpoints across the three basins (Erdozain et al., 2021a, 2021b). Biomass for invertebrates and biofilm was limited because this study was designed to include more sites to increase spatial coverage (n=6 sites/basin) and many sample types at each site, with the trade off there was less time available to collect each sample type. Difficult access meant not all 6 sites were along the same flow path but at least 2-3 were hydrologically connected and the most downstream site in all basins received water from the 5 upstream sites. The minimal basin was in a different ecoregion because it was the only one that could be found that had lower harvesting relative to the intensive and extensive basins and was of a similar size. In the future, follow up studies can be designed to increase sample sites and including replicate treatment basins while focusing on sampling the indicators that showed spatial responses in my study.

4.8 Conclusions

This study examined the cumulative effects of forest management on water and biotic Hg concentrations, the biomagnification of Hg in stream food webs, and the reliance of biota on autochthonous food sources. The main findings were that: 1) the extensive basin had overall higher MeHg concentrations in water, food sources, and Hydropsychidae; 2) dissipative longitudinal trends for food source MeHg in the extensive basin; 3) MeHg biomagnification was greatest in the extensive basin but not spatially at any level; and 4) longitudinal trends in autochthony in sculpin and *Diura* differed with harvesting. These results suggest that forest management did affect the cycling of Hg in these systems, particularly for basal food sources at a basin scale, but that longitudinal effects were not consistent. Most differences were seen in the extensive than the intensive basin, implying that greater forest management (tree removal but also pesticide and fertilizer use for regeneration) does not always mean there will be greater environmental impacts. Few studies have examined how Hg levels vary from upstream to downstream and whether this process is affected by forest management. As such, my thesis work contributes new knowledge that mercury bioaccumulation at the base of the food web was most affected by forestry and that those effects were not translated to higher trophic levels. Future studies are recommended to collect more samples in replicate basins to increase power for analysis and include a true reference basin with no harvesting if possible. Sampling should focus on indicators that showed spatial differences with harvesting, such as water, biofilm, CPOM, Hydropsychidae, Baetidae and sculpin. Collecting abiotic samples such as DOM and DOC would also be useful to see if there is

a correlation between carbon quality or concentration and biotic MeHg concentrations.

Finally, a comparison of the Hg results to harvesting variables like total harvest and clear cut would help understand whether these factors better explain spatial trends than drainage area.

References

- Adams, P., & Froehlich, H. (1984). Compaction of forest soils. USDA. A Pacific Northwest Extension Publication. <https://www.fs.usda.gov/rmrs/documents-and-media/compaction-forest-soils>
- Al-Reasi, H. A., Wood, C. M., & Smith, D. S. (2013). Characterization of freshwater natural dissolved organic matter (DOM): Mechanistic explanations for protective effects against metal toxicity and direct effects on organisms. *Environment International*, 59. <https://doi.org/10.1016/j.envint.2013.06.005>
- Atlantic Provinces Economic Council. (2003). The New Brunswick Forest industry: the potential economic impact of proposals to increase the wood supply. <http://leg-horizon.gnb.ca/e-repository/monographs/30000000043978/30000000043978.pdf>
- Ben-David, M., & Flaherty, E. A. (2012). Stable isotopes in mammalian research: a beginner's guide. *Journal of Mammalogy*, 93(2). <https://doi.org/10.1644/11-MAMM-S-166.1>
- Beschta, R. L. (1978). Long-term patterns of sediment production following road construction and logging in the Oregon Coast Range. *Water Resources Research*, 14(6), 1011–1016. <https://doi.org/10.1029/WR014i006p01011>
- Booth, D. L., Boulter, D. W. K., Neave, D. J., Rotherham, A. A., & Welsh, D. A. (1993). Natural forest landscape management: A strategy for Canada. *The Forestry Chronicle*, 69(2), 141–145. <https://doi.org/10.5558/tfc69141-2>
- Borgå, K., Kidd, K. A., Muir, D. C., Berglund, O., Conder, J. M., Gobas, F. A., Kucklick, J., Malm, O., & Powell, D. E. (2012). Trophic magnification factors: Considerations of ecology, ecosystems, and study design. *Integrated Environmental Assessment and Management*, 8(1), 64–84. <https://doi.org/10.1002/ieam.244>
- Bradley, P. M., Burns, D. A., Murray, K. R., Brigham, M. E., Button, D. T., Chasar, L. C., Marvin-DiPasquale, M., Lowery, M. A., & Journey, C. A. (2011). Spatial and seasonal variability of dissolved methylmercury in two stream basins in the Eastern United States. *Environmental Science & Technology*, 45(6). <https://doi.org/10.1021/es103923j>
- Bueler, C. M. (1984). Feeding preference of *Pteronarcys pictetii* (Plecoptera: Insecta) from a small, acidic, woodland stream. *The Florida Entomologist*, 67(3), 393–401. <https://doi.org/10.2307/3494718>
- Bundschuh, M., & McKie, B. G. (2016). An ecological and ecotoxicological perspective on fine particulate organic matter in streams. *Freshwater Biology*, 61(12). <https://doi.org/10.1111/fwb.12608>

- Cabana, G., & Rasmussen, J. B. (1994). Modelling food chain structure and contaminant bioaccumulation using stable nitrogen isotopes. *Nature*, 372(6503). doi: 10.1038/372255a0
- Campbell, I., & Doeg, T. (1989). Impact of timber harvesting and production on streams: A review. *Australian Journal of Marine and Freshwater Research*, 40(5), 519–539. <https://doi.org/10.1071/MF9890519>
- Caut, S., Angulo, E., & Courchamp, F. (2009). Variation in discrimination factors ($\Delta^{15}\text{N}$ and $\Delta^{13}\text{C}$): the effect of diet isotopic values and applications for diet reconstruction. *Journal of Applied Ecology*, 46(2). <https://doi.org/10.1111/j.1365-2664.2009.01620.x>
- Chételat, J., Richardson, M. C., MacMillan, G. A., Amyot, M., & Poulain, A. J. (2018). Ratio of methylmercury to dissolved organic carbon in water explains methylmercury bioaccumulation across a latitudinal gradient from north-temperate to arctic lakes. *Environmental Science & Technology*, 52(1). <https://doi.org/10.1021/acs.est.7b04180>
- Clayden, M. G., Kidd, K. A., Chételat, J., Hall, B. D., & Garcia, E. (2014). Environmental, geographic and trophic influences on methylmercury concentrations in macroinvertebrates from lakes and wetlands across Canada. *Ecotoxicology*, 23(2). <https://doi.org/10.1007/s10646-013-1171-9>
- Cummins, C.W. (1979). The multiple linkages of forests to streams. In Waring, R.H. (Ed.), *Forests: Fresh perspectives from ecosystem analysis: proceedings of the 40th annual biology colloquium* (pp. 191-198). Corvallis: Oregon State University Press.
- Daguené, V., McFall, E., Yumvihoze, E., Xiang, S., Amyot, M., & Poulain, A. J. (2012). Divalent base cations hamper Hg II uptake. *Environmental Science & Technology*, 46(12). doi: 10.1021/es300760e
- DeForest, D. K., Brix, K. v., & Adams, W. J. (2007). Assessing metal bioaccumulation in aquatic environments: The inverse relationship between bioaccumulation factors, trophic transfer factors and exposure concentration. *Aquatic Toxicology*, 84(2), 236–246. <https://doi.org/10.1016/j.aquatox.2007.02.022>
- DeNiro, M., & Epstein, S. (1981). Hydrogen isotope ratios of mouse tissues are influenced by a variety of factors other than diet. *Science*, 214(4527). <https://doi.org/10.1126/science.7313700>
- Doucett, R. R., Marks, J. C., Blinn, D. W., Caron, M., & Hungate, B. A. (2007). Measuring terrestrial subsidies to aquatic food webs using stable isotopes of hydrogen. *Ecology*, 88(6), 1587–1592. <https://doi.org/10.1890/06-1184>

- Downing, J. (2012). Global abundance and size distribution of streams and rivers. *Inland Waters*, 2(4). <https://doi.org/10.5268/IW-2.4.502>
- Dranguet, P., le Faucheur, S., & Slaveykova, V. I. (2017). Mercury bioavailability, transformations, and effects on freshwater biofilms. *Environmental Toxicology and Chemistry*, 36(12), 3194–3205. <https://doi.org/10.1002/etc.3934>
- Driscoll, C. T., Blette, V., Yan, C., Schofield, C. L., Munson, R., & Holsapple, J. (1995). The role of dissolved organic carbon in the chemistry and bioavailability of mercury in remote Adirondack lakes. *Water, Air, & Soil Pollution*, 80. <https://doi.org/10.1007/BF01189700>
- Eckley, C. S., Eagles-Smith, C., Tate, M. T., Kowalski, B., Danehy, R., Johnson, S. L., & Krabbenhoft, D. P. (2018). Stream mercury export in response to contemporary timber harvesting methods (Pacific Coastal Mountains, Oregon, USA). *Environmental Science & Technology*, 52(4), 1971–1980. <https://doi.org/10.1021/acs.est.7b05197>
- Eklöf, K., Schelker, J., Sørensen, R., Meili, M., Laudon, H., von Brömssen, C., & Bishop, K. (2014). Impact of Forestry on Total and Methyl-Mercury in Surface Waters: Distinguishing Effects of Logging and Site Preparation. *Environmental Science & Technology*, 48(9), 4690–4698. <https://doi.org/10.1021/es404879p>
- England, L. E., & Rosemond, A. D. (2004). Small reductions in forest cover weaken terrestrial-aquatic linkages in headwater streams. *Freshwater Biology*, 49(6). <https://doi.org/10.1111/j.1365-2427.2004.01219.x>
- Erdozain, M., Kidd, K. A., Emilson, E. J. S., Capell, S. S., Kreutzweiser, D. P., & Gray, M. A. (2021a). Forest management impacts on stream integrity at varying intensities and spatial scales: do abiotic effects accumulate spatially? *Science of The Total Environment*, 753. <https://doi.org/10.1016/j.scitotenv.2020.141968>
- Erdozain, M., Kidd, K., Emilson, E., Capell, S., Luu, T., & Gray, M. (2021b) Forest management impacts on stream integrity at varying intensities and spatial scales: do biological effects accumulate spatially. *Science of The Total Environment*, 763. <https://doi.org/10.1016/j.scitotenv.2020.144043>
- Erdozain, M., Kidd, K., Kreutzweiser, D., & Sibley, P. (2018). Linking stream ecosystem integrity to catchment and reach conditions in an intensively managed forest landscape. *Ecosphere*, 9(5). <https://doi.org/10.1002/ecs2.2278>
- Erdozain, M., Kidd, K., Kreutzweiser, D., & Sibley, P. (2019). Increased reliance of stream macroinvertebrates on terrestrial food sources linked to forest management intensity. *Ecological Applications*, 29(4). <https://doi.org/10.1002/eap.1889>

- Ericksen, J. A., Gustin, M. S., Schorran, D. E., Johnson, D. W., Lindberg, S. E., & Coleman, J. S. (2003). Accumulation of atmospheric mercury in forest foliage. *Atmospheric Environment*, 37(12). [https://doi.org/10.1016/S1352-2310\(03\)00008-6](https://doi.org/10.1016/S1352-2310(03)00008-6)
- Finlay, J. (2004). Patterns and controls of lotic algal stable carbon isotope ratios. *Limnology and Oceanography*, 49(3), 850–861. <https://doi.org/10.4319/lo.2004.49.3.0850>
- Fisher, S. G., & Likens, G. E. (1973). Energy Flow in Bear Brook, New Hampshire: An Integrative Approach to Stream Ecosystem Metabolism. *Ecological Monographs*, 43(4), 421–439. <https://doi.org/10.2307/1942301>
- France, R. L., & Peters, R. H. (1997). Ecosystem differences in the trophic enrichment of ^{13}C in aquatic food webs. *Canadian Journal of Fisheries and Aquatic Sciences*, 54(6). <https://doi.org/10.1139/f97-044>
- Fritz, K. M., Schofield, K. A., Alexander, L. C., McManus, M. G., Golden, H. E., Lane, C. R., Kepner, W. G., LeDuc, S. D., DeMeester, J. E., & Pollard, A. I. (2018). Physical and chemical connectivity of streams and riparian wetlands to downstream waters: a synthesis. *JAWRA Journal of the American Water Resources Association*, 54(2). <https://doi.org/10.1111/1752-1688.12632>
- Fry, B. (2006). *Stable isotope ecology*. Springer.
- Giles-Hansen, K., Li, Q., & Wei, X. (2019). The cumulative effects of forest disturbance and climate variability on streamflow in the Deadman River Watershed. *Forests*, 10(2), 1–16. <https://doi.org/10.3390/f10020196>
- Government of New Brunswick. (n.d.). Watershed protection. Retrieved October 3, 2020, from https://www2.gnb.ca/content/gnb/en/departments/elg/environment/content/land_waste/content/reference_manual/watershed_protection.html
- Grigal, D. F. (2002). Inputs and outputs of mercury from terrestrial watersheds: a review. *Environmental Reviews*, 10(1). <https://doi.org/10.1139/a01-013>
- Hall, B. D., Bodaly, R. A., Fudge, R. J. P., Rudd, J. W. M., & Rosenberg, D. M. (1997). Food as the dominant pathway of methylmercury uptake by fish. *Water, Air, and Soil Pollution*, 100, 13–24.
- Hintelmann, H., & Evans, R. D. (1997). Application of stable isotopes in environmental tracer studies - measurement of monomethylmercury (CH_3Hg^+) by isotope dilution ICP-MS and detection of species transformation. *Fresenius' Journal of Analytical Chemistry*, 358(3). <https://doi.org/10.1007/s002160050433>

- Horvat, M., Bloom, N. S., & Liang, L. (1993). Comparison of distillation with other current isolation methods for the determination of methyl mercury compounds in low level environmental samples. *Analytica Chimica Acta*, 281(1).
[https://doi.org/10.1016/0003-2670\(93\)85348-N](https://doi.org/10.1016/0003-2670(93)85348-N)
- Horvat, M., Liang, L., & Bloom, N. S. (1993). Comparison of distillation with other current isolation methods for the determination of methyl mercury compounds in low level environmental samples. *Analytica Chimica Acta*, 282(1).
[https://doi.org/10.1016/0003-2670\(93\)80364-Q](https://doi.org/10.1016/0003-2670(93)80364-Q)
- Iwamoto, R. N., Salo, E. O., Madej, M. A., & McComas, R. L. (1978). Sediment and water quality: A review of literature including a suggested approach for water quality criteria. The Environmental Protection Agency, 248.
<https://www.arlis.org/docs/vol1/Susitna/18/APA1811.pdf>
- Jardine, T. D., Hadwen, W. L., Hamilton, S. K., Hladyz, S., Mitrovic, S. M., Kidd, K. A., Tsoi, W. Y., Spears, M., Westhorpe, D. P., Fry, V. M., Sheldon, F., & Bunn, S. E. (2014a). Understanding and overcoming baseline isotopic variability in running waters. *River Research and Applications*, 30(2), 155–165.
<https://doi.org/10.1002/rra.2630>
- Jardine, T. D., Hadwen, W. L., Hamilton, S. K., Hladyz, S., Mitrovic, S. M., Kidd, K. A., Tsoi, W. Y., Spears, M., Westhorpe, D. P., Fry, V. M., Sheldon, F., & Bunn, S. E. (2014b). Understanding and overcoming baseline isotopic variability in running waters. *River Research and Applications*, 30(2). <https://doi.org/10.1002/rra.2630>
- Jardine, T. D., Kidd, K. A., & Cunjak, R. A. (2009). An evaluation of deuterium as a food source tracer in temperate streams of eastern Canada. *Journal of the North American Benthological Society*, 28(4). <https://doi.org/10.1899/09-046.1>
- Jardine, T. D., Kidd, K. A., & O'Driscoll, N. (2013). Food web analysis reveals effects of pH on mercury bioaccumulation at multiple trophic levels in streams. *Aquatic Toxicology*, 132–133, 46–52. <https://doi.org/10.1016/j.aquatox.2013.01.013>
- Jonsson, M., Polvi, L. E., Sponseller, R. A., & Stenroth, K. (2018). Catchment properties predict autochthony in stream filter feeders. *Hydrobiologia*, 815(1).
<https://doi.org/10.1007/s10750-018-3553-8>
- Kidd, K. A., Muir, D. C. G., Evans, M. S., Wang, X., Whittle, M., Swanson, H. K., Johnston, T., & Guildford, S. (2012). Biomagnification of mercury through lake trout (*Salvelinus namaycush*) food webs of lakes with different physical, chemical and biological characteristics. *Science of The Total Environment*, 438.
<https://doi.org/10.1016/j.scitotenv.2012.08.057>

- Kreutzweiser, D. P., Hazlett, P. W., & Gunn, J. M. (2008). Logging impacts on the biogeochemistry of boreal forest soils and nutrient export to aquatic systems: A review. *Environmental Reviews*, 16(NA), 157–179. <https://doi.org/10.1139/A08-006>
- Krieger, D. (2001). Economic value of forest ecosystem services: A review. <http://www.truevaluemetrics.org/DBpdfs/EcoSystem/The-Wilderness-Society-Ecosystem-Services-Value.pdf>
- Lavoie, R. A., Amyot, M., & Lapierre, J. (2019). Global meta-analysis on the relationship between mercury and dissolved organic carbon in freshwater environments. *Journal of Geophysical Research: Biogeosciences*, 124(6). <https://doi.org/10.1029/2018JG004896>
- Lavoie, R. A., Jardine, T. D., Chumchal, M. M., Kidd, K. A., & Campbell, L. M. (2013). Biomagnification of mercury in aquatic food webs: A worldwide meta-analysis. *Environmental Science & Technology*, 47(23), 13385–13394. <https://doi.org/10.1021/es403103t>
- Lazorchak, J. M., McCormick, F. H., Henry, T. R., & Herlihy, A. T. (2003). Contamination of fish in streams of the Mid-Atlantic Region: An approach to regional indicator selection and wildlife assessment. *Environmental Toxicology and Chemistry*, 22(3). <https://doi.org/10.1002/etc.5620220312>
- Leibowitz, S. G., Wigington, P. J., Schofield, K. A., Alexander, L. C., Vanderhoof, M. K., & Golden, H. E. (2018). Connectivity of streams and wetlands to downstream waters: an integrated systems framework. *JAWRA Journal of the American Water Resources Association*, 54(2). <https://doi.org/10.1111/1752-1688.12631>
- Lescord, G. L., Johnston, T. A., Branfireun, B. A., & Gunn, J. M. (2018). Percentage of methylmercury in the muscle tissue of freshwater fish varies with body size and age and among species. *Environmental Toxicology and Chemistry*, 37(10). <https://doi.org/10.1002/etc.4233>
- Likens, G. E., Bormann, F. H., & Johnson, N. M. (1969). Nitrification: importance to nutrient losses from a cutover forested ecosystem. *Science*, 163(3872), 1205–1206. <https://www.jstor.org/stable/1726549>
- MacDonald, L. H., & Coe, D. (2007). Influence of headwater streams on downstream reaches in forested areas. *Forest Science*, 53(2), 148–168.
- McCutchan, J., Lewis, W., Kendall, C., & McGrath, C. (2003). Variation in trophic shift for stable isotope ratios of carbon, nitrogen, and sulfur. *Oikos*, 102(2), 378–390. <http://www.jstor.org/stable/3548040>

- McNeely, C., Clinton, S., & Erbe, J. (2006). Landscape variation in C sources of scraping primary consumers in streams. *Journal of the North American Benthological Society*, 25(4), 787–799.
- Merritt, R., Cummins, K., & Berg, M. (2008). *An introduction to the aquatic insects of North America* (4th ed.). Kendall Hunt Publishers.
- Miller, E. K., Vanarsdale, A., Keeler, G. J., Chalmers, A., Poissant, L., Kamman, N. C., & Brulotte, R. (2005). Estimation and mapping of wet and dry mercury deposition across northeastern North America. *Ecotoxicology*, 14(1–2).
<https://doi.org/10.1007/s10646-004-6259-9>
- Miura, S., Amacher, M., Hofer, T., San-Miguel-Ayanz, J., Ernawati, & Thackway, R. (2015). Protective functions and ecosystem services of global forests in the past quarter-century. *Forest Ecology and Management*, 352, 35–46.
<https://doi.org/10.1016/j.foreco.2015.03.039>
- Molnar, J. L., & Kubiszewski, I. (2012). Managing natural wealth: Research and implementation of ecosystem services in the United States and Canada. *Ecosystem Services*, 2, 45–55. <https://doi.org/10.1016/j.ecoser.2012.09.005>
- Moore, R., & Wondzell, S. M. (2005). Physical hydrology and the effects of forest harvesting in the pacific northwest: a review. *Journal of the American Water Resources Association*, 41(4). <https://doi.org/10.1111/j.1752-1688.2005.tb03770.x>
- Mulholland, P. J., Helton, A. M., Poole, G. C., Hall, R. O., Hamilton, S. K., Peterson, B. J., Tank, J. L., Ashkenas, L. R., Cooper, L. W., Dahm, C. N., Dodds, W. K., Findlay, S. E. G., Gregory, S. v., Grimm, N. B., Johnson, S. L., McDowell, W. H., Meyer, J. L., Valett, H. M., Webster, J. R., ... Thomas, S. M. (2008). Stream denitrification across biomes and its response to anthropogenic nitrate loading. *Nature*, 452(7184), 202–205. <https://doi.org/10.1038/nature06686>
- Nakano, S., & Murakami, M. (2001). Reciprocal subsidies: dynamic interdependence between terrestrial and aquatic food webs. *Proceedings of the National Academy of Sciences*, 98(1). <https://doi.org/10.1073/pnas.98.1.166>
- National Research Council (US) Committee on the Toxicological Effects of Methylmercury Council (NRC) (2000). 1 Introduction. In *Toxicological Effects of Methylmercury* (pp. 13-30). Washington DC: National Academies Press.
<https://www.ncbi.nlm.nih.gov/books/NBK225769/>
- Natural Resources Canada, & Canadian Forest Services. (2019). The state of Canada's forest: annual report 2019. Government of Canada.
<https://d1ied5g1xfp8x8.cloudfront.net/pdfs/40084.pdf>

- Neary, D. G. (2017). Chapter 13. Forest management and water in the United States. In Garcia-Chevesich, D. G. Neary, D. F. Scott, R. G. Benyon, & T. Reyna (Eds.), *Forest management and the impact on water resources: a review of 13 countries* (pp. 180–203). Paris: UNESCO.
https://www.fs.fed.us/rm/pubs_journals/2017/rmrs_2017_garcia_chevesich_p001.pdf
- Neary, D. G. (2017). Forest Management and the impact on water resources: a review of 13 countries (A. Garcia-Chevesich, D. G. Neary, D. F. Scott, R. G. Benyon, & T. Reyna, Eds.; pp. 180–203). UNESCO.
https://www.fs.fed.us/rm/pubs_journals/2017/rmrs_2017_garcia_chevesich_p001.pdf
- Nislow, K. H., & Lowe, W. H. (2006). Influences of logging history and riparian forest characteristics on macroinvertebrates and brook trout (*Salvelinus fontinalis*) in headwater streams (New Hampshire, U.S.A.). *Freshwater Biology*, 51(2), 388–397.
<https://doi.org/10.1111/j.1365-2427.2005.01492.x>
- Ouédraogo, O., Chételat, J., & Amyot, M. (2015). Bioaccumulation and trophic transfer of mercury and selenium in African sub-tropical fluvial reservoirs food webs (Burkina Faso). *PLOS ONE*, 10(4). doi: 10.1371/journal.pone.0123048
- Pickhardt, P. C., Folt, C. L., Chen, C. Y., Klaue, B., & Blum, J. D. (2002). Algal blooms reduce the uptake of toxic methylmercury in freshwater food webs. *Proceedings of the National Academy of Sciences*, 99(7). <https://doi.org/10.1073/pnas.072531099>
- Pinheiro F. M.R, (2000). Effects of forest fires and clear-cutting on mercury loading to boreal lakes [Master's thesis, McGill University]. *National Library of Canada*.
https://www.collectionscanada.gc.ca/obj/s4/f2/dsk1/tape4/PQDD_0034/MQ64431.pdf
- Pinheiro, F. M. R. (2000). Effects of forest fires and clear-cutting on mercury loading to boreal lakes . In National Library of Canada.
https://www.collectionscanada.gc.ca/obj/s4/f2/dsk1/tape4/PQDD_0034/MQ64431.pdf
- Pirrone, N., Cinnirella, S., Feng, X., Finkelman, R. B., Friedli, H. R., Leaner, J., Mason, R., Mukherjee, A. B., Stracher, G. B., Streets, D. G., & Telmer, K. (2010). Global mercury emissions to the atmosphere from anthropogenic and natural sources. *Atmospheric Chemistry and Physics*, 10(13). <https://doi.org/10.5194/acp-10-5951-2010>
- Plague, G., Wallace, J. B., & Grubaugh, J. (1998). Linkages between trophic variability and distribution of *Pteronarcys* spp. (Plecoptera: Pteronarcyidae) along a stream continuum. *The American Midland Naturalist*, 139(2), 224–234.

- Porvari, P., Verta, M., Munthe, J., & Haapanen, M. (2003). Forestry practices increase mercury and methyl mercury output from boreal forest catchments. *Environmental Science & Technology*, 37(11). <https://doi.org/10.1021/es0340174>
- Post, D. M. (2002). Using stable isotopes to estimate trophic position: models, methods, and assumptions. *Ecology*, 83(3), 703–718. <https://doi.org/10.2307/3071875>
- Poste, A. E., Muir, D. C. G., Guildford, S. J., & Hecky, R. E. (2015). Bioaccumulation and biomagnification of mercury in African lakes: The importance of trophic status. *Science of The Total Environment*, 506–507. doi: 10.1016/j.scitotenv.2014.10.094
- Ravichandran, M. (2004). Interactions between mercury and dissolved organic matter—a review. *Chemosphere*, 55(3). <https://doi.org/10.1016/j.chemosphere.2003.11.011>
- Reinfelder, J. R., Fisher, N. S., Luoma, S. N., Nichols, J. W., & Wang, W.-X. (1998). Trace element trophic transfer in aquatic organisms: A critique of the kinetic model approach. *Science of The Total Environment*, 219(2–3). [https://doi.org/10.1016/S0048-9697\(98\)00225-3](https://doi.org/10.1016/S0048-9697(98)00225-3)
- Reinhart, B. L., Kidd, K. A., Curry, R. A., O’Driscoll, N. J., & Pavey, S. A. (2018). Mercury bioaccumulation in aquatic biota along a salinity gradient in the Saint John River estuary. *Journal of Environmental Sciences*, 68. <https://doi.org/10.1016/j.jes.2018.02.024>
- Richardson, J. S., & Danehy, R. J. (2007). A synthesis of the ecology of headwater streams and their riparian zones in temperate forests. *Forest Science*, 53(2), 131–147.
- Riva-Murray, K., Chasar, L. C., Bradley, P. M., Burns, D. A., Brigham, M. E., Smith, M. J., & Abrahamsen, T. A. (2011). Spatial patterns of mercury in macroinvertebrates and fishes from streams of two contrasting forested landscapes in the eastern United States. *Ecotoxicology*, 20(7). <https://doi.org/10.1007/s10646-011-0719-9>
- Riva-Murray, K., Richter, W., Roxanna Razavi, N., Burns, D. A., Cleckner, L. B., Burton, M., George, S. D., & Freehafer, D. (2020). Mercury in fish from streams and rivers in New York State: Spatial patterns, temporal changes, and environmental drivers. *Ecotoxicology*, 29(10). <https://doi.org/10.1007/s10646-020-02225-0>
- Skyllberg, U., Westin, M. B., Meili, M., & Björn, E. (2009). Elevated concentrations of methyl mercury in streams after forest clear-cut: a consequence of mobilization from soil or new methylation? *Environmental Science & Technology*, 43(22). <https://doi.org/10.1021/es900996z>

- Solomon, C. T., Cole, J. J., Doucett, R. R., Pace, M. L., Preston, N. D., Smith, L. E., & Weidel, B. C. (2009). The influence of environmental water on the hydrogen stable isotope ratio in aquatic consumers. *Oecologia*, 161(2).
<https://doi.org/10.1007/s00442-009-1370-5>
- Sustainable Forestry Initiative. (2015). SFI® works to ensure the health and future of our forests with the launch of the new SFI 2015-2019 standards and rules.
<https://www.forests.org/wp-content/uploads/OnePagerFeb4.pdf>
- Tank, J. L., & Dodds, W. K. (2003). Nutrient limitation of epilithic and epixylic biofilms in ten North American streams. *Freshwater Biology*, 48(6).
<https://doi.org/10.1046/j.1365-2427.2003.01067.x>
- Tsui, M. T. K., & Finlay, J. C. (2011). Influence of dissolved organic carbon on methylmercury bioavailability across Minnesota stream ecosystems. *Environmental Science & Technology*, 45(14). <https://doi.org/10.1021/es200332f>
- Tsui, M. T. K., Finlay, J. C., & Nater, E. A. (2009). Mercury bioaccumulation in a stream network. *Environmental Science & Technology*, 43(18), 7016–7022.
<https://doi.org/10.1021/es901525w>
- U.S. EPA. 2007. Method 7473 (SW-846): Mercury in solids and solutions by thermal decomposition, amalgamation, and atomic absorption spectrophotometry. United States Environmental Protection Agency, Washington, DC.
- Vander Zanden, H. B., Soto, D. X., Bowen, G. J., & Hobson, K. A. (2016). Expanding the isotopic toolbox: applications of hydrogen and oxygen stable isotope ratios to food web studies. *Frontiers in Ecology and Evolution*, 4.
<https://doi.org/10.3389/fevo.2016.00020>
- Vannote, R. L., Minshall, G. W., Cummins, K. W., Sedell, J. R., & Cushing, C. E. (1980). The river continuum concept. *Canadian Journal of Fisheries and Aquatic Sciences*, 37(1). <https://doi.org/10.1139/f80-017>
- Walters, D. M., Raikow, D. F., Hammerschmidt, C. R., Mehling, M. G., Kovach, A., & Oris, J. T. (2015). Methylmercury bioaccumulation in stream food webs declines with increasing primary production. *Environmental Science & Technology*, 49(13).
<https://doi.org/10.1021/acs.est.5b00911>
- Ward, D. M., Nislow, K. H., & Folt, C. L. (2010). Bioaccumulation syndrome: identifying factors that make some stream food webs prone to elevated mercury bioaccumulation. *Annals of the New York Academy of Sciences*, 1195(1).
<https://doi.org/10.1111/j.1749-6632.2010.05456.x>

- Watras, C. J., Back, R. C., Halvorsen, S., Hudson, R. J. M., Morrison, K. A., & Wentz, S. P. (1998). Bioaccumulation of mercury in pelagic freshwater food webs. *Science of The Total Environment*, 219(2–3). [https://doi.org/10.1016/S0048-9697\(98\)00228-9](https://doi.org/10.1016/S0048-9697(98)00228-9)
- Willacker, J. J., Eagles-Smith, C. A., Kowalski, B. M., Danehy, R. J., Jackson, A. K., Adams, E. M., Evers, D. C., Eckley, C. S., Tate, M. T., & Krabbenhoft, D. P. (2019). Timber harvest alters mercury bioaccumulation and food web structure in headwater streams. *Environmental Pollution*, 253. <https://doi.org/10.1016/j.envpol.2019.07.025>
- Woodcock, P., Edwards, D. P., Newton, R. J., Vun Khen, C., Bottrell, S. H., & Hamer, K. C. (2013). Impacts of intensive logging on the trophic organisation of ant communities in a biodiversity hotspot. *PLoS ONE*, 8(4). doi: 10.1371/journal.pone.0060756
- Wulder, M. A., Kurz, W. A., & Gillis, M. (2004). National level forest monitoring and modeling in Canada. *Progress in Planning*, 61(4), 365–381. [https://doi.org/10.1016/S0305-9006\(03\)00069-2](https://doi.org/10.1016/S0305-9006(03)00069-2)
- Yang, Y., Yanai, R. D., Driscoll, C. T., Montesdeoca, M., & Smith, K. T. (2018). Concentrations and content of mercury in bark, wood, and leaves in hardwoods and conifers in four forested sites in the northeastern USA. *PLOS ONE*, 13(4). <https://doi.org/10.1371/journal.pone.0196293>
- Ylla, I., Romani, A. M., & Sabater, S. (2007). Differential effects of nutrients and light on the primary production of stream algae and mosses. *Fundamental and Applied Limnology / Archiv Für Hydrobiologie*, 170(1). <https://doi.org/10.1127/1863-9135/2007/0170-001>
- Zhang, C., Jamieson, R. C., Meng, F.-R., Gordon, R., & Bourque, C. P.-A. (2016). Projecting in-stream dissolved organic carbon and total mercury concentrations in small watersheds following forest growth and clearcutting. *Water, Air, & Soil Pollution*, 227(9), 1–13. <https://doi.org/10.1007/s11270-016-3017-6>

5.0 Supplementary Information

5.1 Isotope data

5.1.1 Carbon, nitrogen, and hydrogen data

Table 5: Average isotopes values for biota and food sources for each stream site and number of replicates per sample

Basin	Site	Sample	$\delta^{13}\text{C}$			$\delta^{15}\text{N}$			$\delta^2\text{H}$			n
			mean	\pm	sd	mean	\pm	sd	mean	\pm	sd	
<i>Extensive</i>	NBE1	Agnestia	-25.5			6.4			-229.5			1
	NBE1	Baetidae	-25.6			4.3			-241.8			1
	NBE1	Biofilm	-30.2			2.5			-246.3			1
	NBE1	Ceratopsyche	-27.0			5.5			-236.6			1
	NBE1	CPOM	-29.2	\pm	0.37	-0.9	\pm	0.26	-137.3	\pm	4.28	3
	NBE1	Dolophilodes	-26.1			5.2			-207.1			1
	NBE1	Epeorus	-28.0			4.1			-204.1			1
	NBE1	FPOM	-27.5	\pm	0.34	2.4	\pm	0.91	-126.0	\pm	2.56	3
	NBE1	Glossosoma	-27.3			3.7			-224.9			1
	NBE1	Isogenoides	-25.0			4.5			-206.3			1
	NBE1	Paraleptophlebia	-25.2			5.7			-182.8			1
	NBE1	Pteronarcys	-28.1			3.5			-173.8			1
	NBE1	Sculpin	-25.9	\pm	1.10	8.5	\pm	0.34	-216.7	\pm	10.94	10
	NBE1	Sweltsa	-26.0			6.6			-183.8			1
	NBE2	Agnestia	-29.1			5.3			-223.7			1
	NBE2	Baetidae	-29.6			4.0			-252.5			1
	NBE2	Biofilm	-32.7			3.3			-246.8			1
	NBE2	Ceratopsyche	-29.7			4.9			-221.2			1
	NBE2	CPOM	-29.3	\pm	0.58	-0.5	\pm	0.46	-152.0	\pm	10.51	3
	NBE2	Dolophilodes	-28.6			4.6						1
	NBE2	Epeorus	-32.3			3.3			-214.9			1
	NBE2	FPOM	-27.8	\pm	0.36	2.3	\pm	0.40	-125.9	\pm	13.83	3
	NBE2	Glossosoma	-28.2			3.4			-239.5			1
	NBE2	Pteronarcys	-27.8			2.3			-148.8			1
	NBE2	Sculpin	-28.6	\pm	0.66	7.8	\pm	0.40	-206.8	\pm	12.24	10
	NBE2	Sweltsa	-27.8			5.9			-188.8			1
	NBE3	Baetidae	-31.7			3.7			-243.8			1
	NBE3	Biofilm	-33.9			3.0			-249.2			1
	NBE3	Ceratopsyche	-29.0			4.9			-170.9			1
	NBE3	CPOM	-29.9	\pm	0.83	-1.6	\pm	0.51	-140.6	\pm	4.63	3
NBE3	Diura	-29.4			6.1			-185.3			1	
NBE3	Dolophilodes	-28.6			4.4			-169.0			1	

NBE3	FPOM	-27.6 ± 0.08	2.3 ± 0.20	-133.2 ± 4.49	3
NBE3	Glossosoma	-30.0	2.8	-245.8	1
NBE3	Heptagenia	-29.4	4.3	-199.0	1
NBE3	Paraleptophlebia	-28.3	4.1	-166.3	1
NBE3	Pteronarcys	-33.5	3.0	-193.5	1
NBE3	Sculpin	-28.1 ± 0.77	7.4 ± 0.27	-193.8 ± 7.39	10
NBE3	Sweltsa	-27.9	6.1	-173.2	1
NBE4	Agnetia	-26.8	7.4	-165.7	1
NBE4	Baetidae	-28.7	5.0	-250.6	1
NBE4	Biofilm	-34.2	3.3	-244.3	1
NBE4	Ceratopsyche	-27.5	7.5	-208.5	1
NBE4	CPOM	-29.4 ± 0.53	0.7 ± 0.34	-149.4 ± 7.07	3
NBE4	Diura	-27.2	7.1	-174.0	1
NBE4	Dolophilodes	-27.4	5.8	-190.4	1
NBE4	Epeorus	-31.2	4.3	-210.7	1
NBE4	FPOM	-27.9 ± 0.14	2.9 ± 0.31	-119.8 ± 9.92	3
NBE4	Glossosoma	-30.8	4.4	-257.9	1
NBE4	Isogenoides	-27.2	5.7	-191.9	1
NBE4	Paraleptophlebia	-26.3	5.4	-171.6	1
NBE4	Pteronarcys	-28.5	4.2	-158.9	1
NBE4	Sculpin	-27.0 ± 0.70	10.6 ± 0.34	-200.3 ± 13.86	5
NBE4	Sweltsa	-26.4	9.0	-157.7	1
NBE5	Agnetia	-28.2	6.1	-197.1	1
NBE5	Baetidae	-29.7	4.5	-247.1	1
NBE5	Biofilm	-32.8	4.1	-244.8	1
NBE5	Ceratopsyche	-28.6	5.3	-200.8	1
NBE5	CPOM	-28.9 ± 0.34	-0.8 ± 0.64	-146.2 ± 8.76	3
NBE5	Diura	-28.0	6.7	-169.5	1
NBE5	Dolophilodes	-29.2	4.6	-185.8	1
NBE5	Epeorus	-32.4	4.1	-219.1	1
NBE5	FPOM	-28.1 ± 0.06	2.2 ± 0.74	-122.5 ± 7.14	3
NBE5	Glossosoma	-30.5	3.4	-235.9	1
NBE5	Heptagenia	-26.8	4.7	-209.6	1
NBE5	Maccaffertium	-26.6	4.0	-208.3	1
NBE5	Paraleptophlebia	-27.0	4.6	-172.0	1
NBE5	Pteronarcys	-29.0	2.6	-151.4	1
NBE5	Sculpin	-27.8 ± 0.51	8.1 ± 0.40	-200.1 ± 13.52	10
NBE5	Sweltsa	-26.8	7.1	-172.3	1
NBE6	Baetidae	-32.6	5.4	-228.3	1
NBE6	Biofilm	-34.3	4.8	-247.0	1
NBE6	Ceratopsyche	-28.7	5.8	-170.0	1

	NBE6	CPOM	-29.4 ± 0.47	-1.4 ± 0.23	-150.3 ± 8.97	3
	NBE6	Diura	-30.2	6.7	-177.5	1
	NBE6	Dolophilodes	-28.6	4.6	-145.0	1
	NBE6	Epeorus	-33.9	4.8	-211.2	1
	NBE6	FPOM	-28.0 ± 0.20	1.6 ± 0.83	-123.4 ± 12.79	3
	NBE6	Glossosoma	-30.9	4.2	-236.5	1
	NBE6	Paraleptophlebia	-28.4	4.4	-151.7	1
	NBE6	Pteronarcys	-29.3	2.7	-151.3	1
	NBE6	Sculpin	-29.0 ± 0.75	8.8 ± 0.24	-203.1 ± 10.40	6
	NBE6	Sweltsa	-27.9	6.9	-166.2	1
<i>Intensive</i>	NBI1	Agnestia	-30.6	4.8	-201.1	1
	NBI1	Baetidae	-31.6	2.8	-240.2	1
	NBI1	Biofilm	-33.5	1.1	-248.7	1
	NBI1	Ceratopsyche	-30.4	4.0	-217.5	1
	NBI1	CPOM	-28.6 ± 0.60	-1.2 ± 0.45	-159.3 ± 3.48	3
	NBI1	Dolophilodes	-28.9	3.7	-186.7	1
	NBI1	Epeorus	-33.2	2.8	-215.3	1
	NBI1	Ephemerella	-30.5	1.9	-200.9	1
	NBI1	FPOM	-28.4 ± 0.23	1.6 ± 0.66	-129.7 ± 13.20	3
	NBI1	Glossosoma	-32.5	2.0	-224.0	1
	NBI1	Isogenoides	-30.2	3.8	-202.9	1
	NBI1	Paraleptophlebia	-28.8 0.46	4.1 1.13	-181.2 2.20	2
	NBI1	Pteronarcys	-30.7	2.4	-207.4	1
	NBI1	Sculpin	-29.6 ± 0.51	7.2 ± 0.43	-198.1 ± 9.48	10
	NBI1	Sweltsa	-29.0	5.2	-175.1	1
	NBI1	Tipula	-30.7	1.0	-173.3	1
	NBI2	Baetidae	-36.1	3.4	-229.4	1
	NBI2	Biofilm	-37.4	2.1	-247.7	1
	NBI2	Ceratopsyche	-31.3	4.7	-214.1	1
	NBI2	CPOM	-29.0 ± 0.51	-1.0 ± 0.39	-137.3 ± 2.92	3
	NBI2	Diura	-31.1	5.0	-172.2	1
	NBI2	Dolophilodes	-29.5	3.6	-157.3	1
	NBI2	Epeorus	-36.3	2.5	-207.5	1
	NBI2	FPOM	-27.8 ± 0.07	2.5 ± 0.05	-115.9 ± 4.40	3
	NBI2	Glossosoma	-37.0	2.1	-222.2	1
	NBI2	Heptagenia	-31.1	2.7	-170.3	1
	NBI2	Isogenoides	-31.2	4.2	-174.8	1
	NBI2	Maccaffertium	-32.0	2.8	-178.6	1
	NBI2	Pteronarcys	-28.2	2.1	-149.5	1
	NBI2	Sculpin	-31.2 ± 0.69	6.7 ± 0.53	-201.9 ± 12.51	5
	NBI2	Sweltsa	-28.9	5.5	-170.5	1

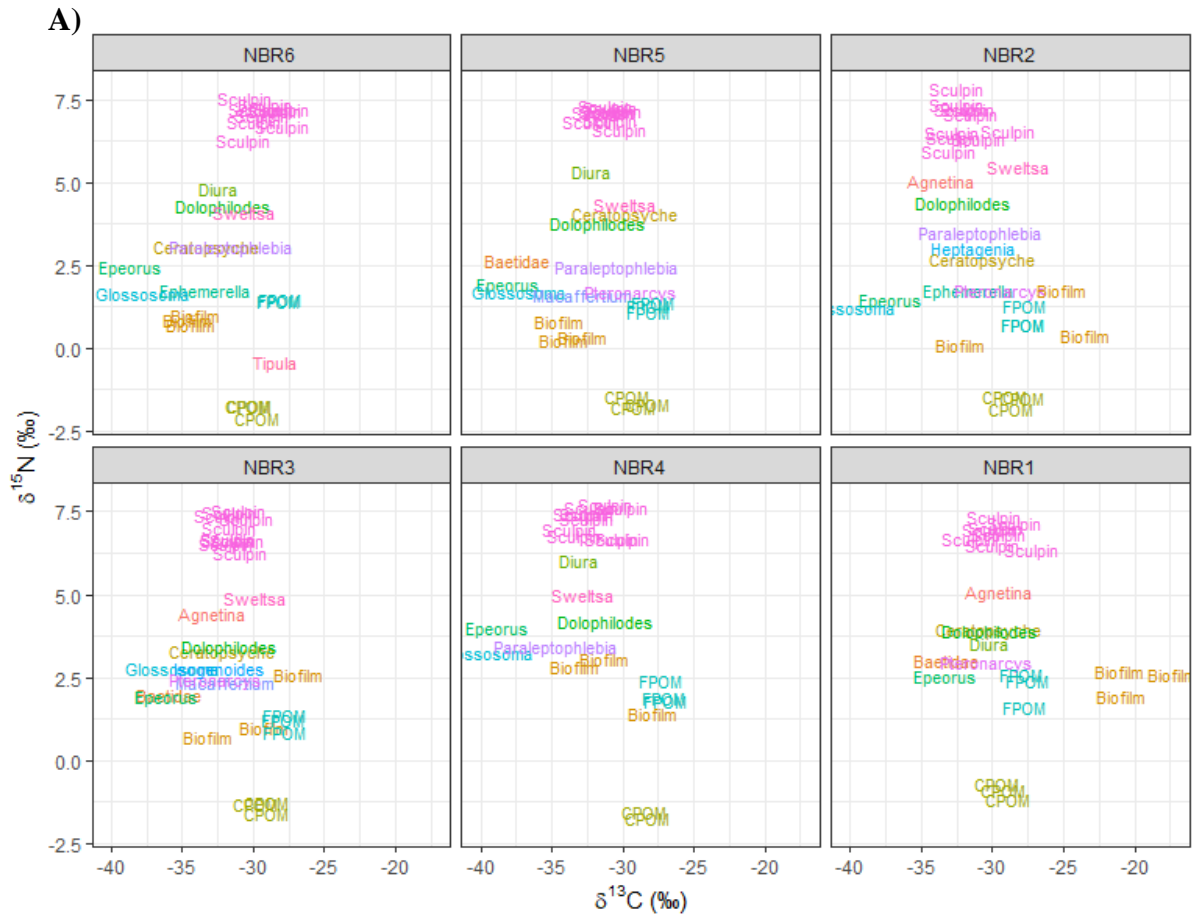
NBI3	Baetidae	-35.0		3.6		-242.3		1
NBI3	Biofilm	-38.1		2.2		-249.5		1
NBI3	Ceratopsyche	-30.2		4.1		-162.6		1
NBI3	CPOM	-29.6	± 0.31	-1.1	± 0.32	-151.1	± 8.05	3
NBI3	Diura	-30.7		5.8		-172.5		1
NBI3	Dolophilodes	-29.3		4.4		-146.8		1
NBI3	Ephemerella	-30.9		2.1		-174.4		1
NBI3	FPOM	-28.6	± 0.16	1.4	± 0.27	-120.1	± 9.50	3
NBI3	Glossosoma	-37.7		2.2		-232.8		1
NBI3	Heptagenia	-32.2		4.3		-176.6		1
NBI3	Paraleptophlebia	-29.3		4.1		-152.2		1
NBI3	Sculpin	-30.8	± 0.84	7.3	± 0.38	-179.4	± 11.13	10
NBI3	Sweltsa	-29.3	± 0.28	5.5	± 0.08	-157.9	± 0.59	2
NBI3	Tipula	-28.7		-1.2		-149.0		1
NBI4	Baetidae	-32.5		2.8		-260.2		1
NBI4	Biofilm	-36.7		2.1		-248.9		1
NBI4	Ceratopsyche	-30.1		3.3		-207.1		1
NBI4	CPOM	-28.6	± 0.63	-1.4	± 0.14	-158.0	± 7.90	3
NBI4	Dolophilodes	-29.4		3.9		-180.6		1
NBI4	Ephemerella	-29.5		1.8		-176.7		1
NBI4	FPOM	-28.0	± 0.31	2.1	± 0.34	-127.4	± 13.18	3
NBI4	Glossosoma	-36.3		2.1		-249.1		1
NBI4	Heptagenia	-30.2		2.8		-196.9		1
NBI4	Isogenoides	-31.1		3.6		-218.9		1
NBI4	Maccaffertium	-28.4		3.2		-196.7		1
NBI4	Pteronarcys	-30.0		1.3		-169.9		1
NBI4	Sculpin	-29.8	± 0.76	7.5	± 0.42	-197.6	± 8.75	10
NBI4	Sweltsa	-28.5		5.3		-175.3		1
NBI4	Tipula	-29.2		-0.4		-157.6		1
NBI5	Baetidae	-31.3		2.9		-272.3		1
NBI5	Biofilm	-33.9		2.8		-249.3		1
NBI5	Ceratopsyche	-30.1		3.9		-225.2		1
NBI5	CPOM	-29.4	± 0.25	-1.4	± 0.22	-150.5	± 2.21	3
NBI5	Dolophilodes	-30.0		4.6		-198.9		1
NBI5	FPOM	-28.1	± 0.28	1.7	± 0.35	-145.0	± 6.71	3
NBI5	Glossosoma	-33.5		2.8		-254.1		1
NBI5	Heptagenia	-29.8		3.7		-190.5		1
NBI5	Isogenoides	-30.3		4.2		-200.9		1
NBI5	Maccaffertium	-29.7		3.2		-229.1		1
NBI5	Pteronarcys	-28.2		2.1		-160.4		1
NBI5	Sculpin	-29.0	± 0.55	7.5	± 0.43	-201.6	± 6.08	9

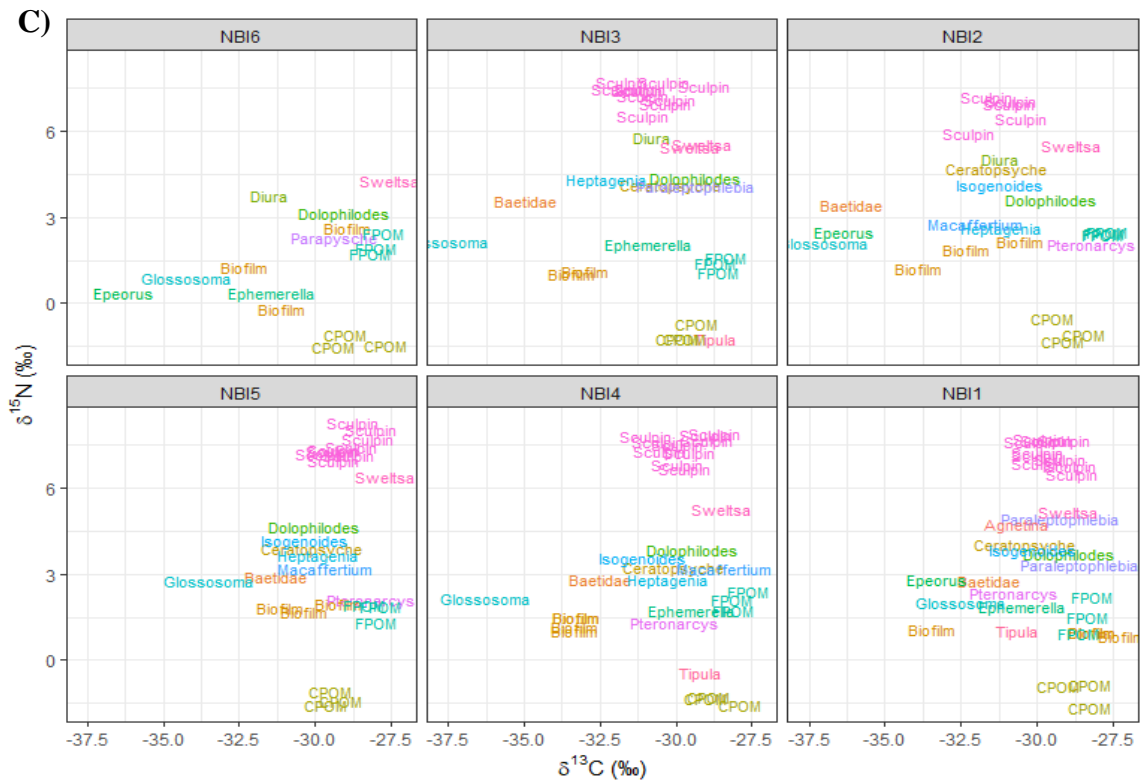
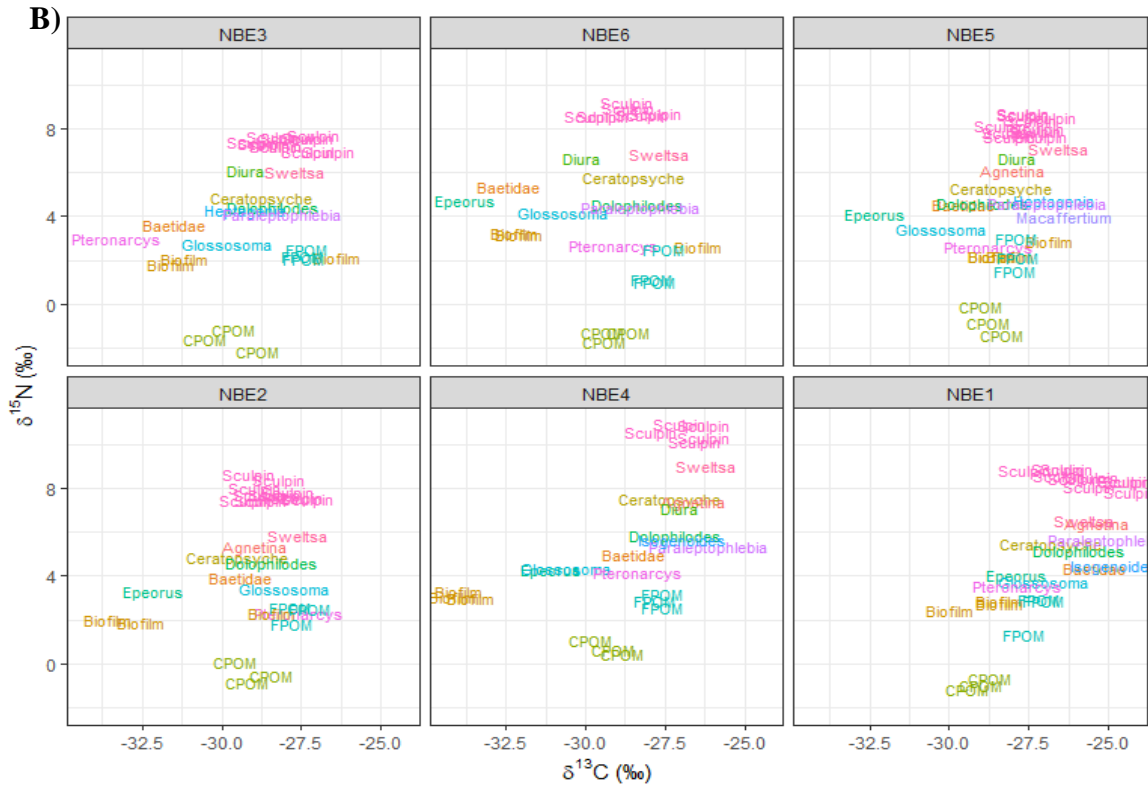
	NBI5	Sweltsa	-27.7		6.4		-172.1		1
	NBI6	Biofilm	-36.6		0.4		-252.4		1
	NBI6	CPOM	-28.7	± 0.89	-1.4	± 0.24	-148.1	± 9.24	3
	NBI6	Diura	-31.4		3.8		-165.3		1
	NBI6	Dolophilodes	-29.0		3.2		-172.1		1
	NBI6	Epeorus	-36.2		0.4		-212.5		1
	NBI6	Ephemerella	-31.5		0.4		-151.0		1
	NBI6	FPOM	-28.0	± 0.21	2.0	± 0.37	-136.7	± 5.61	3
	NBI6	Glossosoma	-34.2		0.9		-188.0		1
	NBI6	Parapysche	-29.4		2.3		-150.8		1
	NBI6	Sweltsa	-27.5		4.3		-152.1		1
<i>Minimally</i>	NBR1	Agnestia	-29.5		5.1		-186.9		1
	NBR1	Baetidae	-33.2		3.0		-267.9		1
	NBR1	Biofilm	-33.6		3.0		-251.2		1
	NBR1	Ceratopsyche	-30.2		4.0		-206.9		1
	NBR1	CPOM	-29.2	± 0.37	-0.9	± 0.23	-159.4	± 2.62	3
	NBR1	Diura	-30.0		3.6		-206.8		1
	NBR1	Dolophilodes	-30.1		3.9		-194.7		1
	NBR1	Epeorus	-33.1		2.6		-225.6		1
	NBR1	FPOM	-27.7	± 0.25	2.2	± 0.52	-122.1	± 7.58	3
	NBR1	Pteronarcys	-30.4		3.0		-215.5		1
	NBR1	Sculpin	-29.5	1.30	6.9	0.32	-199.8	10.73	8
	NBR2	Agnestia	-33.6		5.0		-187.4		1
	NBR2	Biofilm	-40.6		1.2		-251.5		1
	NBR2	Ceratopsyche	-30.8		2.7		-218.6		1
	NBR2	CPOM	-28.5	± 0.62	-1.6	± 0.20	-165.0	± 6.64	3
	NBR2	Dolophilodes	-32.1		4.4		-195.7		1
	NBR2	Epeorus	-37.0		1.5		-205.3		1
	NBR2	Ephemerella	-31.7		1.8		-203.7		1
	NBR2	FPOM	-27.8	± 0.07	0.9	± 0.32	-137.2	± 24.56	3
	NBR2	Glossosoma	-40.2		1.2		-205.0		1
	NBR2	Heptagenia	-31.2		3.0		-170.1		1
	NBR2	Paraleptophlebia	-30.7		3.5				1
	NBR2	Pteronarcys	-29.4		1.8		-194.5		1
	NBR2	Sculpin	-31.9	± 1.26	6.8	± 0.58	-195.5	± 10.34	10
	NBR2	Sweltsa	-28.2		5.5		-166.8		1
	NBR3	Agnestia	-32.9		4.4		-205.6		1
	NBR3	Baetidae	-35.9		2.0		-284.2		1
	NBR3	Biofilm	-36.4		2.0		-250.0		1
	NBR3	Ceratopsyche	-32.2		3.3		-217.6		1
	NBR3	CPOM	-29.3	± 0.45	-1.4	± 0.17	-158.1	± 2.30	3

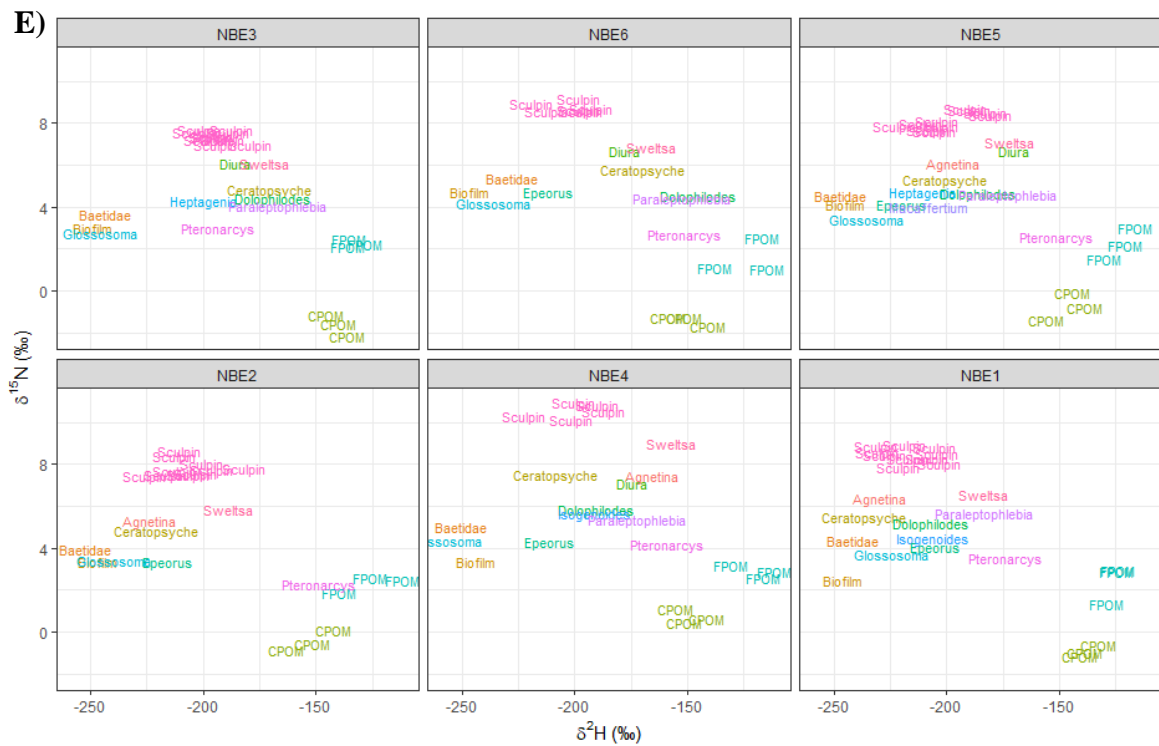
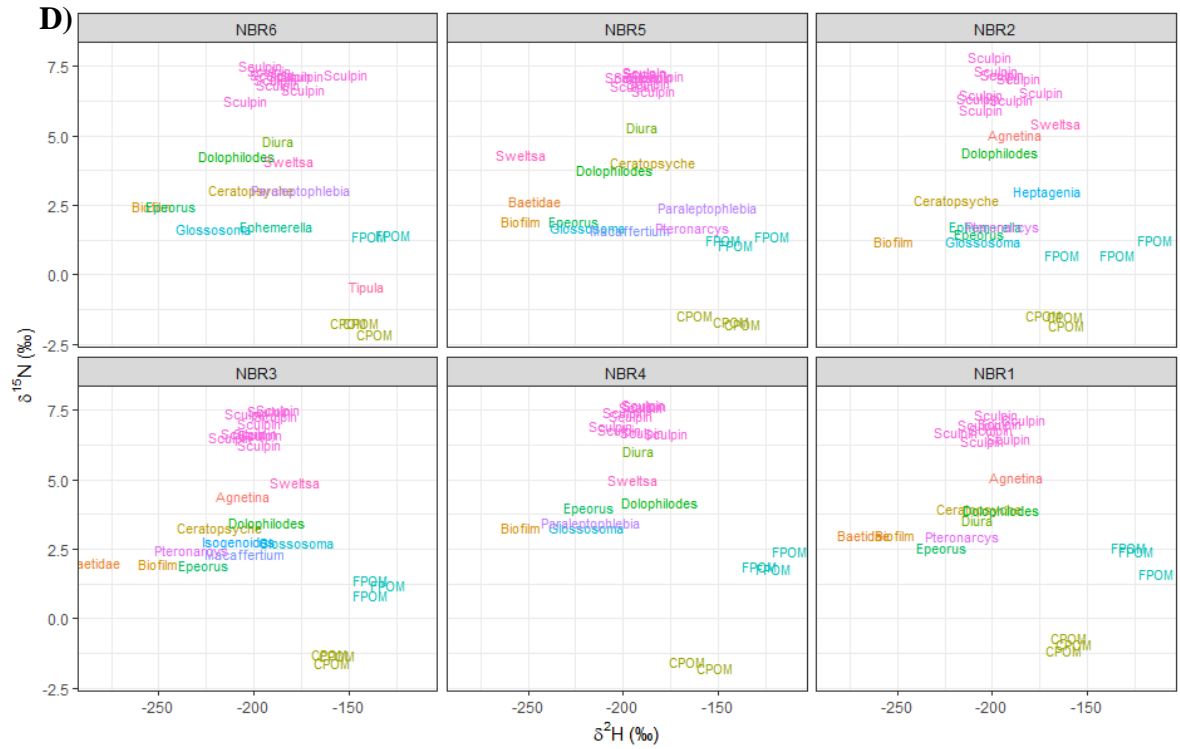
NBR3	Dolophilodes	-31.7		3.5		-193.1		1
NBR3	Epeorus	-35.9		2.0		-225.5		1
NBR3	FPOM	-27.8	± 0.06	1.2	± 0.28	-135.4	± 5.42	3
NBR3	Glossosoma	-35.7		2.8		-177.8		1
NBR3	Isogenoides	-32.4		2.8		-208.3		1
NBR3	Macaffertium	-31.9		2.4		-204.7		1
NBR3	Pteronarcys	-32.6		2.5		-232.7		1
NBR3	Sculpin	-31.4	± 0.55	7.0	± 0.45	-197.5	± 7.79	10
NBR3	Sweltsa	-29.9		4.9		-178.5		1
NBR4	Biofilm	-40.0		3.3		-253.4		1
NBR4	CPOM	-28.3	± 0.13	-1.6	± 0.16	-158.4	± 10.35	2
NBR4	Diura	-32.9		6.0		-191.2		1
NBR4	Dolophilodes	-31.2		4.2		-180.0		1
NBR4	Epeorus	-38.7		4.0		-216.6		1
NBR4	FPOM	-27.1	± 0.17	2.0	± 0.34	-120.4	± 7.99	3
NBR4	Glossosoma	-39.6		3.3		-219.2		1
NBR4	Paraleptophlebia	-34.6		3.5		-216.0		1
NBR4	Sculpin	-31.9	± 1.33	7.2	± 0.41	-193.0	± 8.72	10
NBR4	Sweltsa	-32.8		5.0		-194.7		1
NBR5	Baetidae	-37.5		2.6		-246.2		1
NBR5	Biofilm	-38.3		1.9		-253.9		1
NBR5	Ceratopsyche	-29.9		4.1		-184.1		1
NBR5	CPOM	-29.0	± 0.69	-1.6	± 0.17	-147.0	± 13.03	3
NBR5	Diura	-32.1		5.3		-189.1		1
NBR5	Dolophilodes	-31.7		3.8		-204.2		1
NBR5	Epeorus	-37.9		1.9		-224.9		1
NBR5	FPOM	-28.1	± 0.20	1.3	± 0.15	-136.5	± 13.32	3
NBR5	Glossosoma	-37.4		1.7		-218.7		1
NBR5	Macaffertium	-32.9		1.6		-196.4		1
NBR5	Paraleptophlebia	-30.2		2.4		-154.8		1
NBR5	Pteronarcys	-29.4		1.7		-163.4		1
NBR5	Sculpin	-31.0	± 0.60	7.1	± 0.22	-188.4	± 5.92	9
NBR5	Sweltsa	-29.9		4.3		-253.6		1
NBR6	Biofilm	-38.9		2.5		-253.7		1
NBR6	Ceratopsyche	-33.2		3.1		-201.4		1
NBR6	CPOM	-30.0	± 0.35	-1.9	± 0.23	-142.9	± 6.80	3
NBR6	Diura	-32.2		4.8		-186.4		1
NBR6	Dolophilodes	-32.0		4.3		-208.8		1
NBR6	Epeorus	-38.5		2.5		-242.5		1
NBR6	Ephemerella	-33.3		1.8		-187.9		1
NBR6	FPOM	-28.2	± 0.09	1.4	± 0.03	-132.9	± 8.76	2

NBR6	Glossosoma	-37.8	1.7	-221.5	1
NBR6	Paraleptophlebia	-31.4	3.1	-174.6	1
NBR6	Sculpin	-29.3 ± 0.97	7.1 ± 0.36	-183.7 ± 14.78	10
NBR6	Sweltsa	-30.7	4.1	-181.5	1
NBR6	Tipula	-28.5	-0.4	-140.9	1

5.1.2 Isotope biplots ($\delta^{15}N$ vs $\delta^{13}C$ and $\delta^{15}N$ vs δ^2H)







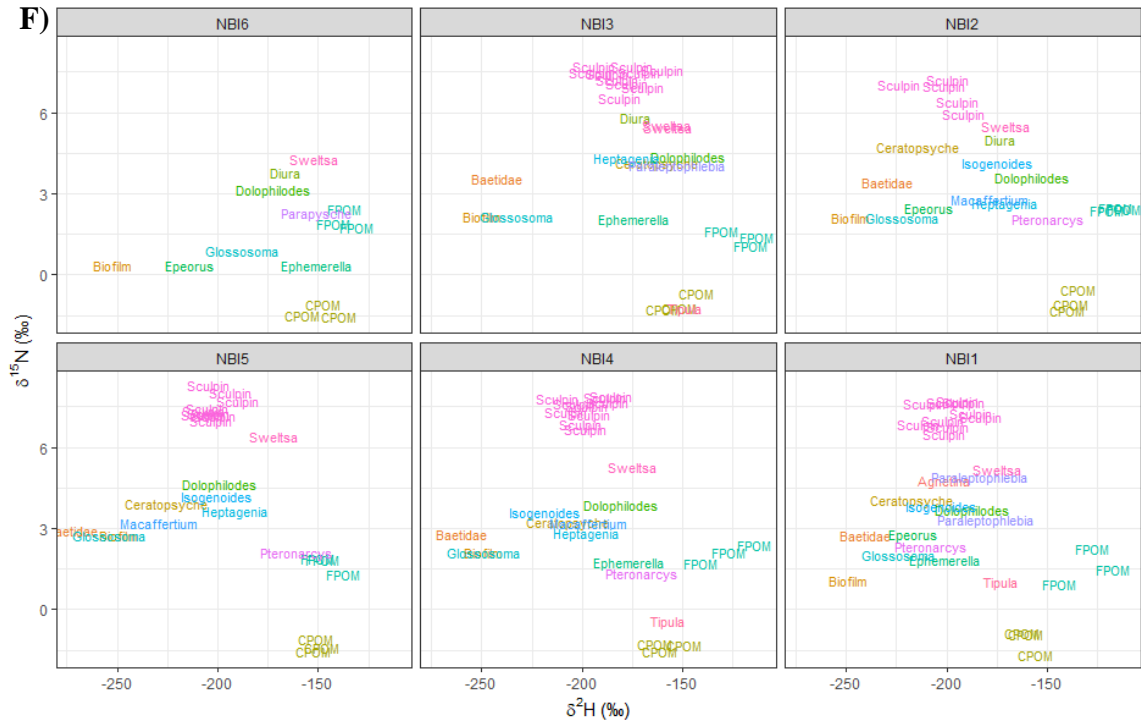


Figure 14: Isotope biplots for food webs of each six sites within the three basins showing either A-C) $\delta^{15}\text{N}$ vs $\delta^{13}\text{C}$ or D-F) $\delta^{15}\text{N}$ vs $\delta^2\text{H}$. Basins are ordered with the minimally managed basin first (NBR), followed by the extensively managed (NBE), then the intensively managed (NBI). Sites are ordered from most upstream from top left to right.

5.2 THg, MeHg and %MeHg in Sculpin

MeHg in a subset of male and female sculpin ($n=5-8/\text{basin}$) ranged from 167 to 588 ng/g dw and % MeHg ranged from 68% to 85% (Figure 15). MeHg measurements in sculpin did not show any significant differences among basins ($p=0.51-0.90$).

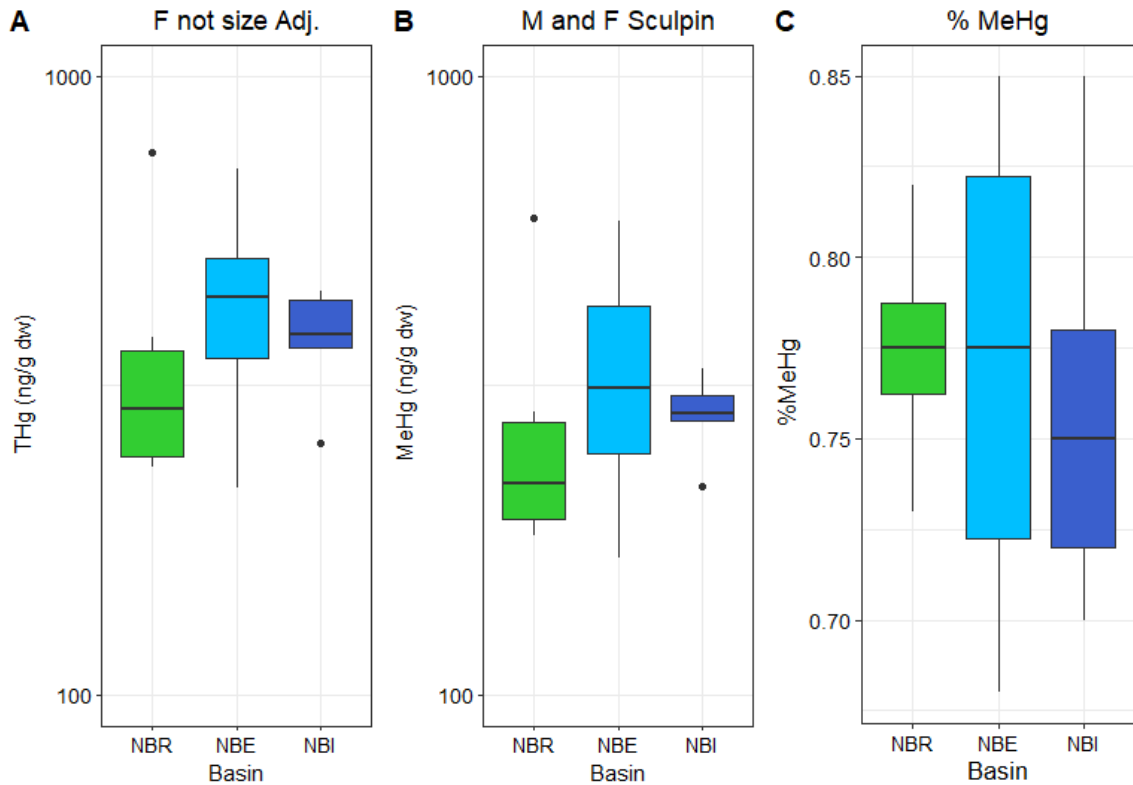


Figure 15: Boxplots showing the differences in different metrics of Hg in slimy sculpin sampled in 2018 in three basins in northern New Brunswick, Canada with varying forest management intensity (5-6 sites/basin). A) shows the differences unadjusted female fish (n=80) among basins. B) shows the difference in MeHg in a subset of sculpin run for MeHg and THg (n= 19). C) shows the difference in %MeHg calculated by dividing MeHg by THg in the 19 fish. Colours represent different basins, green is the minimal basin (NBR), light blue is the extensive basin (NBE), and dark blue is the intensive basin (NBI).

5.3 Mercury entering the food web by proxy with intercept

5.3.1 Intercept comparison of stream sites within basin

Table 6: Intercepts values for each site (n=18) in order of upstream to downstream separated by basin calculated from $\log_{10}\text{Hg}=\delta^{15}\text{N}+\text{Basin}$. Sites were located in northern New Brunswick, Canada in 2018.

Site	Intercepts		
	Minimal	Extensive	Intensive
upstream	0.0414	0.467	NA
2 nd smallest	0.291	0.474	0.272
3 rd smallest	0.293	0.123	0.321
4 th smallest	0.279	0.425	0.184
2 nd largest	0.139	-0.0025	0.353
downstream	0.223	0.18	0.362

Table 7: Output from the ANCOVA analysis to test for differences in intercept of MeHg, or THg, within three basins in northern New Brunswick, Canada in 2018 (6 sites/basin). *p* values for the terms are included for the main effect terms, $\delta^{15}\text{N}$ and Site calculated from $\log_{10}\text{Hg}=\delta^{15}\text{N}+\text{Site}$. Significant *p* values ($p<0.05$) are bolded.

	<i>p</i> $\delta^{15}\text{N}$	<i>p</i> Site
Minimal	<0.001	0.330
Extensive	<0.001	<0.001
Intensive	<0.001	0.479

There were significant differences in the intercepts within the extensively harvested basin, while the minimal and intensive basin intercepts did not differ (Table 7). In the extensive basin, the second largest stream had an intercept smaller than three of the four intercepts upstream (the third smallest not being greater) that suggests that more MeHg is entering the food web in upstream sites than one of the downstream sites ($p=0.009-0.025$).

5.3.2 Intercept values vs drainage area

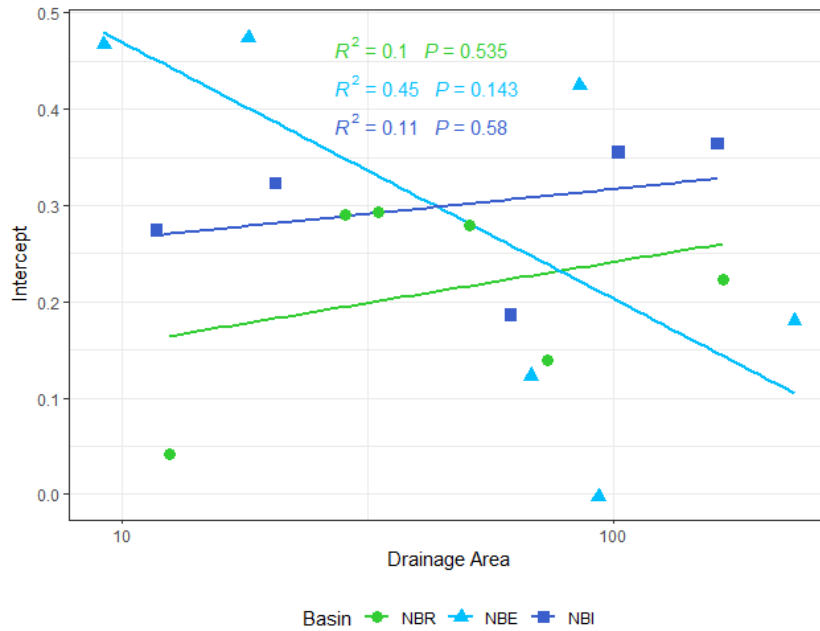


Figure 16: Longitudinal comparison of the intercepts generated from a trophic magnification regression within three basins experiencing different levels of forest management in northern New Brunswick, Canada. The data for each basin is pooled from six sites within each respective basin. Equation of the line and coefficient of determination are shown in each panel. The equation and line are coloured by basin with the minimal basin in green (NBR), extensive basin in light blue (NBE) and intensive basin in dark blue (NBI)

A comparison in overall basin trends and changes in intercept longitudinally can be done by looking at the relationship between intercept and drainage area. An ANCOVA was run that tested $\text{Intercept} = \log_{10}(\text{Area}) * \text{Basin}$ and there was a significant interaction between area and basin. The extensive and intensive basins were significantly different to each other with the extensive basin having a significant decrease in intercept value with increasing area while it was the opposite in the intensive basin. It is important to note that the R^2 values for the minimal, extensive and intensive basins ($R^2 = 0.1$, $R^2 = 0.11$, and $R^2 = 0.45$, respectively) indicates that less than 50% of the variability is explained by this model so some caution is needed when interpreting these results.

5.4 Autochthony

Table 8: ANCOVA for Autochthony= $\log_{10}(\text{Drainage Area}) * \text{Taxon} + \log_{10}(\text{Drainage Area}) + \text{Taxon}$ of data pooled from all taxa for basin. P values are included for the Drainage Area and the interaction between Drainage Area and Taxon, values bolded for $p < 0.05$.

Within Basin¹			
	Log ₁₀ Drainage Area	Taxon	Log ₁₀ Drainage Area*Taxon
Minimal	0.014	<0.001	0.529
Extensive	0.169	<0.001	0.681
Intensive	0.002	<0.001	0.633

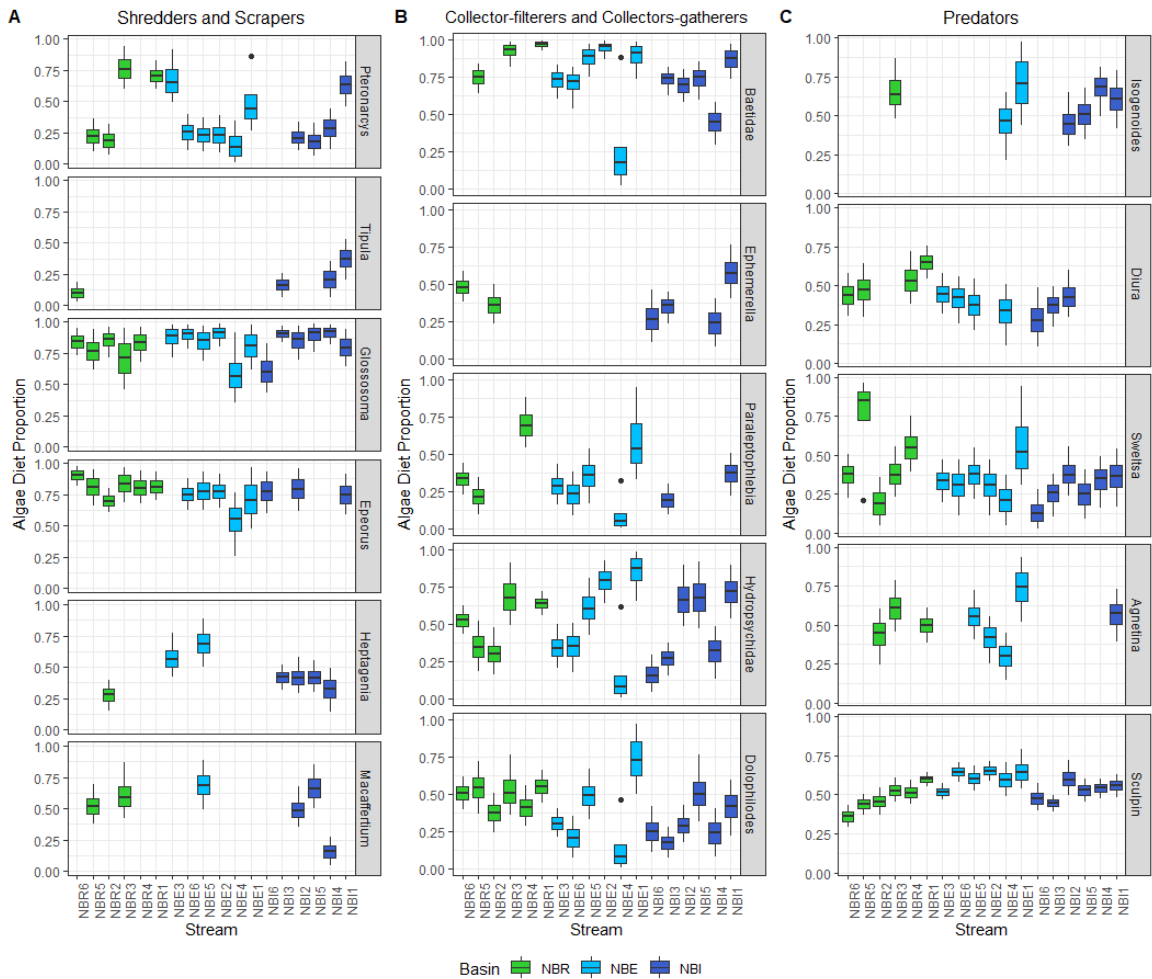


Figure 17: Boxplots showing the dietary contribution of algae (in proportion) to the diets of 16 different benthic macro invertebrate taxa and sculpin separated into three FFG categories: shredders/scrapers, collector-gatherer/collector-filterer, and predator from 12 streams within 3 basins that experience different levels of forest management (northern New Brunswick, Canada). Algal contributions were calculated from a Bayesian 2-isotope mixing model ($\delta^2\text{H}$ and $\delta^{13}\text{C}$) with MixSIAR and the line in the middle of the box is the median algae diet proportion calculated from MixSIAR, the upper and lower hinges match the upper and lower quartiles of the probability distribution around the diet proportion and the whiskers are 5th and 95th percentile of the probability distributions. Green boxes are the minimal basin (NBR), light blue the extensive basin (NBE) and dark blue the intensive basin (NBI).